

**PARAMETRIC FATIGUE ANALYSIS OF
USAF FIGHTER AIRCRAFT**

GEORGE J. ROTH

BLAINE S. WEST

*** Export controls have been removed ***

This document is subject to special export controls and each transmittal to foreign governments or foreign nationals may be made only with prior approval of the Air Force Flight Dynamics Laboratory (AFSC), Wright-Patterson Air Force Base, Ohio 45433. ATTN: FDTR.

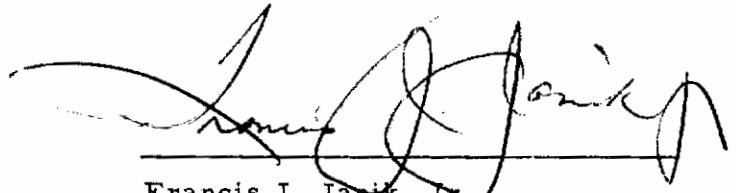
FOREWORD

This report was prepared by the University of Dayton Research Institute, Dayton, Ohio, under Air Force Contract F 33(615)-68-C-1494. The project was initiated under Project 1467, "Structural Analysis Methods", Task 146704, "Structural Fatigue Analysis." The work was administered by the Air Force Flight Dynamics Laboratory, Air Force Systems Command, Wright-Patterson Air Force Base, Ohio. Mr. Howard A. Wood, (FDTR), was the Project Engineer.

The research effort was conducted from 13 May 1968 to 1 July 1969. The report was submitted by the authors in August 1969.

This program was conducted under the general direction of Mr. Dale H. Whitford, Supervisor of Aerospace Mechanics Research.

This technical report has been reviewed and is approved.



Francis J. Janik, Jr.
Chief, Solid Mechanics Branch
Structures Division

ABSTRACT

This report contains the results of a study of the significant parameters that contribute to the fatigue life of USAF fighter aircraft. The variability of the parameters from one aircraft to another was determined in an attempt to use a mean value or a most probable distribution of some parameters so that they could be eliminated from the log sheet or recorded data. The analysis suggests that there is such a wide variation in the load factors, Mach numbers, altitudes and configurations experienced by the F-105D and F-105F aircraft that an average damage model cannot be used to predict damage to individual aircraft. A peak strain cycle counting recorder is suggested as the most practical method of monitoring fatigue damage to individual fighter aircraft. Design concepts of a counting accelerometer and three types of peak strain counters are presented.

This abstract is subject to special export controls and each transmittal to foreign governments or foreign nationals may be made only with prior approval of the Air Force Flight Dynamics Laboratory, Wright-Patterson Air Force Base, Ohio 45433.

Contrails

TABLE OF CONTENTS

	PAGE
SECTION I--INTRODUCTION	1
SECTION II--ANALYSIS OF RECORDED DATA	3
1. F-5A AIRCRAFT	3
a. Fatigue Damage Analysis	3
b. Discussion	5
2. F-105D AIRCRAFT	16
a. Fatigue Damage Analysis	16
(1) Parametric Analysis	17
(2) Damage Analysis by Mission Segment	18
(3) Analysis of Maneuver Mission Segment Data	18
b. Damage Prediction Techniques	18
(1) Mach-Altitude Probability Technique	19
(2) Evaluation of Damage Prediction Techniques	20
(3) Refinement of Damage Prediction Techniques	21
(4) Other Maneuvering in Target Area	23
c. Discussion	23
3. F-105F AIRCRAFT	76
a. Comparison With F-105D Aircraft Analysis	76
b. Fatigue Damage Analysis	76
(1) Parametric Analysis	76
(2) Damage Analysis by Mission Segment	76
(3) Analysis of Maneuver Mission Segment Data	77
c. Damage Prediction Techniques	77
(1) Mach-Altitude Probability Technique	77
(2) Calculation of Damages	77
d. Discussion	78
SECTION III--RECORDER DESIGN	92
1. BACKGROUND	92
2. PEAK COUNTING ACCELEROMETER	93
3. PEAK COUNTING ELECTRO-MECHANICAL OPTICAL STRAIN TRANSDUCER	94
4. RESISTANCE STRAIN GAGE	96
5. MECHANICAL SCRATCH GAGE	97
SECTION IV--DISCUSSION	102
SECTION V--CONCLUSIONS	104
REFERENCES	105

LIST OF ILLUSTRATIONS

		PAGE
Figure 1	Fatigue Damage per Occurrence of Percent Design Limit Load Factor for Various Stores Configurations	13
Figure 2	Cumulative Frequency Distribution of Percent Design Limit Load Factor for Five Different F5A Aircraft	14
Figure 3	Cumulative Frequency Distribution of Load Factors for Five Different F5A Aircraft	15
Figure 4	S-N Curves for 7075-T6 Clad Sheet Notched Sheet under Axial Loading $Kf_{107} = 2.50$	55
Figure 5	S-N Curves for 7075-T6 Clad Sheet Notched Sheet under Axial Loading $Kf_{107} = 2.25$	56
Figure 6	Damage per Cycle vs Load Factor by Configuration for the F-105D Transfer Spar at Fuselage Station 442	57
Figure 7	Damage per Cycle vs Load Factor by Configuration for the F-105D Top Cover Skin at Fuselage Station 509	58
Figure 8	Damage per Cycle vs Load Factor by Gross Weight for the F-105D Transfer Spar at Fuselage Station 442	59
Figure 9	Damage per Cycle vs Load Factor by Gross Weight for the F-105D Top Cover Skin at Fuselage Station 509	60
Figure 10	Damage per Cycle vs Gross Weight by Load Factor for the F-105D Transfer Spar at Fuselage Station 442	61
Figure 11	Damage per Cycle vs Gross Weight by Load Factor for the Top Cover Skin at Fuselage Station 509	62
Figure 12	Damage per Cycle vs Load Factor by Mach-Altitude Condition for the F-105D Transfer Spar at Fuselage Station 442	63
Figure 13	Damage per Cycle vs Load Factor by Mach-Altitude Condition for the F-105D Top Cover Skin at Fuselage Station 509	64
Figure 14	Mach-Altitude Probability Plot for F-105D Pull-up After Weapon Release, Configuration 3, Group 1 Data	65
Figure 15	Mach-Altitude Probability Plot for F-105D Pull-up after Weapon Release, Configuration 3 Data	66
Figure 16	Mach Number Probability by Group for F-105D Pull-up after Weapon Release, Configuration 3 Data	67
Figure 17	Load Factor Probability by Group for F-105D Pull-up after Weapon Release, Configuration 3 Data	68

List of Illustrations, continued

	PAGE	
Figure 18	Damage Ratio vs Pull-up Sample Size for Mach-Altitude Probability Damage Prediction Technique Probability Model Based on Total Configuration 3 Pull-ups, Top Skin at Fuselage Station 509	69
Figure 19	Damage Ratio vs Pull-up Sample Size for Mach-Altitude Probability Damage Prediction Technique Probability Model Based on Total Configuration 3 Pull-ups, Transfer Spar at Fuselage Station 442	70
Figure 20	Mach-Altitude Probability Plot for First 114 F-105D Pull-ups After Weapon Release, Configuration 3 Data	71
Figure 21	Mach-Altitude Probability Plot for Last 114 F-105D Pull-ups After Weapon Release, Configuration 3 Data	72
Figure 22	Comparison of Probability of Occurrence by Load Factor for F-105D, Configuration 3 Pull-up and Non Pull-up Data	73
Figure 23	Mach-Altitude Probability Plot by Load Factor Magnitude for F-105D Pull-up after Weapon Release, Configuration 3 Data	74
Figure 24	Mach-Altitude Probability Plot for F-105D Non Pull-up, Configuration 3 Data for Two Typical Aircraft	75
Figure 25	Mach-Altitude Probability Plot for F-105F Configuration 3, Base 2 Pull-ups After Weapon Release or Gunfiring	90
Figure 26	Probability of Occurrence by Load Factor Magnitude and Mach Number for F-105F, Base 2, Configuration 3 Pull-ups	91
Figure 27	Schematic Diagram of Counting Accelerometer System	98
Figure 28	Design Concept of Electro-Mechanical-Optical Peak Strain Transducer	99
Figure 29	Schematic Diagram of Electro-Mechanical-Optical Peak Strain Counting System	100
Figure 30	Schematic Diagram of Resistance Strain Gage Peak Strain Counting System	101

LIST OF TABLES

TABLE		PAGE
I	Distribution of Fatigue Damage at Wing Station 26.6 for F5A SEA Data Sample	9
II	Comparison of the Predicted Damage to Actual Damage from Average Damage per Flight Hour	10
III	Comparison of Predicted Damage to Actual Damage Based on Average Damage per Flight	11
IV	Percentage of Combat Mission by Flight Length Duration and by Recording Phase	12
V	Major and Minor Configuration Definition for F-105D	27
VI	F-105D Mach-Altitude Subdivision for Damage Calculations	28
VII	Load Factor Definition Used for Computing F-105D Damage	28
VIII	Tabulation of Damage by Mission Segment for the F-105D Transfer Spar at Fuselage Station 442 by A/C Serial Number	29
IX	Tabulation of Damage by Mission Segment for the F-105D Top Cover Skin at Fuselage Station 509 by A/C Serial Number	30
X	Tabulation of Damage due to Pull-up after Weapon Release for Transfer Spar at Fuselage Station 442 on F-105D Aircraft	31
XI	Tabulation of Damage due to Pull-up after Weapon Release for Top Cover Skin at Fuselage Station 509 on F-105D Aircraft	32
XII	Data Groups for Probability Analysis of Load Factor Occurrences During Pull-up after Weapon Release	33
XIII	Distribution of Pull-up Peaks by Group and Configuration	33
XIV	Mach-Altitude Probability Distribution for F-105D, Configuration 3 Pull-up after Weapon Release	34

Contrails

List of Tables, continued

TABLE		PAGE
XV	Predicted Damages, $(D_{K_i})_i$, for Transfer Spar at Fuselage Station 442	36
XVI	Predicted Damages, $(D_{K_i})_i$, for Top Cover Skin at Fuselage Station 509	37
XVII	Damage Predicted for Pull-ups after Weapon Release by Group 1, Configuration 3 Probability Model Fuselage Station 509	38
XVIII	Damage Predicted for Pull-ups after Weapon Release by Group 1, Configuration 3 Probability Model Fuselage Station 442	39
XIX	Damage Predicted for Pull-ups after Weapon Release by Total Configuration 3 Probability Model Fuselage Station 509	40
XX	Damage Predicted for Pull-ups after Weapon Release by Total Configuration 3 Probability Model Fuselage Station 442	41
XXI	Comparison of Damage Prediction Techniques for Top Cover Skin at Fuselage Station 509 for F-105D	42
XXII	Comparison of Damage Prediction Techniques for Transfer Spar at Fuselage Station 442 for F-105D	43
XXIII	Predicted Damage per Flight Hour, F-105D SEA Total Data Sample at Fuselage Station 509	44
XXIV	Predicted Damage per Flight Hour, F-105D SEA Total Data Sample at Fuselage Station 442	45
XXV	Predicted Damage per Flight, F-105D SEA Total Data Sample at Fuselage Station 509	46
XXVI	Predicted Damage per Flight, F-105D SEA Total Data Sample at Fuselage Station 442	47
XXVII	Predicted Damage per Pull-up after Weapon Release, F-105D, Configuration 3, SEA Data Sample at Fuselage Station 509	48
XXVIII	Predicted Damage per Pull-up after Weapon Release, F-105D, Configuration 3, SEA Data Sample at Fuselage Station 442	49

Contrails

List of Tables, continued

TABLE		PAGE
XXIX	Variance Calculations for F-105D Truncated Data Sample	50
XXX	Variance Calculations for F-105D Damage Ratios Computed by Base	51
XXXI	Damage Prediction Ratios for Mach-Altitude Probability Model Based on First 114 F-105D Configuration 3 Pull-ups	52
XXXII	Damage Prediction Ratios for Mach-Altitude Probability Model Based on Last 114 F-105D Configuration 3 Pull-ups	53
XXXIII	Comparison of Damage Ratios and Variance for Four Mach-Altitude Probability Models	54
XXXIV	Definition of Mission Type for the F-105F SEA Data Sample	79
XXXV	Recorded Data by Mission Type and Air Base for F-105F Data Sample	79
XXXVI	Tabulation of Damage by Mission Segment for the F-105F Transfer Spar at Fuselage Station 442 by Aircraft Serial Number	80
XXXVII	Tabulation of Damage by Mission Segment for the F-105F Top Cover Skin at Fuselage Station 509 by Aircraft Serial Number	81
XXXVIII	Tabulation of Damage due to Pull-up after Weapon Release for Transfer Spar at Fuselage Station 442 on F-105F Aircraft	82
XXIX	Tabulation of Damage due to Pull-up after Weapon Release for Top Cover Skin at Fuselage Station 509 on F-105F Aircraft	83
XL	Pull-up after Weapon Release or Gunfiring Occurrences by Configuration, Mission Type, and Air Base for F-105F Aircraft	84

Contrails

List of Tables, concluded

TABLES		PAGE
XLI	Mach-Altitude Probability Distribution for F-105F, Base 2, Configuration 3 Pull-up after Weapon Release	85
XLII	Damage Predicted for Pull-ups Using Base 2, Configuration 3 Probability Model for F-105F	86
XLIII	Predicted Damage Ratios per Flight Hour for F-105F Data Sample	87
XLIV	Predicted Damage Ratios per Flight for F-105F Data Sample	88
XLV	Predicted Damage Ratio per Pull-up for F-105F Data Sample	89

SECTION I

INTRODUCTION

This report is written in support of the Air Force Fatigue Certification Program and the Aircraft Structural Integrity Program. The Fatigue Certification Program has these overall objectives: (a) to provide the Air Force with aircraft which have specified life capabilities; (b) to provide the Air Force with a rational means of scheduling aircraft for required structural modifications so that the required life can be achieved with minimum downtime and loss of combat capability; and (c) to provide the Air Force with a means to assess the life trade-off requirements for various mission mixes and subsequent long range planning for aircraft replacement. The objectives of the Structural Integrity Program are: (a) to establish, evaluate, and substantiate structural integrity of aircraft systems; (b) to continually evaluate the structural integrity program by utilizing inputs from operational usage; (c) to develop statistical techniques for the evaluation of operational usage and for logistic support (maintenance, inspection, suppliers); and (d) to develop and incorporate improved structural criteria and methods of design, evaluation, and substantiation of aircraft systems.

To achieve these objectives it is necessary to know the accumulated fatigue damage to each individual aircraft in the fleet. The Air Force document, ASD-TR-66-57, "Air Force Aircraft Structural Integrity Program Requirements", as revised in 1969, states in paragraph 2.5.2.1 that,

"Individual aircraft or groups of aircraft can accumulate fatigue damage at widely varying rates depending on usage. These variations from the fleet average must be assessed to prevent catastrophic failures or unscheduled maintenance in the fleet."

For fighter aircraft the fatigue damage is a function of gross weight, Mach number, altitude, stores configuration, and load factor experienced. These parameters vary from flight to flight and also are dependent on the type of mission. Aircraft are currently programmed for modification on the basis of total flight hours, regardless of the utilization of the individual aircraft. This philosophy is based on the assumption that each aircraft will experience the same number of combinations of the above parameters during its life. Recorders are installed on a small percent of the fleet and from these recordings the average fatigue damage per hour is calculated. This average damage rate is then applied to each aircraft in the fleet.

In 1967, a study was conducted (Reference 1), wherein 120 flights were analyzed to determine if each aircraft was experiencing the same damage rate

Contrails

when the rate was normalized to different parameters. Since that time, data has become available on 3407 flights involving three different types of aircraft.

This report presents the analysis of these flights and defines the parameters necessary to monitor the damage on individual aircraft. Presentations are made of the expected accuracy of the fatigue damage to individual aircraft when one uses an average damage per hour, average damage per flight, average damage per weapon pass and a calculation based on the recorded load factor level with a distribution of Mach-altitude conditions. A design concept of a low cost recorder that could be installed in each aircraft is also presented.

SECTION II

ANALYSIS OF RECORDED DATA

Fatigue damage during flight of a fighter aircraft is a function of the aircraft's load factor, gross weight, stores configuration, Mach number, and altitude. This section presents an analysis of the effect of each of these parameters and an analysis of the consistency of the distribution of them from aircraft to aircraft. Each of the three aircraft, the F-5A, F-105D, and the F-105F will be analyzed and the results presented separately.

1. F-5A AIRCRAFT

The F-5A aircraft parametric study was based on the analysis of data reported in References 2 and 3. The fatigue damage calculations were based on the loads and stresses presented in Reference 4. Reference 2, which is a VGH flight loads report, contains composited data from 1638 flights in the SEA war zone. Reference 3 contains the load factor data for the weapon passes of this same data.

The F-5A aircraft known as the "Freedom Fighter" is a light-weight single-seat fighter-bomber built by the Norair Division of the Northrop Corporation and was used in SEA as a close air support bomber. The analysis of the data by the Northrop Corporation as presented in Reference 4 was used whenever possible to perform the parametric study.

a. Fatigue Damage Analysis

The ground rules for the fatigue analysis were the same as those used in Reference 4. As stated previously, fatigue damage is a function of the load factor, gross weight, stores configuration, Mach number, and altitude. For the F-5A aircraft the most critical location for determining the fatigue life is the wing root section at wing station 26.6. Reference 4 states that

"... 89.5 percent of the flight time occurred at altitudes below 15,000 feet and 89.3 percent of the flight time occurred in the equivalent airspeed range of 250 to 400 knots. These conditions result in a maximum Mach range from 0.4 to 0.76. Under these flight conditions the wing loads do not vary appreciably and, therefore, no attempt has been made to vary the loads to account for altitude and airspeed."

Contrails

Therefore, the fatigue damage has been reduced to a function of load factor, gross weight, and stores configuration. The data in Reference 2 that is most usable is presented in terms of percent design limit load factor (PDLLF), where

$$\text{PDLLF} = \frac{N_z W}{N_{zd} W_d} \times 100$$

where

N_{zd} = design limit load factor for a configuration

N_z = actual maneuver load factor

W_d = design gross weight for a configuration

W = actual aircraft gross weight at time of load factor experience

Therefore, to analyze the available data, damage is only a function of PDLLF and stores configuration. Figure 1 is a plot of damage per occurrence versus PDLLF for the configurations represented in the data sample. As can be observed from the figure, the amount of damage is a strong function of the stores configuration. Using the data from Figure 1 and the load experiences as reported in Reference 2, the damage by mission segment was calculated. Table I is a listing of these damages by mission segment. The data presented in Table I is the sum of all aircraft and indicates that 97.5 percent of the fatigue damage occurs during air to ground combat activities.

In order to calculate the damage on an aircraft tail number basis, we must look at the distribution of load factors and configurations by aircraft tail numbers. Table 11 of Reference 2 lists the PDLLF versus configurations for the total data sample and Table 13 lists the distribution of PDLLF by aircraft serial number. Assuming that each aircraft had the same distribution of PDLLF versus configuration as shown in Table 11 of Reference 2, the data in Table 13 of Reference 2 was used to calculate the damage by aircraft. The results of these calculations, shown in Table II of this report, were the best estimates of the damage to each individual aircraft that could be made with the data available. The listing in Table II shows that the average damage fraction was 0.000045553 per hour. Assuming that each aircraft accumulates damage at the same rate, a predicted damage for each aircraft is also presented in Table II and shows that the damage could be over- or under-predicted by 42% on two of the aircraft. The aircraft which was under-predicted by 42% had only 67 hours of recorded flight time. Two other aircraft which had 16.9 and 2.3 hours were also badly under-predicted. If one were to remove these three aircraft, i. e., numbers 3, 7, and 8, only aircraft number 1 would be poorly estimated.

Contrails

Since most of the damage is done during the weapon passes, a more reasonable method of monitoring the damage would be to determine the average damage per flight instead of per hour. Table III lists the percent of error of the predicted damage to actual damage.

Before presenting any more data, some comments are in order about the data sample that was used. The recorded data was collected in five phases. The first, third, and fifth were recorded at Bien Hoa airbase while the second and fourth were at DaNang. The aircraft were moved from one base to the other with the change in the recording phases. In analyzing the data on a per-hour or per-flight basis, it is important to know if all the aircraft were used in the same manner at each of the bases. Figure 7 of Reference 2 shows the percentage of flights within different flight length bands. This data is repeated here as Table IV and shows that the flights from Bien Hoa were generally of a shorter duration than those at DaNang. If some aircraft had a higher percentage of their flights at Bien Hoa, one would expect that the damage rate per hour would be higher for those aircraft. This is true because a great majority of the damage occurs during air-to-ground activities, which is not a function of the flight duration. The data available does not list the mission mix flown by each aircraft; therefore, no analysis was possible regarding the lengths of flights by aircraft serial number. However, since both Tables II and III show reasonably good predicted damages, it indicates that all the aircraft must have flown approximately the same mission mix. Another interesting fact about the data as pointed out in Reference 4 is that the ground gunnery passes during Phase I represented 80.9% of the maneuver load factors for all ground gunnery. These gunnery passes during Phase I, which was a 2-month period, were a result of an evaluation of the F-5/M-39 gun where approximately 50,000 rounds of ammunition were fired by each aircraft. "Thus, essentially every mission included firing all of the ammunition carried in the aircraft."* After the first data-collecting phase, the guns were used only as needed to fulfill the requirements of each mission. The total fatigue damage due to ground gunnery during Phase I was 0.0354, which was 50% of the total damage for the entire data sample. One can see from these figures that the evaluation of the gun greatly affects the damage rate of the data sample. This could explain why aircraft numbers 3, 7, and 8 received more damage than would be predicted by either the per-hour or per-flight average, since these three aircraft had a small number of recorded flights and most of these were probably during recording Phase I.

b. Discussion

The parametric fatigue analysis of the F-5A aircraft indicated that the great majority of the damage was due to air-to-ground activity. Therefore, an average damage rate based on a per-flight rather than a per-hour basis is a better predictor of damage, since the length of the flight has little to do with the activity in the target area. Also, since most of the damage was due to the

* Reference 3

Contrails

pull-up after weapon release or due to ground gunnery, the majority of the load factors occurred when the aircraft was in a clean configuration. Gunfire passes are usually made after weapon passes. This fact reduces the importance of the earlier assumption that the distribution of configurations for each individual aircraft was the same as the distribution for the entire instrumented fleet.

It is the authors' opinion that for the data sample analyzed, the use of an average damage per flight is an adequate method for monitoring the fatigue damage on the F-5A aircraft. Some improvement in the calculation of the damage to individual aircraft could be realized by the use of a load factor recorder that segregated the occurrences into grouping by stores configuration. However, because of the large scatter factor associated with fatigue failures, even for constant amplitude cycling, an improvement on the $\pm 30\%$ error does not appear to be justified. This conclusion is based on the analysis of the recorded data for SEA operations. The success of the predictor based on the average damage per flight may be the result of a fortuitous combination of load factors, gross weight, and configurations. There is some reason to be suspicious of the success obtained by the average damage per flight predictor, since the cumulative frequency distribution of PDLDF, as presented in Figure 2, shows a large variation from one aircraft to another. A comparison of Figure 3, which is a cumulative frequency distribution of load factors, with Figure 2 shows the effect that weight and configuration mix has on the conversion of load factor distribution to PDLDF distributions.

From the analysis of the distribution of the damage to the individual aircraft, it appears that a substantial improvement in the confidence of the damage calculations would result from the use of some type of recorded data. The data could be in the form of load factor level as a function of (a) weight, (b) stores configuration, (c) altitude, and (d) airspeed. The use of a peak counting accelerometer that segregated the occurrences by these parameters would eliminate the costly data processing task of a time history recorder. However, the number of storage registers would be equal to the product of the number of bands of each of the parameters. For example, on the F-5A aircraft, 45 storage registers would be required if one used three weight bands, three configurations, and five load levels. These are the only important parameters for this aircraft. This number could be reduced with some sacrifice in accuracy and introduction of some conservatism. Using the F-5A as an example, one could base all of the calculations on the most damaging configuration, which happens to be Configuration 1 (see Figure 1). The data shows that 90% of the damage occurred during Configuration 1, 8.3% during Configuration 2, and 1.5% during Configuration 3. If Configuration 1 had been used for all of the damaging load cycles, then the sum of the estimated damage for all the aircraft would have been 155% of the actual damage. This is definitely conservative and less accurate than predictions based on either the per-hour or per-flight averages. However, this assumption would reduce the number of storage registers to 15, since the load factors would only be segregated by weight.

Contrails

Another approach would be to segregate the load factors by three configurations and assume a mean value for the weight which could be a function of the configuration. For the data sample analyzed it was found that the mean weight for Configuration 1 at the time of the peak load after weapon release or ground fire was 12,979 lbs., with a standard deviation of 726 lbs. For configurations 2 and 3, the numbers were 14,421 lbs. mean with 638 lbs. standard deviation, and 14,667 lbs. mean with 797 lbs. standard deviation, respectively. The design gross weight for Configuration 1 was 11,600 lbs. Therefore, an error of 726 lbs. would cause an error in the PDLL of 5.2% at 5 g's.

$$PDLL = \frac{5(12,979 + 726)}{7(11,600)}$$

$$PDLL = 84.39$$

$$PDLL = \frac{5(12,979)}{7(11,600)}$$

$$PDLL = 79.92$$

$$\text{Error} = \frac{4.47}{84.39} = 5.2\%$$

This error of 5.2% at the 84.39% level for Configuration 1 would cause an underestimation of the damage per load cycle occurrence, see Figure 1, of $(0.0000190 - 0.0000138) = 0.0000052$ which is 27.4%. For those weights which are less than the mean by 1σ , at the same load factor and configuration, the damage would be overestimated by 31.1%. Now, if the actual weights are symmetrically distributed about the mean, over- and underestimates would be offsetting so that the cumulative damage over a long period of time would be very nearly correct. It therefore appears that the best type of load factor monitor for the F-5A would be one that segregated the load factor by three configurations and five load factor levels. This would then require 15 storage registers. The design of such a system is presented in Section IV.

Another recording system that would eliminate the problems associated with knowing the gross weight and/or configuration would be a strain amplitude cycle counter. This recorder would accumulate in storage registers the number of times that various strain amplitudes were equaled or exceeded. These strain cycle counts would then be plotted as the number of times that a given strain level was exceeded versus the strain level. From this plot a fatigue analysis could be performed with the very simple calculation of determining the life cycles at each stress level. The accuracy of this technique would depend on only two factors: (1) the ability of the analyst to determine a transfer factor from the gage location to the fatigue critical location, and (2) the effect of the variation in the 1-g trim stress. The complexity of the first factor depends on the aircraft structure, the location of the fatigue critical point, and the response of the aircraft to the various types of loads. Two approaches can be taken to the second factor. It can be assumed that the 1-g strain is a constant or that each aircraft

Contrails

has the same probability of various 1-g trim stresses. The use of a constant 1-g trim stress should be adequate for most fighter aircraft since there is little variation in the trim stress for the weight range and configurations that exist at the time the damaging loads occur. For example, the fatigue analysis presented in Reference 4 for the F-5A had only a 1083 psi variation in the 1-g trim stress over the entire range of the nine configurations. Therefore, the use of a constant 1-g trim stress would mean that the assumed 1-g stress would have a deviation from an existing practice of only ± 540 psi, which is well within the capability to calculate the stress from any set of parameters. The concept of an electro-mechanical-optical strain transducer which would accumulate these strain counts is presented in Section IV.

TABLE I

Distribution of Fatigue Damage at Wing Station 26.6
for F5A SEA Data Sample

<u>Mission Segment</u>	<u>Wing Station 26.6 Damage</u>	<u>Percent Damage</u>
Ascent	0	0
Descent	.0000625539	.09
Cruise Out	.0000219635	.03
Cruise Back	.0012011469	1.69
Loiter	.0001375018	.19
Refuel	0	0
Low Angle Bomb	.0251612405	35.50
Rocket Firing	.0011593153	1.63
Ground Gunnery	.0427923695	60.38
Photo	<u>.0003380570</u>	<u>.48</u>
Total	.0708741484	99.99

Percent of Total Damage Due to Air-to-Ground
Activities

Low Angle Bombing	35.50%
Rocket Firing	1.63%
Ground Gunnery	<u>60.38%</u>
	97.51%

TABLE II

Comparison of the Predicted Damage to Actual Damage
from Average Damage Per Flight Hour

A/C Number	Recorded Flight Time (hours)	Actual Damage (x 10 ³) (B)	Predicted Damage (damage/hr x hrs) x 10 ³ (A)	% Error
1	184.53	5.89632	8.40594	42.60
2	153.28	7.11406	6.98240	- 1.85
3	16.90	1.02444	0.76985	-24.90
4	205.90	9.17693	9.37942	2.21
5	172.57	7.00650	7.86113	12.20
6	195.03	10.18678	8.88425	-12.80
7	2.32	0.16262	0.10568	-35.00
8	67.93	5.27875	3.09443	-41.40
9	185.08	7.81347	8.43010	7.90
10	166.10	6.87209	7.56640	10.10
11	<u>201.03</u>	<u>10.10611</u>	9.15757	- 9.40
Total	1550.67	70.63807		

Average Damage Per Hour = .000045553

$$\% \text{ Error} = \frac{\text{(A)} - \text{(B)}}{\text{(B)}} \times 100$$

TABLE III

Comparison of Predicted Damage to Actual Damage
Based on Average Damage Per Flight

A/C Number	Flights	Actual Damage (x 10 ³) (B)	Predicted Damage (damage/flight x flights) 10 ³ (A)	% Error
1	172	5.89632	7.41742	+26
2	168	7.11406	7.24493	+ 1.8
3	23	1.02444	.99186	- 3.2
4	196	9.17693	8.45241	- 7.9
5	187	7.00650	8.06429	+15.1
6	217	10.18678	9.35803	- 8.1
7	3	0.16262	0.12937	-20.4
8	82	5.27875	3.53621	-33.0
9	194	7.81347	8.36616	+ 7.1
10	183	6.87209	7.89179	+14.8
11	<u>213</u>	<u>10.10611</u>	9.18553	- 9.1
Total	1638	70.63807		

$$\text{Average damage/flight} = \frac{70.63807 \times 10^{-3}}{1638} = .000043125$$

$$\% \text{ Error} = \frac{(A) - (B)}{(B)} \times 100$$

TABLE IV

Percentage of Combat Mission by Flight Length Duration
and by Recording Phase

Recording Phase	Base	Duration of Flight Hours				
		0-.5	.5-1	1-1.5	1.5-2	2-6.5
1	Bien Hoa	0	78.4	21.5	0.1	0
2	Da Nang	0	12.2	60.5	26.2	1.1
3	Bien Hoa	1.6	84.1	15.3	0	0
4	Da Nang	0	6.4	39.1	30.9	23.6
5	Bien Hoa	0	86.2	13.8	0	0

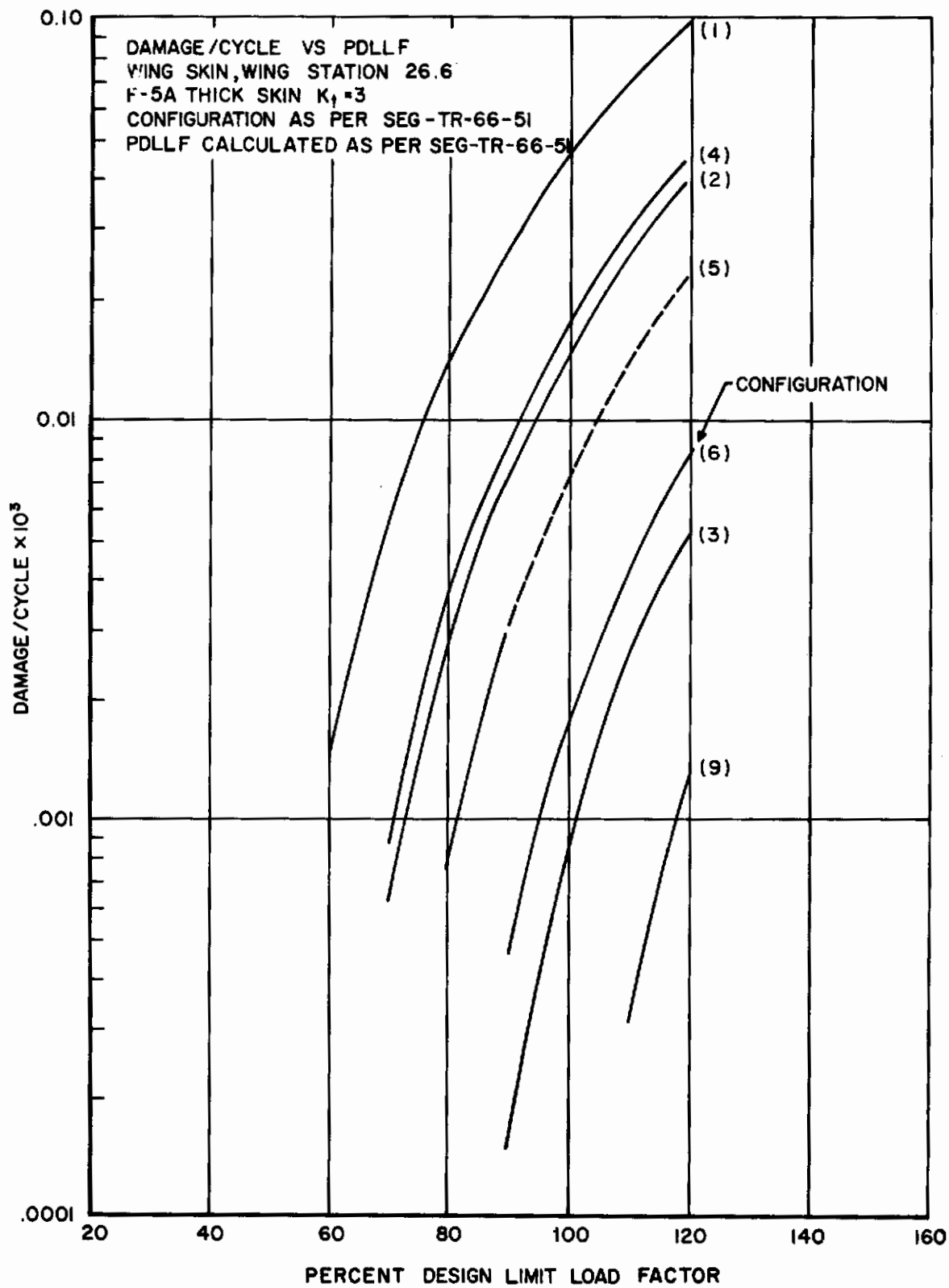


Figure 1 Fatigue Damage per Occurrence of Percent Design Limit Load Factor for Various Stores Configurations

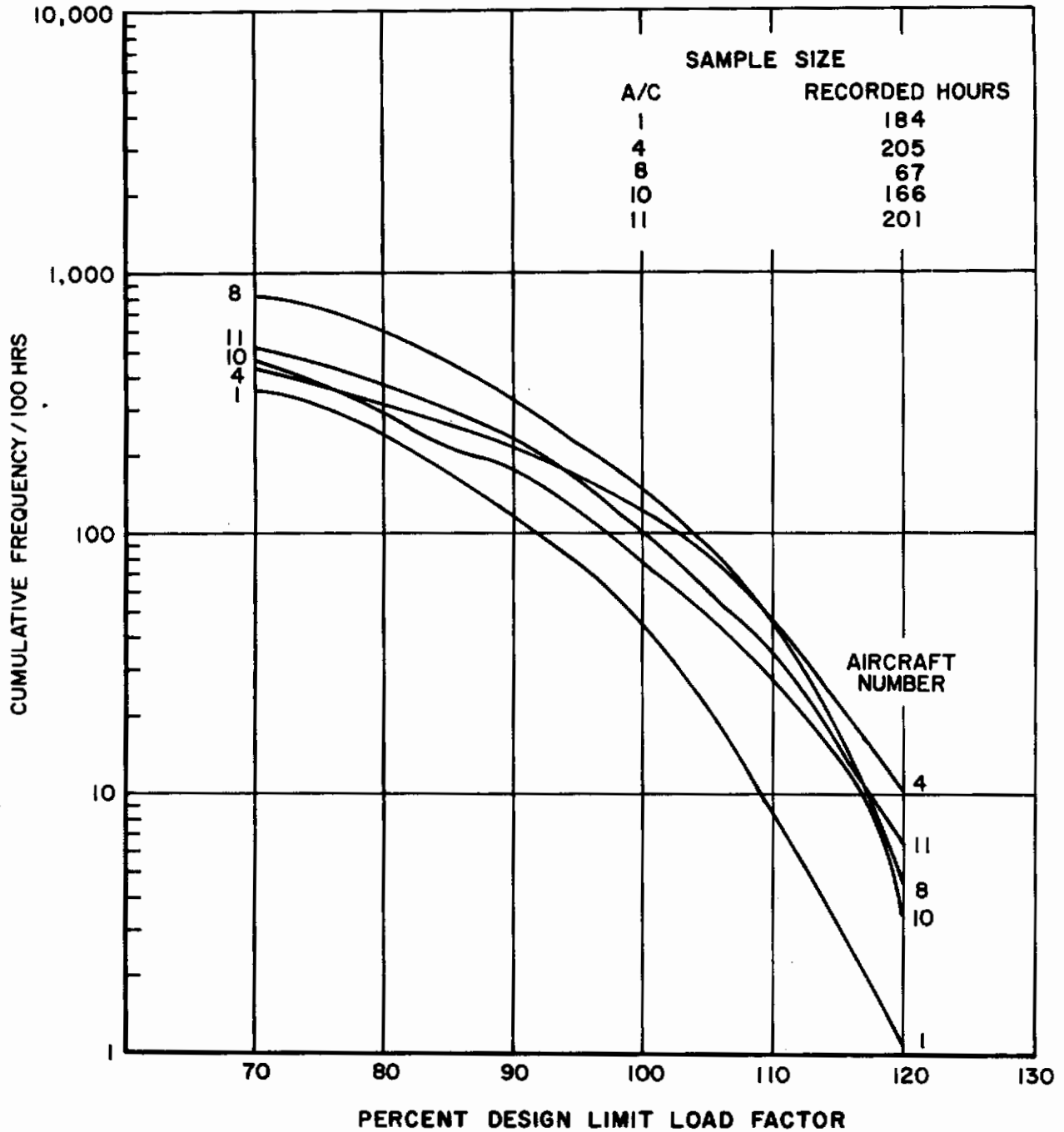


Figure 2 Cumulative Frequency Distribution of Percent Design Limit Load Factor for Five Different F5A Aircraft

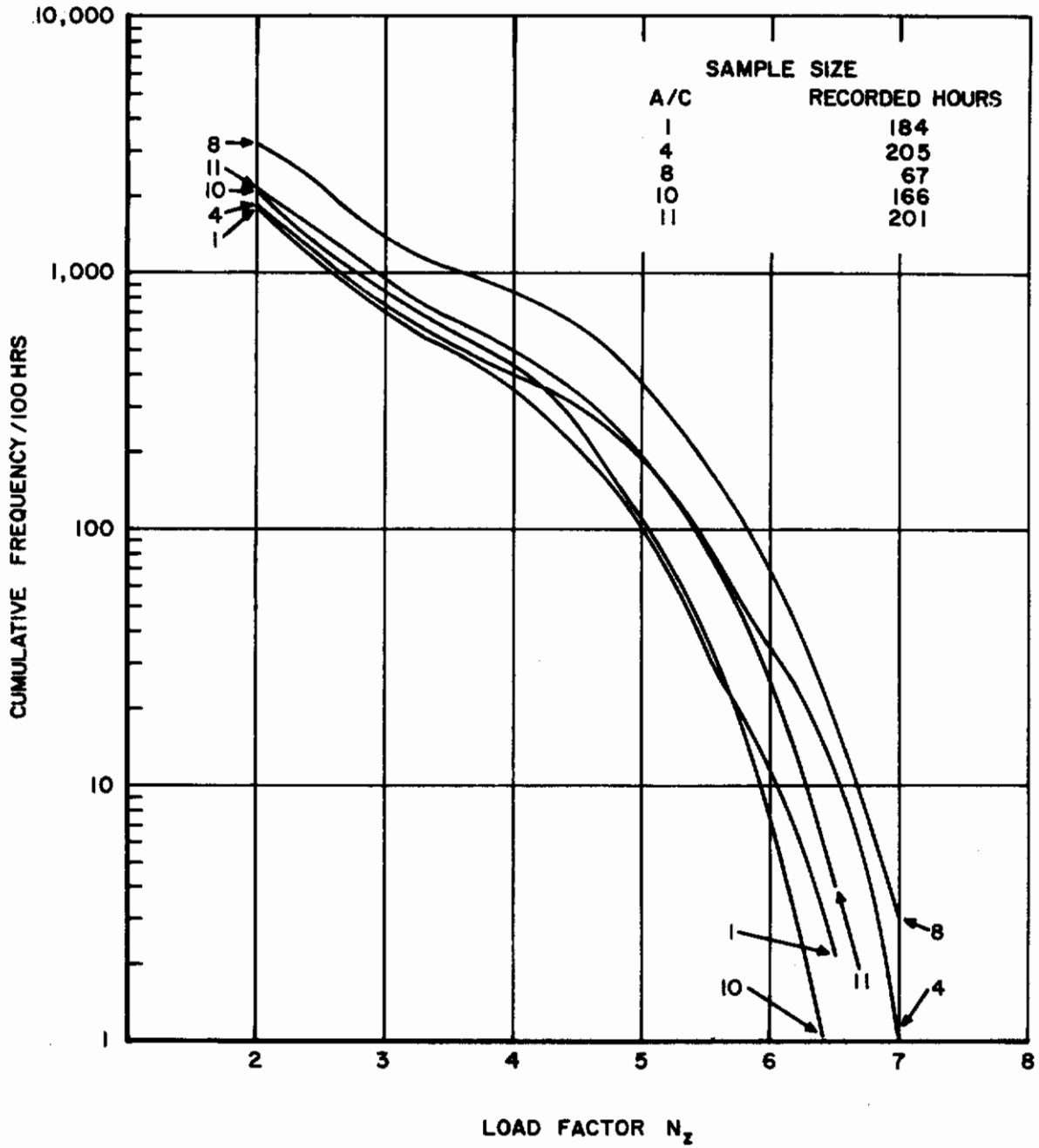


Figure 3 Cumulative Frequency Distribution of Load Factors for Five Different F5A Aircraft

2. F-105D AIRCRAFT

The purpose of this analysis is to determine the relative importance of each of the parameters affecting fatigue damage and to determine what parameters must be known to conduct a tail number fatigue damage monitoring program for the F-105D. The fatigue damage analysis reported herein is based on a 3,056 hour VGH data sample obtained in the Southeast Asia combat zone. The data was recorded on 1,319 flights from two air bases as reported in Reference 5.

a. Fatigue Damage Analysis

For the purpose of this study the fatigue damage was calculated for two critical locations, the transfer spar at fuselage station 442 and the top cover skin at the access door at fuselage station 509. Stress versus center of gravity normal load factor curves were extracted from a computer program output tab obtained from Republic Aviation. These stresses were used with the S-N curves presented in Figures 4 and 5 to calculate damage rates for 185 combinations of Mach number, altitude, gross weight, and major configuration.

For purposes of classifying the data at any time during flight, five major and 23 minor configurations were defined for the aircraft. The definition of these configurations is presented in Table V. Only the classification by major configuration was utilized in this analysis.

The Mach-altitude conditions were categorized into blocks for purposes of calculating damage. The points for which damage was calculated as defined in Reference 6 are shown in Table VI. Grouping of all possible flight conditions into the Mach-altitude conditions shown was determined, in the reference, to be sufficient for computing aircraft damage.

The aircraft gross weight was defined in increments of two-thousand pounds between 34,000 and 42,000 pounds. Damages for gross-weights less than 34,000 pounds were computed at 33,000 pounds and gross weights greater than or equal to 42,000 pounds were computed at 44,000 pounds. Damage was computed for all load factors greater than or equal to 2.5 g's in 0.5 g increments. Load factors less than 2.5 g's did not cause fatigue damage to the aircraft at the two locations being monitored. The classification of the data by load factor level used in this analysis is presented in Table VII. Load factor peaks were defined during the reduction of the data according to the following criteria: (1) the incremental peak value must be at least ± 1.0 g from the 1.0 g level flight condition, and (2) the trace must have a rise and fall of at least 1.0 g and 50 percent of the incremental peak value.

All damages computed for this analysis were found by treating each load factor occurrence as an independent stress cycle. The damages were then accumulated utilizing Miner's linear cumulative damage rule. This rule is stated mathematically as follows:

Contrails

$$D = \sum_{i=1}^j \frac{n_i}{N_i}$$

- where N_i = Number of cycles to failure under a specified cyclic loading condition i
- n_i = Number of cycles experienced at a specified loading condition
- D = Accumulated damage
- j = Number of loading conditions experienced

Failure is indicated when the accumulated damage D is equal to one.

(1) Parametric Analysis

The variation of the damage rate with configuration and load factor for a typical Mach-altitude-gross weight combination is presented in Figures 6 and 7 for fuselage stations 442 and 509, respectively. Examination of these figures reveals that damage is quite dependent on major configuration. For an N_z value of 4 there is an order of magnitude difference at fuselage station 509. At fuselage station 442 the difference in the damages varies by a factor of four.

The variation of damage rate with gross weight and load factor for a typical Mach-altitude-configuration is presented in Figures 8 and 9 for fuselage stations 442 and 509, respectively. As might be expected, the fatigue damage is much more sensitive to gross weight at fuselage station 442 than at fuselage station 509. This is due to the fact that the stress at fuselage station 442 is dependent on the wing loading, whereas the stress at fuselage station 509 is only indirectly related to the wing loading.

The variation of damage rate with load factor and gross weight for a typical Mach-altitude-configuration combination is presented in Figures 10 and 11. This is a cross-plot of the data in Figures 8 and 9. The damage rate at both aircraft locations is sensitive to load factor magnitude at all aircraft gross weights. The decrease in damage sensitivity to load factor at fuselage station 442 for the higher load factor levels reflects the effects of wing tip stalling.

The variation of the damage rate with Mach-altitude block and load factor for a typical gross weight-configuration combination is shown in Figures 12 and 13 for fuselage stations 442 and 509, respectively. The effect of wing tip stalling is reflected in the damage rate at fuselage station 442 by the gross nonlinearity at the higher values of normal load factor.

During the data acquisition program, the mission types which the F-105D aircraft was expected to experience in the SEA combat zone were divided into six classifications. Ninety-six percent of the flight hours, 92 percent of the load factor occurrences, and 92 percent of the flights occurred during the mission type denoted as conventional bombing. Therefore, mission type was eliminated as a variable for the purposes of this analysis.

The results of the damage sensitivity study reveal that damage rate is most sensitive to normal load factor. Gross weight and configuration are also of importance along with the Mach-altitude condition.

(2) Damage Analysis by Mission Segment

The airborne portion of the flight was classified into the mission segments of ascent, maneuver, cruise, refuel, and descent. Based on the results of Reference 1, it was anticipated that a large percent of the damage experienced by the F-105D would occur during the maneuver mission segment. This was further verified for the F-105D Southeast Asia combat data sample reported in Reference 5. Computer tabs for each flight contained in the F-105D SEA data sample reported in Reference 5 were obtained from Technology Incorporated, Dayton, Ohio, and damages were computed for each of the 10,610 N_z occurrences having a magnitude greater than or equal to 2.5 g's. The results are presented in Tables VIII and IX for fuselage stations 442 and 509, respectively. Approximately 99 percent of the total damage, exclusive of the ground-air-ground cycle, occurred during the maneuver mission segment (mission segment 2) at both aircraft fatigue critical locations.

(3) Analysis of Maneuver Mission Segment Data

On the basis of the data presented in Tables VIII and IX, the parametric analysis was confined to the determination of damage in the maneuver mission segment. If damage prediction techniques can be developed for this portion of the flight, the damage occurring in all other mission segments can be neglected as insignificant.

The damage in the maneuver mission segment was separated into two categories; maneuvering in the target area and pull-up after weapon release. The results of these calculations are presented in Tables X and XI for fuselage stations 442 and 509, respectively. It can be concluded that in general more than three-fourths of the total aircraft damage, exclusive of the ground-air-ground cycle, occurs during pull-up after weapon release for both fatigue critical points under consideration.

b. Damage Prediction Techniques

Based on the relative importance of the load factor occurrences during pull-up after weapon release, the primary effort was directed toward development of a method for predicting damage resulting from these occurrences.

(1) Mach-Altitude Probability Technique

On the basis of the findings of Section II -2a and of Reference 1, a damage prediction technique based on Mach-altitude probability was investigated. The Mach-altitude probabilities as a function of load factor and configuration and independent of gross weight were determined for the pull-up data. The total data sample of pull-up occurrences was divided into four groups by aircraft tail number as defined in Table XII. The aircrafts were divided into four groups in an attempt to show that a damage model derived from a few aircraft could be used to predict the damage on the remaining aircraft in the fleet. Each group contained a representative sample by base and hours of data recorded as reported in Table 6 of Reference 5. Table XIII of this report shows the distribution of pull-up occurrences by group and by configuration. Approximately 83 percent of all pull-ups occurred in exit Configuration 3. Therefore, the exit Configuration 3 data was selected for analysis.

The Mach-altitude probabilities for Configuration 3 by group and by load factor level are presented in Table XIV. As can be seen, the probability distributions as a function of load factor are in general slightly skewed, indicating some correlation between Mach number and load factor magnitude. Representative three-dimensional Mach-altitude probability plots for the Group I and total Configuration 3 data samples are presented in Figures 14 and 15, respectively. These plots are independent of load factor level. Figure 16 shows these pull-up distributions with the altitude variable eliminated. The consistency of the data by Group is further exemplified by cross-plotting the data presented in Table XIV. These results in the form of histograms showing the probability of occurrences as a function of load factor level are presented in Figure 17.

The fatigue damage due to pull-up after weapon release for the F-105D aircraft was calculated using two different Mach-altitude probability models. The first model was based on the Mach-altitude probabilities associated with the exit Configuration 3 pull-ups experienced by the Group I aircraft. The second model was based on the total exit Configuration 3 pull-up experience.

The probability of occurrence for each Mach-altitude block was determined as a function of load factor level and independent of aircraft gross weight. The damage per occurrence as a function of Mach-altitude block and load factor level was then determined for each aircraft gross weight condition. This data was used with the probability model to calculate damage per occurrence as a function of load factor level and gross weight. This calculation is represented mathematically by the following equation:

$$D_{ki} = \sum_{j=1}^n p_{ij} d_{kij}$$

- p_{ij} = probability of occurrence of Mach-altitude block j at load factor level i
- d_{kij} = damage at load factor level i, Mach-altitude block j and gross weight k
- D_{ki} = predicted damage per occurrence at load factor level i and aircraft gross weight k

These calculations resulted in a matrix of D_{ki} as a function of gross weight and load factor. These results are presented in Tables XV and XVI for the two aircraft locations and Mach-altitude probability models. Each pull-up occurrence was then assigned a damage D_{ki} and the total damage was found by summing over the total number of occurrences.

The results of these calculations are presented in Tables XVII through XX. Tables XVII and XVIII show the damage predicted using the Group I probability model for the top cover skin at fuselage station 509 and the transfer spar at fuselage station 442, respectively. The variation in the ratio of the predicted damage to the calculated damage is greater than had been expected. Tables XIX and XX show the corresponding data for the probability model constructed from the total data sample. Based on these results, it appears that the damage predicted for an individual aircraft using this technique is subject to a significant error. This can probably be attributed to the diverse experience accumulated on a fighter aircraft of this type in a combat zone.

The correlation between the ratio of the predicted damage to the actual damage and the sample size for an individual aircraft is presented in Figures 18 and 19 for the two aircraft fatigue critical locations. Each point on the curve represents the experience for a particular aircraft. The top curve on each figure connects those points for which the predicted damage was too high, the bottom curve connects those points for which the predicted damage was too low. Examination of these curves reveals that there is little improvement in the damage ratio within the range of the sample size represented.

(2) Evaluation of Damage Prediction Techniques

Comparison of the fatigue damage predicted by the Mach-altitude probability technique with damage predictions based on per-hour, per-flight, and per pull-up calculations is presented in Tables XXI and XXII. The actual damages on which these comparisons are based are presented in Tables XXIII through XXVII. It should be noted that not all damage ratios are computed from a common basis. The per hour and per flight ratios are based on the damage for the total SEA data sample. However, the damage ratios for the pull-ups and the Mach-altitude prediction model are based on the damage due to pull-up after weapon release in exit Configuration 3.

A qualitative examination of the results presented in Tables XXI and XXII does not suggest a strong preference for any of the damage prediction techniques under consideration. Therefore, a statistical evaluation of the four techniques was attempted. First, the available data was truncated by arbitrarily eliminating those aircraft that experienced less than twenty-eight pull-ups. Next the damage ratios were assumed to be an indicator of the relative merit of the different techniques and the variance was computed independently for each of the damage prediction techniques using the formula

$$S^2 = \frac{n\sum(X_i)^2 - (\sum X_i)^2}{n(n-1)}$$

where S^2 = sample variance
 n = sample size
 X_i = the i th data point in sample n

The results of these calculations are presented in Table XXIX for fuselage stations 509 and 442. A significance test was made on the variances assuming that the deviations have a Gaussian distribution. For a probability of 1 in 20 ($\alpha = .05$) of concluding that there was a difference when there was not, there was no significant statistical difference in the variances. However, a qualitative comparison shows a trend which indicates that the variance in the tail number fatigue damage prediction for a fleet of aircraft can be minimized by using the Mach-altitude probability prediction technique. The relative advantage of the method is greater at fuselage station 509 than for fuselage station 442.

(3) Refinement of Damage Prediction Techniques

Initially it was assumed that the accumulated fatigue damage could be predicted independently of air base for the SEA data sample. This assumption was based on a qualitative evaluation of the data presented in Reference 5, the results presented in Reference 1, and the desire to minimize the number of variables required for damage prediction.

Examination of the data contained in Tables XXIII through XXVIII reveals that there is a difference in the damage rates at the two bases, particularly at fuselage station 509. Therefore, the fatigue damage was calculated using the damage rates at each base on a per-hour, per-flight, and per pull-up basis. The resulting damage ratios are presented in Table XXX. The variances for these data were calculated using the same ground rules as were employed in the previous section. The results of these calculations are shown at the bottom of Table XXX. There was no significant improvement in the variances at either aircraft location as a result of considering the samples obtained at each base to be independent.

Due to the differences in fatigue damage prediction, utilizing the Mach-altitude probability technique, between this investigation and that reported in Reference 1, it was decided to investigate the possibility that more than one statistical population was contained in the total F-105D SEA data sample. To accomplish this a Mach-altitude probability model was formulated from the first 114 Configuration 3 pull-up occurrences. Another model was constructed from the last 114 Configuration 3 pull-ups contained in the data sample (pull-ups 1084 through 1198).

The three dimensional Mach-altitude probability plots for these two models are presented in Figures 20 and 21. Comparison of these two figures reveals some difference in the aircraft utilization. The primary difference is in the Mach 1.2 probability. Since this Mach-altitude block encompasses all altitudes, it is difficult to determine from the plots whether the difference reflects a variation in airspeed, altitude, or both. Examination of the altitude for each of the occurrences at Mach 1.2 showed them to be comparable. Therefore, it was concluded that the increase in the number of occurrences at Mach 1.2 could be attributed to an increase in the airspeed at the time of pull-up after weapon release for the last 114 pull-ups. Comparison of Figures 20 and 21 with Figure 15 reveals that the Mach-altitude probability plot for the last 114 pull-ups agrees more closely with the corresponding plot for the total Configuration 3 Mach-altitude probabilities, particularly at Mach 1.2.

The first of these models was used to predict damage for the first 114, first 228, and first 345 Configuration 3 pull-up occurrences as well as for the total data sample. The results of these calculations are presented in Table XXXI in the form of damage ratios. The variance with the corresponding sample size is shown at the bottom of each column for fuselage stations 509 and 442, respectively. Although the damage ratio deviates from one by a considerable margin for the total data sample, the variance decreases with increasing data sample size. This might be expected since fighter aircraft in combat utilization generally show a large scatter in the amount of damage accumulated on any one given flight. In addition, it should be noted that the sample size N for which the variance is calculated increases as the data sample is expanded to include more aircraft. Therefore, this difference must be accounted for in interpreting the variances.

The corresponding results for the predicted damage using the Mach-altitude probability model for the last 114 pull-ups are shown in Table XXXII. The results are similar to those obtained from the Mach-altitude probability model based on the first 114 Configuration 3 pull-ups. It is interesting to note that the actual damage predicted for the total data sample using the model from the last 114 pull-ups is considerably better at both aircraft fatigue critical locations, as would be expected from the results of comparing the Mach-altitude probability plots. However, the variance is minimized for the non-truncated data sample if the model based on the first 114 pull-ups is used. For the truncated data sample presented in Table XXXIII, the variance is smaller for the model based on the last 114 pull-ups.

The total damage due to the 1198 Configuration 3 pull-ups has now been predicted using four different Mach-altitude probability models (i. e., models based on the Group I pull-ups, the total pull-ups, the first 114 pull-ups, and the last 114 pull-ups). The damage ratios and the variances for the truncated data sample are shown in Table XXXIII for comparison.

(4) Other Maneuvering in Target Area

Approximately twenty to twenty-five percent of the fatigue damage, exclusive of the ground-air-ground cycle, resulted from load factor occurrences other than pull-up after weapon release (see Tables X and XI). This data was analyzed to see if the Mach-altitude probability damage prediction technique could be utilized for predicting this damage.

Probability distributions of the pull-up after weapon release and the pull-ups due to other maneuvering in the target area were plotted. These results are presented in Figure 22. The plot for pull-up after weapon release is for the total Configuration 3 pull-ups. The plots for the load factor occurrences due to other maneuvering in the target area are for two typical aircraft, one at each base. The distribution of the pull-ups is approximately symmetrical about a mean of 4.7 to 5.2 g's. The distribution of the non-pull-up data displays the shape of the familiar exponential exceedance curve.

It was anticipated that the Mach-altitude probability data might lend itself to division into two models according to load factor magnitude. The total Configuration 3 pull-up data sample was separated into two parts; load factor peaks ≥ 4.2 , and load factor peaks ≤ 3.7 . The corresponding Mach-altitude probability models are presented in Figure 23. As was pointed out previously, there is some correlation between Mach number and load factor magnitude.

Next, it was attempted to correlate the Mach-altitude probability distribution for the non-pull-up data, independent of load factor magnitude, with the Mach-altitude probability for pull-ups having a load factor magnitude ≤ 3.7 . The Mach-altitude probability distributions for the non-pull-up data in the maneuver mission segment for aircraft serial numbers 130 and 422 are presented in Figure 24. Comparison of Figure 24 with Figure 23 reveals some similarity, with respect to Mach number, between the two probability models.

Although this investigation showed some promise, application of the method for predicting fatigue damage due to the non-pull-up load factors was not pursued further because of the relative lack of success encountered in predicting the damage due to pull-up after weapon release.

c. Discussion

The prediction of accumulated fatigue damage on a fighter aircraft presents a formidable problem. There are a multitude of parameters that affect the fatigue life. Some of these remain constant during the life of the aircraft while others are quite sensitive to aircraft utilization.

Contrails

Laboratory fatigue test results on controlled specimens subjected to cyclic loads having constant amplitude alternating and mean stresses show a significant scatter factor in fatigue life. If one were to use any of the prediction techniques presented to this point he would have to increase the scatter factor by a factor of two due to the usage.

Efforts to predict the stress level encountered during operation of fighter aircraft are complicated by the wide latitude in usage. Loads encountered on a specific mission are affected by the pilot, the type and location of the target, enemy activity, visibility and weather conditions. Mission definition is dependent on base location, intensity of the conflict and military philosophy, and is subject to continuous redefinition. Therefore, it would seem that a fighter aircraft deployed in a combat zone could be expected to experience a random input spectrum with regard to fatigue damage accumulation. Thus, in the authors' opinion, the use of statistical methods for predicting fatigue damage could not rationally be expected to yield precise results.

The relative merits of the various methods employed to predict fatigue damage to the F-105D aircraft are not easily defined. For the data sample analyzed, there was no significant difference in the ability of the various methods used. However, care must be exercised in generalizing these results to the total problem of evaluating the accumulated fatigue damage to the aircraft for all utilization. For example, the damage rate per hour would be quite sensitive to target location relative to the base. The damage rate per flight would be more sensitive to target type and the weapon delivery modes. The damage per pull-up would be sensitive to target topography and fortification as well as pilot reaction and time of day. This means that continuous flight load or strain recording would be necessary on a number of aircraft to provide a basis for establishing and revising damage rates or damage prediction models. This might be required on a squadrom basis or an even finer breakdown depending on the aircraft utilization.

Keeping these general observations in mind, the following specific remarks concerning the analysis reported herein are presented. There was some advantage in the Mach-altitude probability technique of damage prediction. This advantage was not significant for the data sample analyzed. However, the advantage might be more distinct for a more general data sample.

A comparison of the variances for the different Mach-altitude probability models presented in Table XXVII indicates that better results are obtained when the model is based on a chronological sample rather than a sample by aircraft serial number. This indicates that there was a greater inconsistency with respect to aircraft serial number than with mission variation. This was also true for the data sample reported in Reference 1. However, the basic differences between the results of this study and those of Reference 1 can apparently be attributed to the difference in the S-N curves and the Mach-altitude breakdown used in the two studies. The S-N curves used in Reference 1 attached more significance

Contrails

to the damage resulting from the high load factor levels whereas the damage at the lower load factor levels was the same in both studies. The S-N data used in the Reference 1 study for life cycles less than 300 was extrapolated by the University of Dayton whereas the data for this study used data extrapolated by Republic Aviation. The study in Reference 1 placed all Mach numbers greater than .9 at .92 whereas this study placed Mach numbers greater than .95 at Mach 1.2. Reference to Figures 12 and 13 will show the significance of this Mach effect. Also the stress vs. N_z data were calculated based on the SEA Weapon Configuration whereas Reference 1 used stresses based on peacetime training flights that had approximately the same configuration.

In view of the results of this study there appear to be three alternatives available for achieving, with some degree of success, the objectives of the Air Force Fatigue Certification Program and the Aircraft Structural Integrity Program.

(1) The first alternative would be the use of per-hour, per-flight or per pull-up calculations. This would require instrumentation of a portion of the fleet to provide damage rates for the remainder of the fleet. Considering the diverse utilization of fighter aircraft, this method has some obvious shortcomings as discussed previously and the confidence in the predicted damage, particularly on an aircraft serial number basis, would be low.

(2) A second alternative would be to install a peak counting accelerometer on each aircraft, together with the necessary instrumentation and logic circuitry for determining Mach number, altitude, gross weight, and configuration at the time of each load factor occurrence. The load factor occurrences would be segregated by these parameters and recorded in storage registers. The number of storage registers would be equal to the product of the number of bands required for each of the parameters. If the data were categorized by the five major configurations, 11 load factor levels, six gross weights, and the Mach-altitude breakdown of Table VI a total of 3,310 storage registers would be required. For the SEA data sample analyzed during this study, the number of storage registers could be reduced to 396 with little loss in accuracy. This number could be pared even further by accepting some sacrifice in accuracy.

Although this method of monitoring fatigue damage eliminates the cost of recording and processing VGH time history data, it still requires a fairly sophisticated instrumentation and recording system. Also, while it is relatively easy to eliminate or consolidate variables, and thus decrease the number of storage registers required, for a given data sample the judicious choice of these variables without this prior knowledge would prove a more difficult problem.

(3) The third alternative would be to eliminate the necessity for knowing parameters such as gross weight, configuration, airspeed, altitude and load factor. This could be accomplished by using a strain amplitude cycle counter.

Contrails

The frequency at which selected strain levels were equaled or exceeded could be sensed and recorded in accumulating storage registers. This strain exceedance data could then be used directly with an S-N curve to determine the cumulative damage at a fatigue critical location. Since only the magnitude of the strain peaks would be measured, a constant mean stress could be assumed or the mean stress could be expressed as a function of the aircraft gross weight and configuration. However, this added breakdown of the peaks would require additional storage registers.

TABLE V

Major and Minor Configuration Definition for F-105D

<u>Major Config.</u>	<u>Minor Config.</u>	<u>Center Line Station</u>	<u>Inboard Station</u>	<u>Outboard Station</u>
1	A	Clean	Clean	Clean
1	B	Clean	Clean	Any Store
1	C	Clean	≤1000# Store	Clean
1	D	Clean	≤1000# Store	≤700# Store
1	E	Any Store	Clean	Clean
1	F	Any Store	Clean	Any Store
1	G	Any Store	≤1000# Store	Clean
1	H	Any Store	≤1000# Store	≤700# Store
1	I	650 Gal. Tank	Clean	Clean
1	J	650 Gal. Tank	Clean	Any Store
1	K	650 Gal. Tank	≤1000# Store	Clean
1	L	650 Gal. Tank	≤1000# Store	≤700# Store
2	M	650 Gal. Tank	>700# Store	>700# Store
2	N	650 Gal. Tank	>1000# Store	Clean
2	O	650 Gal. Tank	>1000# Store	Any Store
3	P	Clean	450 Gal. Tank	Clean
3	Q	Clean	450 Gal. Tank	≤700# Store
3	R	≤1000# Store	450 Gal. Tank	Clean
3	S	≤1000# Store	450 Gal. Tank	≤700# Store
4	T	Clean	450 Gal. Tank	>700# Store
4	U	≤1000# Store	450 Gal. Tank	>700# Store
5	V	>1000# Store	450 Gal. Tank	Clean
5	W	>1000# Store	450 Gal. Tank	Any Store

TABLE VI

F-105D Mach-Altitude Subdivision for Damage Calculations

Altitude	Mach Numbers					
		.65		.85	.92	1.2
1,000			2,000			
					5,000	
7,000	10,000					
12,000			15,000			
20,000						

TABLE VII

Load Factor Definition Used for Computing F-105D Damages

<u>Load Factor Interval</u>	<u>Value for Which Damage was Computed</u>
≥ 2.5 - < 3.0	2.7
≥ 3.0 - < 3.5	3.2
≥ 3.5 - < 4.0	3.7
≥ 4.0 - < 4.5	4.2
≥ 4.5 - < 5.0	4.7
≥ 5.0 - < 5.5	5.2
≥ 5.5 - < 6.0	5.7
≥ 6.0 - < 6.5	6.2
≥ 6.5 - < 7.0	6.7
≥ 7.0 - < 7.5	7.2
≥ 7.5	7.7

TABLE VIII

Tabulation of Damage by Mission Segment for the F-105D
Transfer Spar at Fuselage Station 442 by A/C Serial Number

1	2	3	4	5
<u>Damage Summary</u>				
A/C	M. S. 2 (Maneuver)	All Other M. S.	Total	<u>Damage M. S. 2</u> <u>Total Damage</u> x 100
130	.047292898	.000135848	.047428746	99.71
160	.007393539	.000046220	.007439759	99.38
240	.024659128	.000122500	.024781628	99.51
357	.016063090	.000020446	.016083536	99.87
367	.037294519	.000258924	.037553443	99.31
720	.000035452	-----	.000035452	100.00
731	.003086485	.000023310	.003109795	99.25
732	.029523458	.000183697	.029707155	99.38
762	.000428973	.000003754	.000432727	99.13
Subtotal				
Base 1	.165777542	.000794699	.166572241	99.52
68	.024607462	.000177036	.024784498	99.29
69	.034840997	.000121454	.034962451	99.65
132	.042614288	.000151869	.042766157	99.64
167	.003267466	.000012909	.003280375	99.61
205	.030545950	.000165749	.030711699	99.46
352	.004220838	.000001384	.004222222	99.97
378	.045659687	.000143400	.045803087	99.69
422	.011572689	.000089483	.011662172	99.23
424	.003939580	.000003434	.003943014	99.91
469	.005396200	.000029239	.005425439	99.46
Subtotal				
Base 2	.206665157	.000895957	.207561114	99.57
Total	.372442699	.001690656	.374133355	99.55

TABLE IX

Tabulation of Damage by Mission Segment for the F-105D
Top Cover Skin at Fuselage Station 509 by A/C Serial Number

A/C	<u>Damage Summary</u>			$\frac{\text{Damage M. S. 2}}{\text{Total Damage}} \times 100$
	M. S. 2 (Maneuver)	All Other M. S.	Total	
130	.015133408	.000144693	.015278101	99.05
160	.004614652	.000044801	.004659453	99.04
240	.006885296	.000103627	.006988923	98.52
357	.004427206	.000017938	.004445144	99.60
367	.011342031	.000322921	.011664952	97.23
720	.000008603	-----	.000008603	100.00
731	.000729279	.000023988	.000747140	97.61
732	.010193342	.000205703	.010399045	98.02
762	.000060579	.000004671	.000065250	92.84
Subtotal				
Base 1	.053394396	.000868342	.054256611	98.41
68	.012076296	.000157801	.012234097	98.71
69	.014791108	.000110809	.014901917	99.26
132	.019692062	.000139962	.019832024	99.29
167	.001108912	.000015433	.001124345	98.63
205	.011121770	.000135154	.011256924	98.80
352	.003049063	.000000493	.003049556	99.98
378	.025906307	.000172216	.026078523	99.34
422	.003900497	.000056418	.003956915	98.57
424	.001561174	.000001320	.001562494	99.91
469	.001750460	.000020006	.001770466	98.87
Subtotal				
Base 2	.094957649	.000809612	.095767261	99.15
Total	.148352045	.001677954	.150023872	98.89

TABLE X

Tabulation of Damage due to Pull-up after Weapon Release for
Transfer Spar at Fuselage Station 442 on F-105D Aircraft

<u>A/C</u>	Number of Pull-up	<u>Damages</u>		<u>Damage Pull-up</u> <u>Damage M. S. 2</u> x 100
		M. S. 2 (Maneuver)	Pull-up after Weapon Release	
130	126	.047292898	.037451294	79.19
160	40	.007393539	.003290226	44.50
240	128	.024659128	.017532723	71.10
357	54	.016063090	.014507099	90.31
367	137	.037294519	.024853427	66.64
720	0	.000035452	- - - - -	- - -
731	15	.003086485	.002817961	91.30
732	148	.029523458	.023655876	80.13
762	4	.000428973	.000421885	98.35
Subtotal Base 1		.165777542	.124530491	75.12
68	130	.024607462	.020583639	83.65
69	116	.034840997	.030027328	86.18
132	123	.042614288	.033047298	77.55
167	12	.003267466	.002917203	89.28
205	138	.030545950	.028625917	93.71
352	9	.004220838	.003880182	91.93
378	149	.045659678	.038848251	85.08
422	77	.011572689	.009992032	86.34
424	11	.003939580	.003492819	88.66
469	31	.005396200	.004706186	87.21
Subtotal Base 2		.206665157	.176120855	85.22
Total		.372442699	.300651346	80.72

TABLE XI

Tabulation of Damage due to Pull-up after Weapon Release for
Top Cover Skin at Fuselage Station 509 on F-105D Aircraft

A/C	Number of Pull-up	Damages		Damage Pull-up Damage M. S. 2 x 100
		M. S. 2 (Maneuver)	Pull-up after Weapon Release	
130	126	.015133408	.012318943	81.40
160	40	.004614652	.002038340	44.17
240	128	.006885296	.004977942	72.30
357	54	.004427206	.004022334	90.85
367	137	.011342031	.007289099	64.27
720	0	.000008603	- - - - -	- - -
731	15	.000729279	.000649082	89.00
732	148	.010193342	.007854239	77.05
762	4	.000060579	.000058955	97.32
Subtotal Base 1		.053394396	.039208934	73.43
68	130	.012076296	.007970412	66.00
69	116	.014791108	.012399450	83.83
132	123	.019692062	.015785158	80.16
167	12	.001108912	.000723382	65.23
205	138	.011121770	.009894261	88.96
352	9	.003049063	.002971337	97.45
378	149	.025906307	.018890256	72.91
422	77	.003900497	.003199132	82.02
424	11	.001561174	.001290189	82.64
469	31	.001750460	.001594274	91.08
Subtotal Base 2		.094957649	.074717801	78.69
Total		.148352045	.113926735	76.79

TABLE XII

Data Groups for Probability Analysis of Load Factor Occurrences During Pull-up after Weapon Release

<u>Group</u>	<u>Aircraft No.</u>
1	130, 132, 357, 422
2	160, 240, 378, 469
3	731, 732, 69, 167
4	367, 720, 762, 68, 205, 352, 424

TABLE XIII

Distribution of Pull-up Peaks by Group and Configuration
Number of Pull-up Occurrences

Group	Configuration					Total
	1	2	3	4	5	
1	32	1	309	4	34	380
2	26	1	290	7	24	348
3	18	4	245	6	18	291
4	32	6	354	0	37	429
Total	108	12	1198	17	113	1448

TABLE XIV

**Mach-Altitude Probability Distribution for F-105D,
Configuration 3 Pull-up After Weapon Release**

Mach-Altitude Blocks										
N _z	.65	.65	.85	.85	.85	.92	.92	.92	.92	1.2
	7	20	1	7	20	1	7	12	20	20
Group 1 Probabilities										
2.7	.500				.500					
3.2	.182				.818					
3.7	.210				.737				.053	
4.2	.057		.029		.629		.029		.143	
4.7					.632		.015		.044	
5.2			.029		.629		.014		.114	
5.7			.036		.473		.091		.182	
6.2			.039		.500		.077		.039	
6.7					.375				.188	
7.2									.200	
7.7									.500	
Totals	.029		.019		.576		.006		.036	
Group 2 Probabilities										
2.7					1.000					
3.2					.889		.111			
3.7	.048				.667				.095	
4.2					.650		.025		.025	
4.7			.014		.800		.057		.071	
5.2	.016		.016		.619		.032		.032	
5.7					.625		.075		.225	
6.2					.483				.241	
6.7					.100		.100		.300	
7.2					.500				.250	
7.7					.333				.333	
Totals	.007		.003		.645		.014		.038	
Group 3 Probabilities										
2.7					.100					
3.2	.250				.625		.125			
3.7	.063				.813				.063	
4.2	.029		.059		.618		.029		.029	
4.7	.021				.646		.021		.042	
5.2	.019				.556		.047		.241	
5.7					.543		.022		.196	
6.2					.588		.059		.176	
6.7					.429		.071		.071	
7.2					.200		.200			
7.7									1.00	
Totals	.024				.588		.012		.045	

(Table XIV continued on next page)

TABLE XIV, Continued

Mach-Altitude Blocks										
N _z	.65	.65	.85	.85	.85	.92	.92	.92	.92	1.2
	7	20	1	7	20	1	7	12	20	20
Group 4 Probabilities										
2.7	.250			.500		.250				
3.2			.091	.727		.091	.091			
3.7	.050			.750	.100		.050			.050
4.2	.024		.049	.634	.024		.220			.049
4.7				.682	.015	.045	.121			.136
5.2	.011			.652		.043	.163	.043		.087
5.7				.580		.160	.180			.080
6.2				.545		.091	.227			.136
6.7				.211		.158	.368			.263
7.2				.333			.167			.500
7.7										1.00
Totals	.011		.088	.607	.011	.068	.172	.011		.110
All Group Probabilities										
2.7	.222			.667		.111				
3.2	.103		.026	.769	.051	.026	.026			
3.7	.092			.737	.026		.053	.026		.065
4.2	.027		.033	.633	.027	.013	.153	.013		.100
4.7	.004		.004	.694	.012	.048	.127			.111
5.2	.011	.004	.007	.620	.007	.039	.161	.014		.136
5.7			.010	.550		.089	.194			.157
6.2			.009	.526		.060	.181			.224
6.7				.289		.085	.237	.016		.373
7.2				.250		.050	.150			.550
7.7				.143			.286			.571
Totals	.018	.001	.010	.604	.011	.048	.152	.008		.149

Altitudes are in feet x 10⁻³

TABLE XV
 Predicted Damages, $(D_K)_i$, for Transfer Spar
 at Fuselage Station 442
 Group 1, Configuration 3, Pull-up Probability Model

N_z	Gross Weight x 10^{-3}					
	33	35	37	39	41	44
2.7	0.0	0.0356	0.0742	0.1626	0.1812	0.0933
3.2	0.0743	0.1402	0.2182	0.4317	0.5226	0.2105
3.7	0.2649	0.3871	0.6193	1.2670	1.8011	0.5908
4.2	0.7347	1.1932	1.9030	3.7938	5.7061	1.9214
4.7	1.9010	2.9068	4.8353	8.8939	10.4686	3.7459
5.2	4.3727	6.3983	8.0073	14.0436	23.8068	6.4495
5.7	8.8831	10.0655	15.9244	28.9518	37.3640	33.1591
6.2	15.2591	19.8803	30.4564	53.7918	89.7596	49.0379
6.7	25.1247	39.7110	52.7412	108.5148	173.6502	80.9299
7.2	54.2750	100.3309	157.4869	185.3413	290.3087	201.8780
7.7	75.7472	110.9637	150.9013	195.7983	205.3322	163.4993

Total Configuration 3 Pull-up Probability Model

N_z	Gross Weight x 10^{-3}					
	33	35	37	39	41	44
2.7	0.0	0.0158	0.0497	0.1334	0.1770	0.0514
3.2	0.0705	0.1350	0.2176	0.4386	0.5637	0.1995
3.7	0.2733	0.4157	0.6724	1.4112	1.9946	0.6476
4.2	0.7303	1.1857	1.9082	3.8223	5.6889	1.9012
4.7	1.7570	2.6766	4.4594	8.3511	9.1097	3.0817
5.2	4.3895	5.7069	6.8679	12.2716	20.7205	4.8845
5.7	8.0823	8.8684	13.9157	25.8944	31.3149	32.6247
6.2	12.9191	15.1622	22.5681	41.3216	65.8760	40.9756
6.7	25.9428	36.9441	50.5491	101.5327	155.9376	70.4541
7.2	41.8744	73.8877	114.6699	133.5362	210.7528	147.4712
7.7	79.0918	118.7365	162.3092	214.5017	215.9111	185.0529

$$(D_K)_i = \sum_{j=1}^n P_{ij} (d_{Kij})$$

= predicted damage per occurrence at load factor
 level i and aircraft gross weight K.

Numbers in the table are damage x 10^5 .

TABLE XVI
 Predicted Damages, $(D_{K'})_i$, for Top Cover Skin
 at Fuselage Station 509

Group 1, Configuration 3, Pull-up Probability Model

N_z	Gross Weight x 10^{-3}					
	33	35	37	39	41	44
2.7	0.0	0.0	0.0	0.0	0.0	0.0
3.2	0.0090	0.0083	0.0090	0.0938	0.0052	0.0
3.7	0.1862	0.2304	0.2988	0.4697	0.2742	0.1174
4.2	0.5719	0.6742	0.8620	1.2674	0.9393	0.6176
4.7	1.2540	1.5281	1.8677	2.6329	1.9158	1.2332
5.2	2.5944	3.1411	3.4523	5.1769	4.2900	2.7303
5.7	4.2539	5.1286	5.7892	7.8724	6.9810	5.0255
6.2	9.1723	10.1891	13.1929	10.9450	5.0988	11.0083
6.7	17.8354	22.5190	26.4770	48.1508	41.1749	23.1038
7.2	47.0834	55.3134	70.7774	131.2717	120.4984	64.3467
7.7	52.3390	60.5907	124.6507	167.6208	144.0159	77.5987

Total Configuration 3 Pull-up Probability Model

N_z	Gross Weight x 10^{-3}					
	33	35	37	39	41	44
2.7	0.0	0.0	0.0	0.0	0.0	0.0
3.2	0.0086	0.0085	0.0112	0.0911	0.0053	0.0
3.7	0.1828	0.2323	0.3070	0.4919	0.3063	0.1353
4.2	0.5389	0.6385	0.8154	1.2049	0.8814	0.5753
4.7	1.0865	1.2933	1.5683	2.2009	1.5486	0.9661
5.2	2.1306	2.5156	2.7706	4.0983	3.4934	2.0776
5.7	3.5758	4.2853	4.8082	6.2907	5.7614	4.0377
6.2	7.2214	7.9838	10.2447	16.1498	5.3022	8.2150
6.7	16.2845	20.3791	24.1537	43.7488	36.9666	21.0706
7.2	34.5693	40.7783	52.2527	97.6245	90.2766	45.9856
7.7	55.1865	64.3317	134.5567	183.2314	161.8594	83.4041

$$(D_{K'})_i = \sum_{j=1}^n P_{ij}(d_{K'})_{ij}$$

= predicted damage per occurrence at load factor
 level i and aircraft gross weight K.

Numbers in the table are damage x 10^5 .

TABLE XVII

Damage Predicted for Pull-ups after Weapon Release
by Group 1, Configuration 3 Probability ModelFuselage Station 509

A/C	Predicted Damage	Actual Damage	No. Pull-ups	<u>Predicted Damage</u> <u>Actual Damage</u>
130	.011101328	.011054771	105	1.00
132	.009941412	.009308585	94	1.07
357	.003434372	.003770050	43	0.91
422	.003933254	.003051069	67	1.29
160	.002678943	.001265232	28	2.12
240	.006356793	.004634964	116	1.37
378	.014935296	.012418496	118	1.20
469	.001513419	.001518588	28	1.00
731	.000926601	.000637889	13	1.45
732	.009410448	.006262450	128	1.50
69	.008092920	.009463007	93	0.86
167	.000638259	.000722062	11	0.88
367	.009620021	.006353593	109	1.51
720	- - - - -	- - - - -	0	--
762	.000147953	.000047762	3	3.10
68	.011233754	.005434180	112	2.07
205	.007378656	.007211458	112	1.02
352	.001980458	.002971337	9	0.67
424	.000811469	.001278468	9	0.63
Total	.104135356	.087403961	1198	1.19

TABLE XVIII

Damage Predicted for Pull-ups after Weapon Release
by Group 1, Configuration 3 Probability Model

Fuselage Station 442

A/C	Predicted Damage	Actual Damage	No. Pull-ups	<u>Predicted Damage</u> <u>Actual Damage</u>
130	.030695597	.035629394	105	0.86
132	.025075527	.026087360	94	0.96
357	.012272102	.014136603	43	0.87
422	.015274948	.009666610	67	1.58
160	.005837160	.002654828	28	2.20
240	.023035078	.017132062	116	1.34
378	.039599059	.031232314	118	1.27
469	.004423352	.004588783	28	0.96
731	.004000717	.002803357	13	1.43
732	.031093000	.022037530	128	1.41
69	.021704972	.027515075	93	0.79
167	.002250145	.002914833	11	0.77
367	.032601718	.023243259	109	1.40
720	- - - - -	- - - - -	0	--
762	.000616525	.000407993	3	1.51
68	.032030401	.015493040	112	2.07
205	.023715802	.024954671	112	0.95
352	.002865961	.003880182	9	0.74
424	.002113829	.003475942	9	0.61
Total	.309205893	.267853836	1198	1.15

TABLE XIX

Damage Predicted for Pull-ups after Weapon Release
by Total Configuration 3 Probability Model

Fuselage Station 509

A/C	Predicted Damage	Actual Damage	No. Pull-ups	<u>Predicted Damage</u> Actual Damage
130	.010061774	.011054771	105	0.91
132	.007774021	.009308585	94	0.84
357	.002958563	.003770050	43	0.78
422	.003387564	.003051069	67	1.11
160	.002616828	.001265232	28	2.07
240	.005198587	.004634964	116	1.12
378	.012989552	.012418496	118	1.05
469	.001273420	.001518588	28	0.84
731	.000785918	.000637889	13	1.23
732	.007811945	.006262450	128	1.25
69	.006793217	.009463007	93	0.72
167	.000507983	.000722062	11	0.70
367	.007851088	.006353593	109	1.24
720	- - - - -	- - - - -	0	--
762	.000119850	.000047762	3	2.51
68	.009084963	.005434180	112	1.67
205	.006308707	.007211458	112	0.87
352	.002073974	.002971337	9	0.70
424	.000704458	.001278468	9	0.55
Total	.088302412	.087403961	1198	1.01

TABLE XX

Damage Predicted for Pull-ups after Weapon Release
by Total Configuration 3 Probability Model

Fuselage Station 442

A/C	Predicted Damage	Actual Damage	No. Pull-ups	<u>Predicted Damage</u> <u>Actual Damage</u>
130	.026970951	.035629394	105	0.76
132	.020161120	.026087360	94	0.77
357	.010859514	.014136603	43	0.77
422	.013521032	.009666610	67	1.40
160	.005422644	.002654828	28	2.04
240	.019359242	.017132062	116	1.13
378	.033754140	.031232314	118	1.08
469	.003943526	.004588783	28	0.86
731	.003576185	.002803357	13	1.28
732	.026967903	.022037530	128	1.22
69	.018710929	.027515075	93	0.68
167	.001912396	.002914833	11	0.66
367	.027337999	.023243259	109	1.18
720	- - - - -	- - - - -	0	--
762	.000549660	.000407993	3	1.35
68	.026369567	.015493040	112	1.70
205	.020481797	.024954671	112	0.82
352	.002906484	.003880182	9	0.75
424	.001916828	.003475942	9	0.55
Total	.264721917	.267853836	1198	0.99

TABLE XXI

Comparison of Damage Prediction Techniques for
Top Cover Skin at Fuselage Station 509 for F-105D

A/C	<u>Dam. /Hr. *</u> Actual Damage	<u>Dam. /Flt. **</u> Actual Damage	<u>Dam. /Pull-up †</u> Actual Damage	<u>M-A Predicted Dam. ††</u> Actual Damage
130	.79	.77	.69	.91
160	1.13	1.17	1.61	2.07
240	2.50	2.20	1.82	1.12
357	1.10	.97	.83	.78
367	1.64	1.45	1.25	1.24
720	4.39	1.32	--	--
731	2.01	2.13	1.49	1.23
732	1.52	1.31	1.49	1.25
762	4.51	5.23	4.58	2.51
Base 1	1.41	1.28	1.17	1.10
68	1.03	1.02	1.50	1.67
69	.64	.69	.72	.72
132	.49	.61	.74	.84
167	1.29	1.72	1.11	.70
205	1.26	1.31	1.13	.87
352	.18	.22	.22	.70
378	.56	.60	.69	1.05
422	1.50	1.64	1.60	1.11
424	.72	.87	.51	.55
469	2.07	2.31	1.35	.84
Base 2	.77	.83	.89	.95
Total	1.00	1.00	1.00	1.01

*Damage/Hour = $\left(\frac{\text{total damage for data sample}}{\text{total hours of data}}\right)$ (hours per aircraft)

**Damage/Flight = $\left(\frac{\text{total damage for data sample}}{\text{total number of flights}}\right)$ (flights per aircraft)

†Damage/Pullup = $\left(\frac{\text{total damage for all Configuration 3 pull-ups after weapon release}}{\text{total number of Configuration 3 pull-up after weapon release}}\right)$
(Configuration 3 pull-ups per aircraft)

††M-A Predicted Damage = Configuration 3 pull-up damage predicted using Mach-altitude model based on total of all Configuration 3 pull-ups

Actual Damage = Damage calculated using measured Mach, altitude, gross weight, configuration and load factor

= Total damage for per hour and per flight calculations

= Damage due to Configuration 3 pull-ups for per pull-up and Mach-altitude probability calculations

TABLE XXII

Comparison of Damage Prediction Techniques for
Transfer Spar at Fuselage Station 442 for F-105D

A/C	<u>Dam. /Hr. *</u> Actual Damage	<u>Dam. /Flt. **</u> Actual Damage	<u>Dam. /Pull-up †</u> Actual Damage	<u>M-A Predicted Dam. ††</u> Actual Damage
130	.64	.62	.66	.76
160	1.77	1.83	2.36	2.05
240	1.76	1.55	1.51	1.13
357	.76	.67	.68	.77
367	1.27	1.13	1.05	1.18
720	2.66	8.01	--	--
731	1.20	1.28	1.04	1.28
732	1.33	1.15	1.30	1.22
762	1.70	1.97	1.64	1.35
Base 1	1.14	1.04	1.03	1.03
68	1.27	1.26	1.62	1.70
69	.68	.74	.76	.68
132	.57	.70	.81	.77
167	1.10	1.47	.84	.66
205	1.15	1.20	1.00	.82
352	.32	.40	.52	.75
378	.80	.85	.84	1.08
422	1.27	1.39	1.55	1.40
424	.72	.86	.58	.55
469	1.68	1.88	1.36	.86
Base 2	.88	.96	.97	.96
Total	1.00	1.00	1.00	.99

*Damage/Hour = $\left(\frac{\text{total damage for data sample}}{\text{total hours of data}}\right)$ (hours per aircraft)

**Damage/Flight = $\left(\frac{\text{total damage for data sample}}{\text{total number of flights}}\right)$ (flights per aircraft)

†Damage/Pull-up = $\left(\frac{\text{total damage for all Configuration 3 pull-ups after weapon release}}{\text{total number of Configuration 3 pull-ups after weapon release}}\right)$
(Configuration 3 pull-ups per aircraft)

††M-A Predicted Damage = Configuration 3 pull-up damage predicted using Mach-altitude model based on total of all Configuration 3 pull-ups

Actual Damage = Damage calculated using measured Mach, altitude, gross weight, configuration and load factor data

= Total Damage for per hour and per flight calculations

= Damage due to Configuration 3 pull-ups for per pull-up and Mach-altitude probability calculations

TABLE XXIII

Predicted Damage per Flight Hour, F-105D
SEA Total Data Sample at Fuselage Station 509

A/C	Flight Time	Total Damage	<u>A/C Damage</u> A/C Time	Predicted Damage	<u>Predicted Damage</u> Actual Damage
130	247.13	.015278101	.000061822	.01213398	.79
160	107.44	.004659453	.000043368	.00527526	1.13
240	355.54	.006988923	.000019657	.01745687	2.50
357	99.55	.004445144	.000044652	.00488787	1.10
367	388.49	.011664952	.000030026	.01907410	1.64
720	.77	.000008603	.000011173	.00003781	4.39
731	30.57	.000747140	.000024440	.00150097	2.01
732	322.03	.010399045	.000032292	.01581154	1.52
762	6.0	.000065250	.000010875	.00029460	4.51
Subtotal					
Base 1	1557.52	.054256611	.000034835	.07647361	1.41
68	257.61	.012234097	.000047491	.01264855	1.03
69	194.31	.014901917	.000076692	.00954054	.64
132	199.48	.019832024	.000099419	.00979439	.49
167	29.46	.001124345	.000038165	.00144647	1.29
205	289.30	.011256924	.000038911	.01420451	1.26
352	11.19	.003049556	.000272525	.00054942	.18
378	298.45	.026078523	.000087380	.01465378	.56
422	120.50	.003956915	.000032838	.00591650	1.50
424	23.04	.001562494	.000067817	.00113125	.72
469	74.64	.001770466	.000023720	.00366479	2.07
Subtotal					
Base 2	1497.98	.095767261	.000063931	.07355022	.77
Total	3055.50	.15002342	.000049100	.15002387	1.00

$$\text{Predicted Damage} = \left(\frac{\text{Total Damage}}{\text{Total Flight Hours}} \right) (\text{Flight Hours})$$

$$\text{Average Damage Rate} = \left(\frac{\text{Total Damage}}{\text{Total Flight Hours}} \right) = .000049$$

TABLE XXIV

Predicted Damage per Flight Hour, F-105D
SEA Total Data Sample at Fuselage Station 442

A/C	Flight Time	Total Damage	<u>A/C Damage</u> A/C Time	Predicted Damage	<u>Predicted Damage</u> Actual Damage
130	247.13	.047428746	.000191918	.03026008	.64
160	107.44	.007439759	.000069246	.01315560	1.77
240	355.54	.024781628	.000069701	.04353445	1.76
357	99.55	.016083536	.000161562	.01218950	.76
367	388.49	.037553443	.000096665	.04756905	1.27
720	.77	.000035452	.000046042	.00009428	2.66
731	30.57	.003109795	.000101727	.00374317	1.20
732	322.03	.029707155	.000092249	.03943129	1.33
762	6.00	.000432727	.000072121	.00073468	1.70
Subtotal					
Base 1	1557.52	.166572241	.000106947	.19071209	1.14
68	257.61	.024784498	.000096209	.03154331	1.27
69	194.31	.034962451	.000179931	.02379248	.68
132	199.48	.042766157	.000214388	.02442553	.57
167	29.46	.003280375	.000111350	.00360726	1.10
205	289.30	.030711699	.000106159	.03542363	1.15
352	11.19	.004222222	.000377321	.00137017	.32
378	298.45	.045803087	.000153470	.03654401	.80
422	120.50	.011662172	.000096782	.01475474	1.27
424	23.04	.003943014	.000171138	.00282116	.72
469	74.64	.005425439	.000072688	.00913937	1.68
Subtotal					
Base 2	1497.98	.207561114	.000138561	.18342166	.88
Total	3055.50	.374133355	.000122446	.37413375	1.00

$$\text{Predicted Damage} = \left(\frac{\text{Total Damage}}{\text{Total Flight Hours}} \right) (\text{Flight Hours})$$

$$\text{Average Damage Rate} = \left(\frac{\text{Total Damage}}{\text{Total Flight Hours}} \right) = .000122$$

TABLE XXV
 Predicted Damage per Flight, F-105D
 SEA Total Data Sample at Fuselage Station 509

A/C	Number Flights	Total Damage	Predicted Damage	<u>Predicted Damage</u> <u>Actual Damage</u>
130	103	.015278101	.011724181	.77
160	48	.004659453	.005463696	1.17
240	135	.006988923	.015366645	2.20
357	38	.004445144	.004325426	.97
367	149	.011664952	.016960223	1.45
720	1	.000008603	.000113827	13.23
731	14	.000747140	.001593578	2.13
732	120	.010399045	.013659240	1.31
762	3	.000065250	.000341481	5.23
Subtotal				
Base 1	611	.054256611	.069548297	1.28
68	110	.012234097	.012520970	1.02
69	91	.014901917	.010358257	.70
132	106	.019832024	.012065662	.61
167	17	.001124345	.001935059	1.72
205	130	.011256924	.014797510	1.31
352	6	.003049556	.000682962	.22
378	137	.026078523	.015594299	.60
422	57	.003956915	.006488139	1.64
424	12	.001562494	.001365924	.87
469	30	.001770466	.004097772	2.31
Subtotal				
Base 2	702	.095767261	.079906554	.83
Total	1313	.150023872	.150023872	1.00

$$\text{Predicted Damage} = \left(\frac{\text{Total Damage}}{\text{Total Number of Flights}} \right) (\text{No. of Flights})$$

$$\text{Average Damage Rate} = \left(\frac{\text{Total Damage}}{\text{Total Number of Flights}} \right) = .000114$$

TABLE XXVI

Predicted Damage per Flight, F-105D
SEA Total Data Sample at Fuselage Station 442

A/C	Number Flights	Damage	Predicted Damage	<u>Predicted Damage</u> <u>Actual Damage</u>
130	103	.047428746	.029237992	.62
160	48	.007439759	.013625472	1.83
240	135	.024781628	.038321640	1.55
357	38	.016083536	.010786822	.67
367	149	.037553443	.042295736	1.13
720	1	.000035452	.000283864	8.00
731	14	.003109795	.003974096	1.28
732	120	.029707155	.034063680	1.15
762	3	.000432727	.000851592	1.97
Subtotal				
Base 1	611	.166572241	.173440904	1.04
68	110	.024784498	.031225040	1.26
69	91	.034962451	.025831624	.74
132	106	.042766157	.030089584	.70
167	17	.003280375	.004825688	1.47
205	130	.030711699	.036902320	1.20
352	6	.004222222	.001703184	.40
378	137	.045803087	.038889368	.85
422	57	.011662172	.016180248	1.39
424	12	.003943014	.003406368	.86
469	36	.005425439	.010219104	1.88
Subtotal				
Base 2	702	.207561114	.149272528	.96
Total	1313	.374133355	.374133355	1.00

$$\text{Predicted Damage} = \left(\frac{\text{Total Damage}}{\text{Total Number of Flights}} \right) (\text{No. of Flights})$$

$$\text{Average Damage Rate} = \left(\frac{\text{Total Damage}}{\text{Total Number of Flights}} \right) = .000285$$

TABLE XXVII

Predicted Damage per Pull-up after Weapon Release,
F-105D, Configuration 3, SEA Data Sample
at Fuselage Station 509

A/C	Number Pull-ups	Damage due to Pull-ups	Predicted Damage	<u>Predicted Damage</u> <u>Actual Damage</u>
130	105	.011054771	.007660590	.69
160	28	.001265232	.002042824	1.61
240	116	.004634964	.008463128	1.83
357	43	.003770050	.003137194	.83
367	109	.006353593	.007952422	1.25
720	0			
731	13	.000637889	.000948454	1.49
732	128	.006262450	.009338624	1.49
762	3	.000047762	.000218874	4.58
Base 1	545	.034026711	.039762110	1.17
68	112	.005434180	.008171296	1.50
69	93	.009463007	.006785094	.72
132	94	.009308585	.006858052	.74
167	11	.000722062	.000802538	1.11
205	112	.007211458	.008171296	1.13
352	9	.002971337	.000656622	.22
378	118	.012418496	.008609044	.69
422	67	.003051069	.004888186	1.60
424	9	.001278468	.000656622	.51
469	28	.001518588	.002042824	1.35
Base 2	653	.053377250	.047641574	.89
Total	1198	.087403961	.087403961	1.00

$$\text{Predicted Damage} = \left(\frac{\text{Total Damage}}{\text{Total Number Pull-ups}} \right)^* (\text{No. Pull-ups})$$

$$\text{Average Damage Rate} = \left(\frac{\text{Total Damage}}{\text{Total Number Pull-ups}} \right)^* = .000073$$

* Configuration 3 Data

TABLE XXVIII
 Predicted Damage per Pull-up After Weapon Release,
 F-105D, Configuration 3, SEA Data Sample
 at Fuselage Station 442

A/C	Number Pull-ups	Damage due to Pull-ups	Predicted Damage	<u>Predicted Damage</u> <u>Actual Damage</u>
130	105	.035629344	.023476320	.66
160	28	.002654828	.006260352	2.36
240	116	.017132062	.025935744	1.51
357	43	.014136603	.009614112	.68
367	109	.023243259	.024370656	1.05
720	0			
731	13	.002803357	.002906592	1.04
732	128	.022037530	.028618752	1.30
762	3	.000407993	.000670752	1.64
Base 1	545	.118045026	.121853280	1.03
68	112	.015493040	.025041408	1.62
69	93	.027515075	.020793312	.76
132	94	.026087360	.021016896	.81
167	11	.002914833	.002459424	.84
205	112	.024954671	.025041408	1.00
352	9	.003880182	.002012256	.52
378	118	.031232314	.026382912	.84
422	67	.009666610	.014980128	1.55
424	9	.003475942	.002012256	.58
469	28	.004588783	.006260352	1.36
Base 2	653	.149808810	.146000352	.97
Total	1198	.267853836	.267853836	1.00

$$\text{Predicted Damage} = \left(\frac{\text{Total Damage}}{\text{Total Number Pull-ups}} \right)^* (\text{No. of Pull-ups})$$

$$\text{Average Damage Rate} = \left(\frac{\text{Total Damage}}{\text{Total Number Pull-ups}} \right)^* = .000224$$

* Configuration 3 Data

TABLE XXIX
Variance Calculations for F-105D Truncated Data Sample

A/C	<u>Damage/Hr.</u> Actual Damage	<u>Damage/Flight</u> Actual Damage	<u>Damage/Pull-up</u> Actual Damage	<u>M-A Predicted Damage</u> Actual Damage
<u>Fuselage Station 509</u>				
130	.79	.77	.69	.91
160	1.13	1.17	1.61	2.07
240	2.50	2.20	1.82	1.12
357	1.10	.97	.83	.78
367	1.64	1.45	1.25	1.24
732	1.52	1.31	1.49	1.25
68	1.03	1.02	1.50	1.67
69	.64	.69	.72	.72
132	.49	.61	.74	.84
205	1.26	1.31	1.13	.87
378	.56	.60	.69	1.05
422	1.50	1.64	1.60	1.11
469	2.07	2.31	1.35	.84
S ² =	.354	.311	.168	.148

<u>Fuselage Station 442</u>				
130	.64	.62	.66	.76
160	1.77	1.83	2.36	2.05
240	1.76	1.55	1.51	1.13
357	.76	.67	.68	.77
367	1.27	1.13	1.05	1.18
732	1.33	1.15	1.30	1.22
68	1.27	1.26	1.62	1.70
69	.68	.74	.76	.68
132	.57	.70	.81	.77
205	1.15	1.20	1.00	.82
378	.80	.85	.84	1.08
422	1.27	1.39	1.55	1.40
469	1.68	1.88	1.36	.86
S ² =	.184	.183	.240	.168

$$S^2 = \frac{n\sum(X_i)^2 - (\sum X_i)^2}{n(n-1)}$$

TABLE XXX

Variance Calculations for F-105D Damage Ratios
Computed by Base

A/C	Predicted Damage/Actual Damage		
	Damage/Hour	Damage/Flight	Damage/Pull-up
<u>Fuselage Station 509</u>			
130	.56	.60	.59
160	.80	.91	1.38
240	1.77	1.71	1.56
357	.78	.76	.71
367	1.16	1.13	1.07
732	1.08	1.02	1.28
68	1.34	1.23	1.68
69	.83	.83	.80
132	.64	.73	.83
205	1.64	1.58	1.27
378	.73	.72	.78
422	1.94	1.97	1.80
469	2.69	2.77	1.51
S ² =	.394	.393	.163

Fuselage Station 442

130	.56	.59	.64
160	1.54	1.76	2.28
240	1.53	1.49	1.47
357	.66	.64	.66
367	1.11	1.08	1.02
732	1.16	1.10	1.26
68	1.44	1.31	1.66
69	.77	.77	.78
132	.65	.73	.83
205	1.31	1.25	1.03
378	.90	.88	.87
422	1.43	1.45	1.59
469	1.91	1.96	1.40
S ² =	.176	.187	.228

$$S^2 = \frac{n \sum (X_i)^2 - (\sum X_i)^2}{n(n-1)}$$

Contrails

TABLE XXXI
 Damage Prediction Ratios for Mach-Altitude Probability Model
 Based on First 114 F-105D Configuration 3 Pull-ups

A/C	Peaks 1-114	Peaks 1-228	Peaks 1-345	All Peaks
	$\frac{\text{Predicted Damage}}{\text{Actual Damage}}$	$\frac{\text{Predicted Damage}}{\text{Actual Damage}}$	$\frac{\text{Predicted Damage}}{\text{Actual Damage}}$	$\frac{\text{Predicted Damage}}{\text{Actual Damage}}$
<u>Fuselage Station 509</u>				
130	--	.57	.77	.72
132	1.95	2.01	1.60	.31
357	--	--	--	.65
422	--	--	--	.94
160	2.26	1.79	1.79	1.79
240	--	1.87	.81	.73
378	.94	.98	.84	.70
469	.66	.65	.65	.65
731	--	--	--	1.05
732	1.57	1.57	1.11	.90
69	.50	.49	.54	.46
167	--	--	--	.48
367	1.03	1.20	1.20	.79
720	--	--	--	--
762	--	--	--	1.91
68	--	1.91	2.03	.94
205	1.50	1.77	1.67	.71
352	.60	.60	.60	.60
424	--	--	--	.44
Totals	.96	.91	.92	.69
Variance	.3939 N=9	.3605 N=12	.2695 N=12	.1788 N=18
<u>Fuselage Station 442</u>				
130	--	.54	.90	.61
132	1.36	1.48	1.33	.43
357	--	--	--	.68
422	--	--	--	1.21
160	3.08	1.69	1.67	1.68
240	.74	1.50	.74	.83
378	.95	1.04	1.02	.76
469	.72	.74	.74	.74
731	--	--	--	1.15
732	1.97	1.57	1.24	1.00
69	.65	.56	.60	.49
167	--	--	--	.52
367	1.44	1.29	1.34	.88
720	--	--	--	--
762	--	--	--	1.22
68	--	2.10	2.68	1.14
205	1.41	1.73	1.56	.68
352	.62	.62	.62	.62
424	--	--	--	.48
Totals	1.07	1.03	1.03	.75
Variance	.5920 N=10	.2718 N=12	.3478 N=12	.1113 N=18

Contrails

TABLE XXXII

Damage Prediction Ratios for Mach-Altitude Probability Model
Based on Last 114 F-105D Configuration 3 Pull-ups

A/C	Peaks 1084-1198	Peaks 971-1198	Peaks 857-1198	Peaks 1-1198
	<u>Predicted Damage</u> Actual Damage	<u>Predicted Damage</u> Actual Damage	<u>Predicted Damage</u> Actual Damage	<u>Predicted Damage</u> Actual Damage
<u>Fuselage Station 509</u>				
130	2.57	1.70	1.70	.60
132	1.05	.27	.45	.55
357	.82	.95	.95	.95
422	.53	1.23	1.11	1.29
160	----	----	----	.79
240	----	.89	.89	1.02
378	----	.80	.77	.71
469	----	----	----	.94
731	1.46	1.46	1.46	1.46
732	3.24	1.26	1.31	1.29
69	----	----	----	.60
167	.69	.74	.74	.74
367	1.94	1.42	1.60	1.17
720	----	----	----	----
762	2.69	2.69	2.69	2.69
68	1.01	.89	1.03	1.40
205	.88	.95	.85	.99
352	----	----	----	.08
424	----	.68	.68	.68
Totals	1.05	.87	.86	.85
Variances	.8657 N=11	.3354 N=14	.3257 N=14	.2999 N=18
<u>Fuselage Station 442</u>				
130	1.69	1.50	1.50	.68
132	.69	.25	.47	.60
357	.87	.93	.93	.93
422	.81	1.66	1.38	1.62
160	----	----	----	1.23
240	----	.95	1.21	1.07
378	----	1.02	.93	.92
469	----	----	----	.96
731	1.50	1.51	1.51	1.51
732	1.80	.98	1.01	1.34
69	----	----	----	.61
167	.67	.69	.69	.69
367	1.60	1.20	1.30	1.21
720	----	----	----	----
762	1.37	1.37	1.37	1.37
68	.86	1.08	1.24	1.60
205	.63	.69	.69	.92
352	----	----	----	.20
424	----	.68	.68	.68
Totals	.96	.95	.93	.95
Variances	.2076 N=11	.1520 N=14	.1161 N=14	.1547 N=18

TABLE XXXIII

Comparison of Damage Ratios and Variance for
Four Mach-Altitude Probability Models

A/C	Mach-Altitude Probability Models			
	Group I	Total	First 114	Last 114
<u>Fuselage Station 509</u>				
130	1.00	.91	.72	.60
132	1.07	.84	.31	.55
357	.91	.78	.65	.95
422	1.29	1.11	.94	1.29
160	2.12	2.07	1.79	.79
240	1.37	1.12	.73	1.02
378	1.20	1.05	.70	.71
469	1.00	.84	.65	.94
732	1.50	1.25	.90	1.29
69	.86	.72	.46	.60
367	1.51	1.24	.79	1.17
68	2.07	1.67	.94	1.40
205	1.02	.87	.71	.99
Variance	.1684	.1483	.1215	.0814
<u>Fuselage Station 442</u>				
130	.86	.76	.61	.68
132	.96	.77	.43	.60
357	.87	.77	.68	.93
422	1.58	1.40	1.21	1.62
160	2.20	2.04	1.68	1.23
240	1.34	1.13	.83	1.07
378	1.27	1.08	.76	.92
469	.96	.86	.74	.96
732	1.41	1.22	1.00	1.34
69	.79	.68	.49	.61
367	1.40	1.18	.88	1.21
68	2.07	1.70	1.14	1.60
205	.95	.82	.68	.92
Variance	.2078	.1667	.1140	.1133

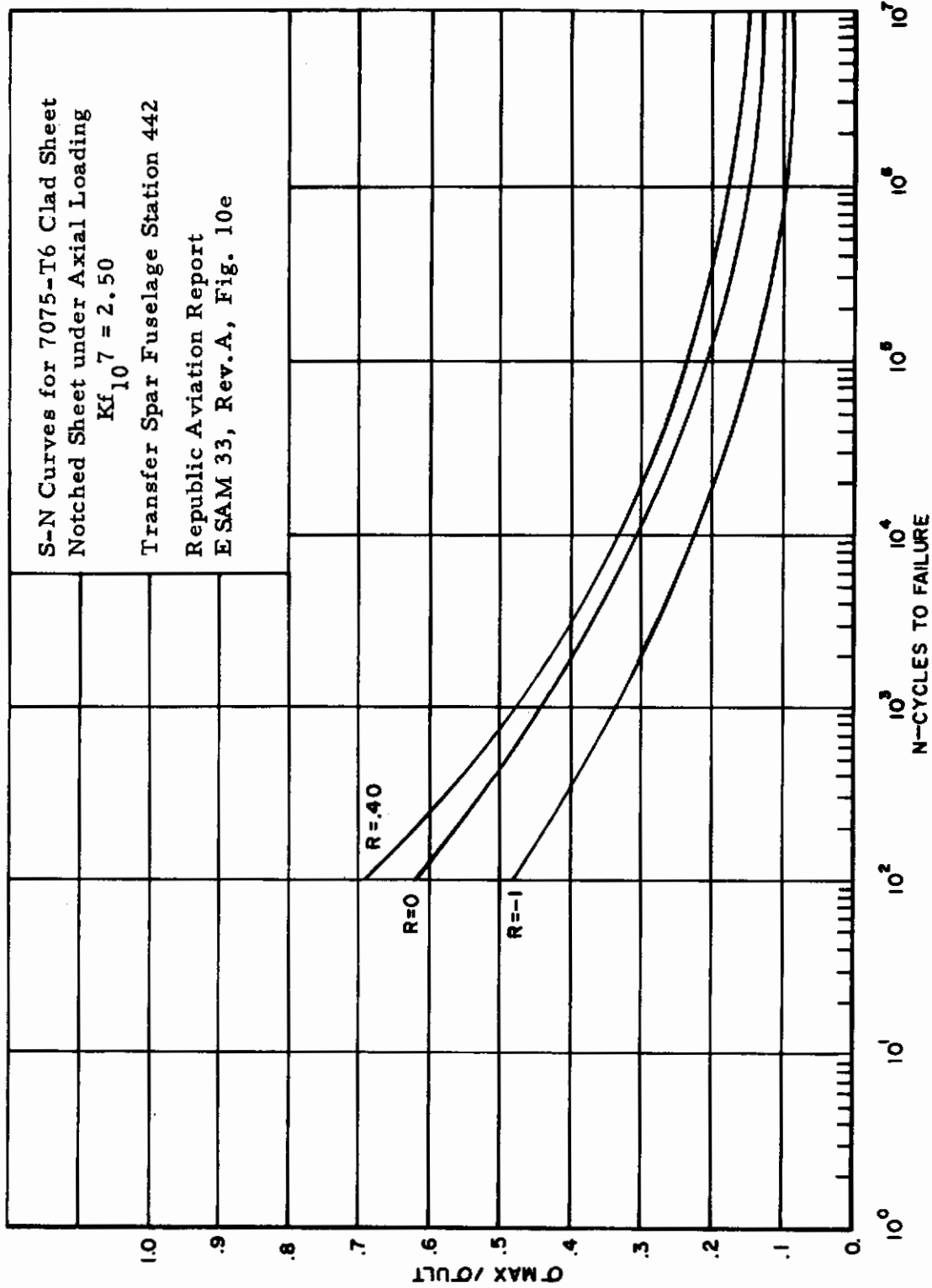


Figure 4 S-N Curves for 7075-T6 Clad Sheet Notched Sheet under Axial Loading
 $Kf_{10} = 2.50$

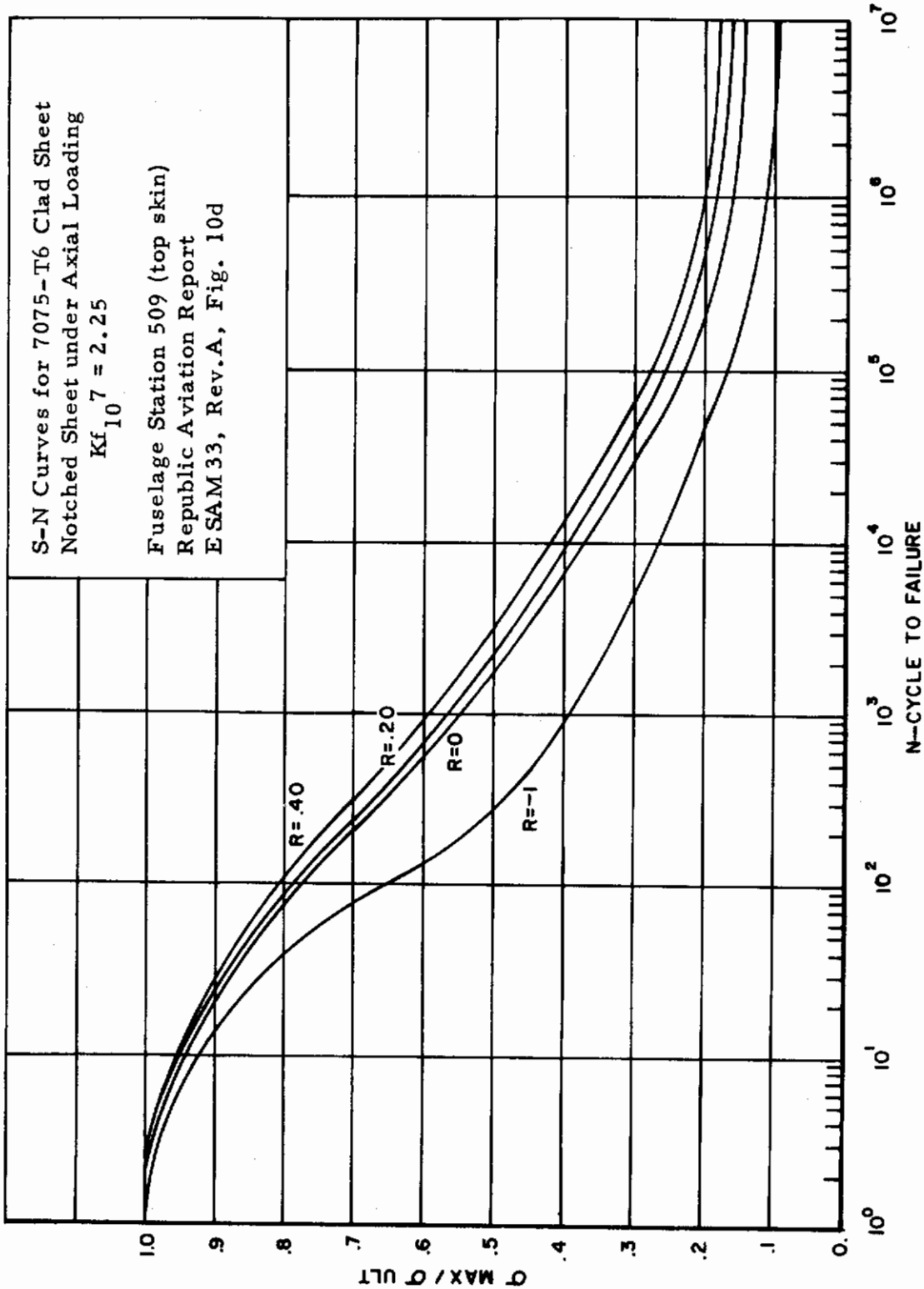


Figure 5 S-N Curves for 7075-T6 Clad Sheet Notched Sheet under Axial Loading
 $Kf_{10} = 2.25$

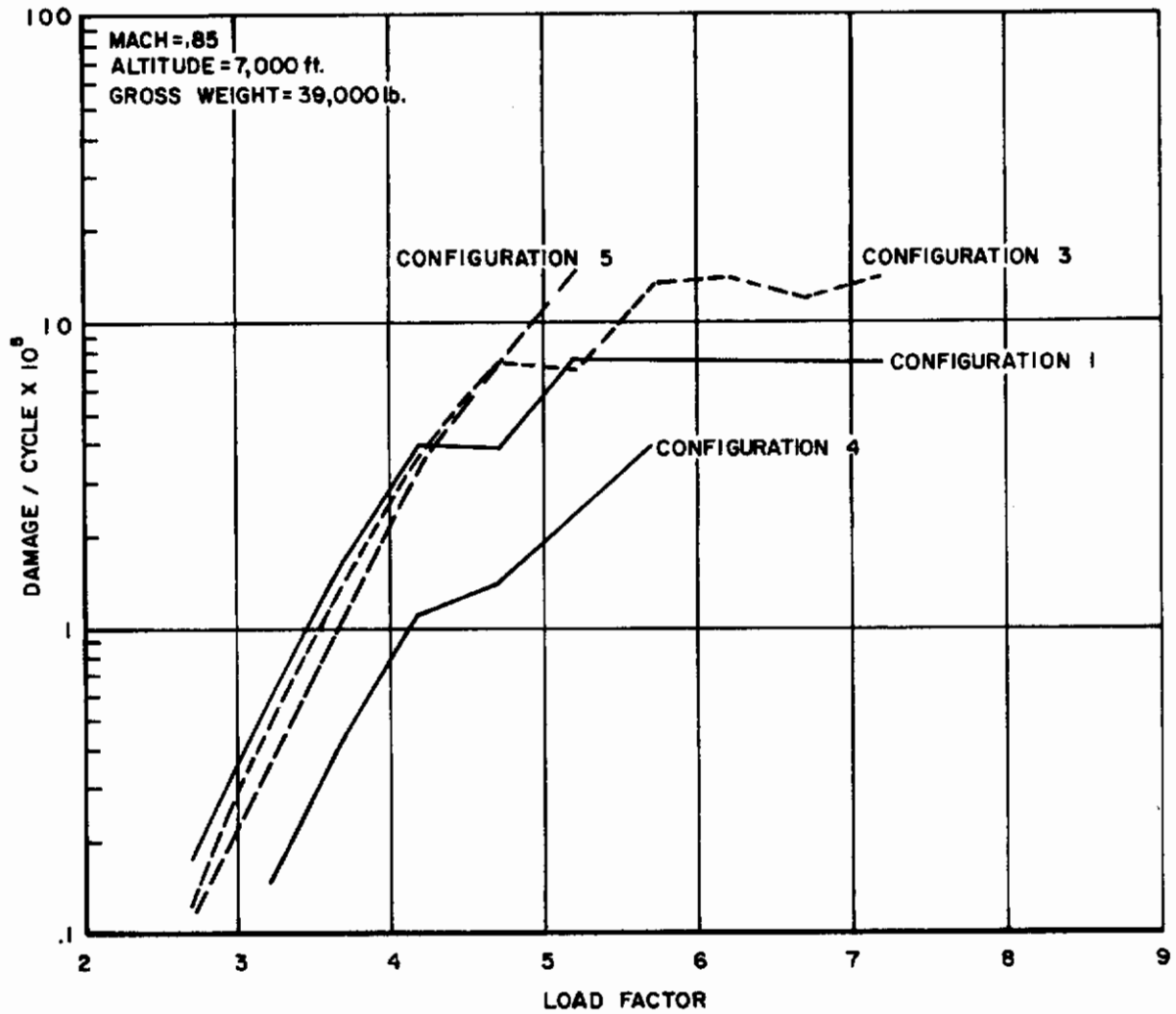


Figure 6 Damage per Cycle vs Load Factor by Configuration for the F-105D Transfer Spar at Fuselage Station 442

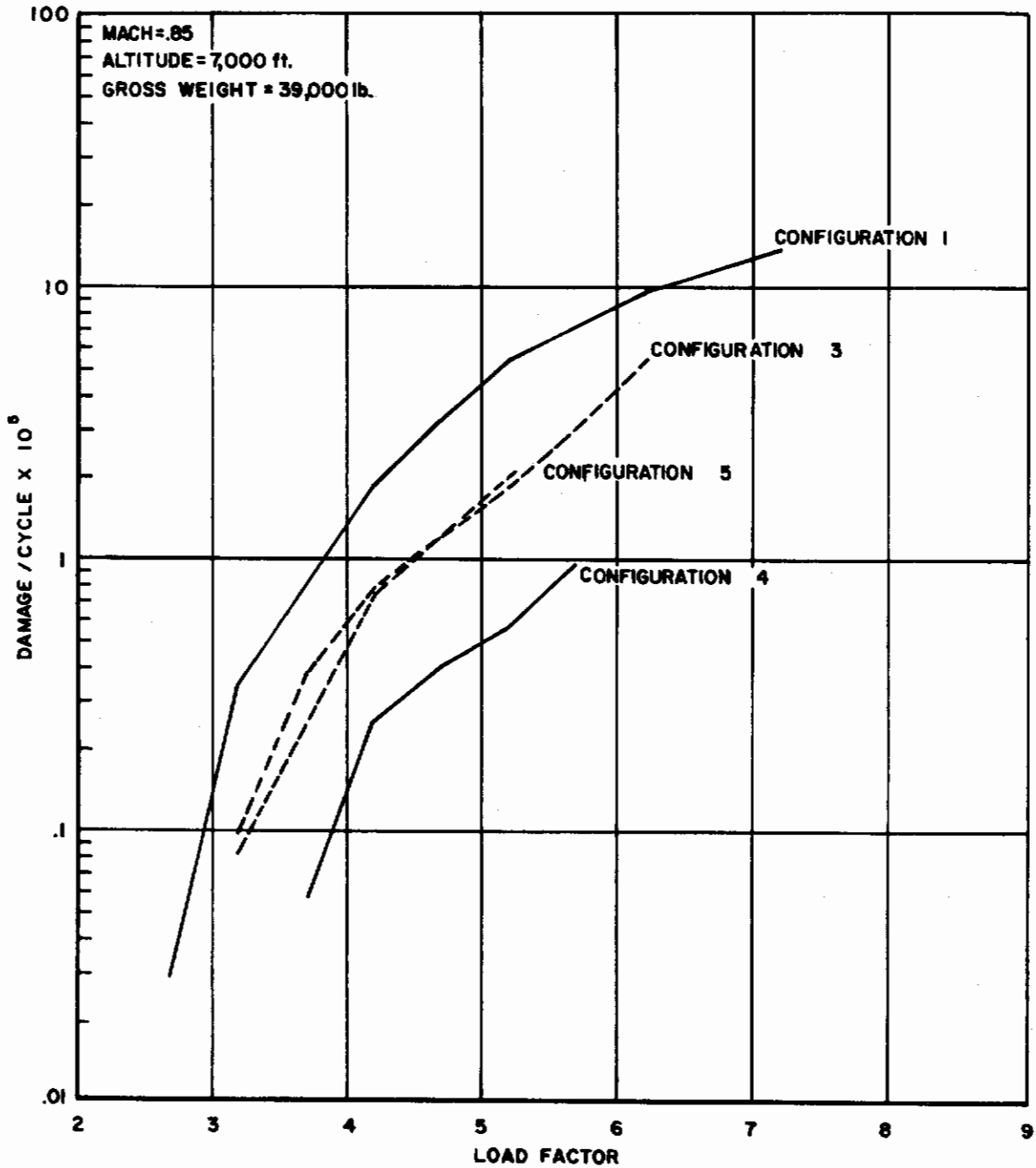


Figure 7 Damage per Cycle vs Load Factor by Configuration for the F-105D Top Cover Skin at Fuselage Station 509

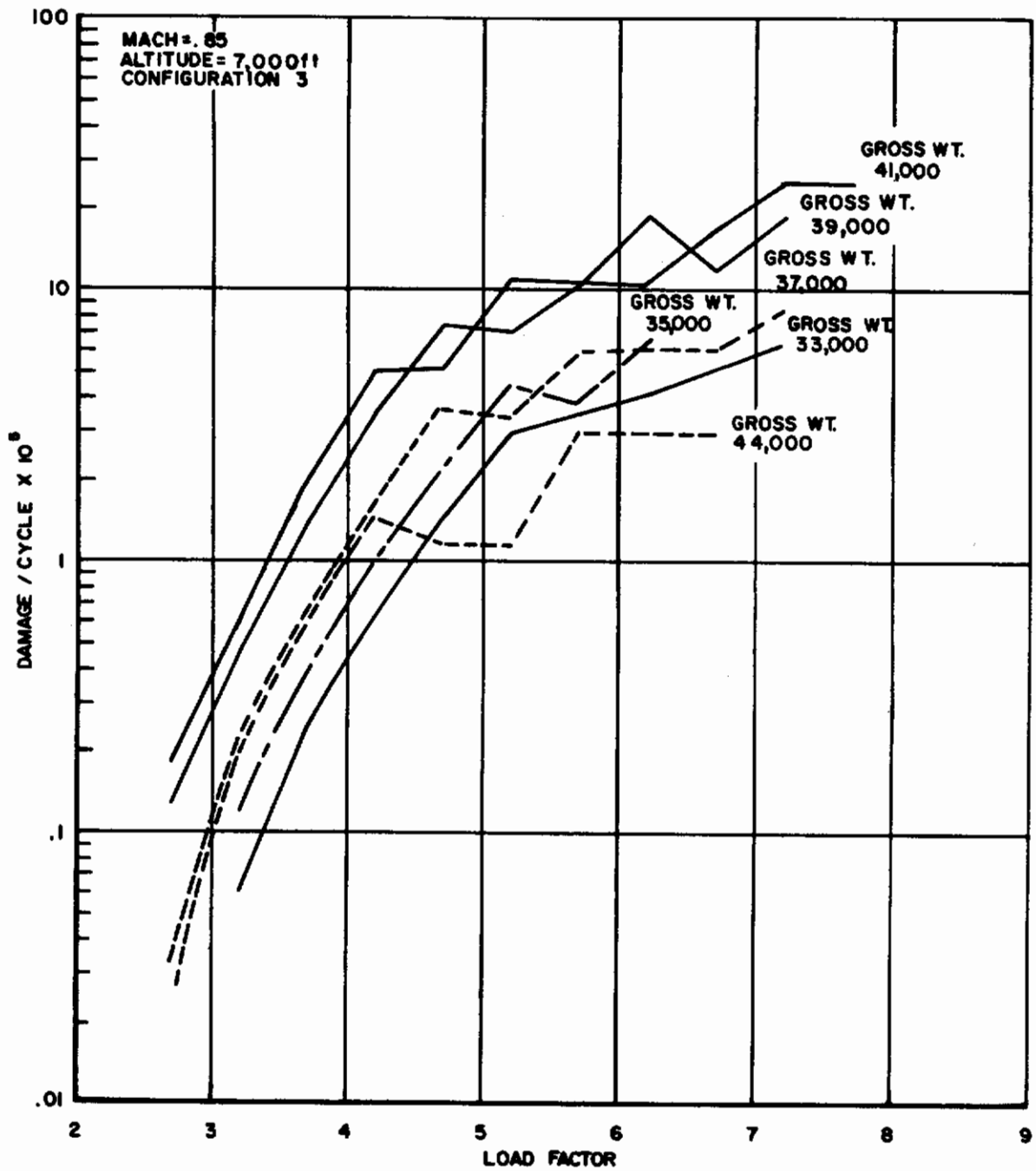


Figure 8 Damage per Cycle vs Load Factor by Gross Weight for the F-105D Transfer Spar at Fuselage Station 442

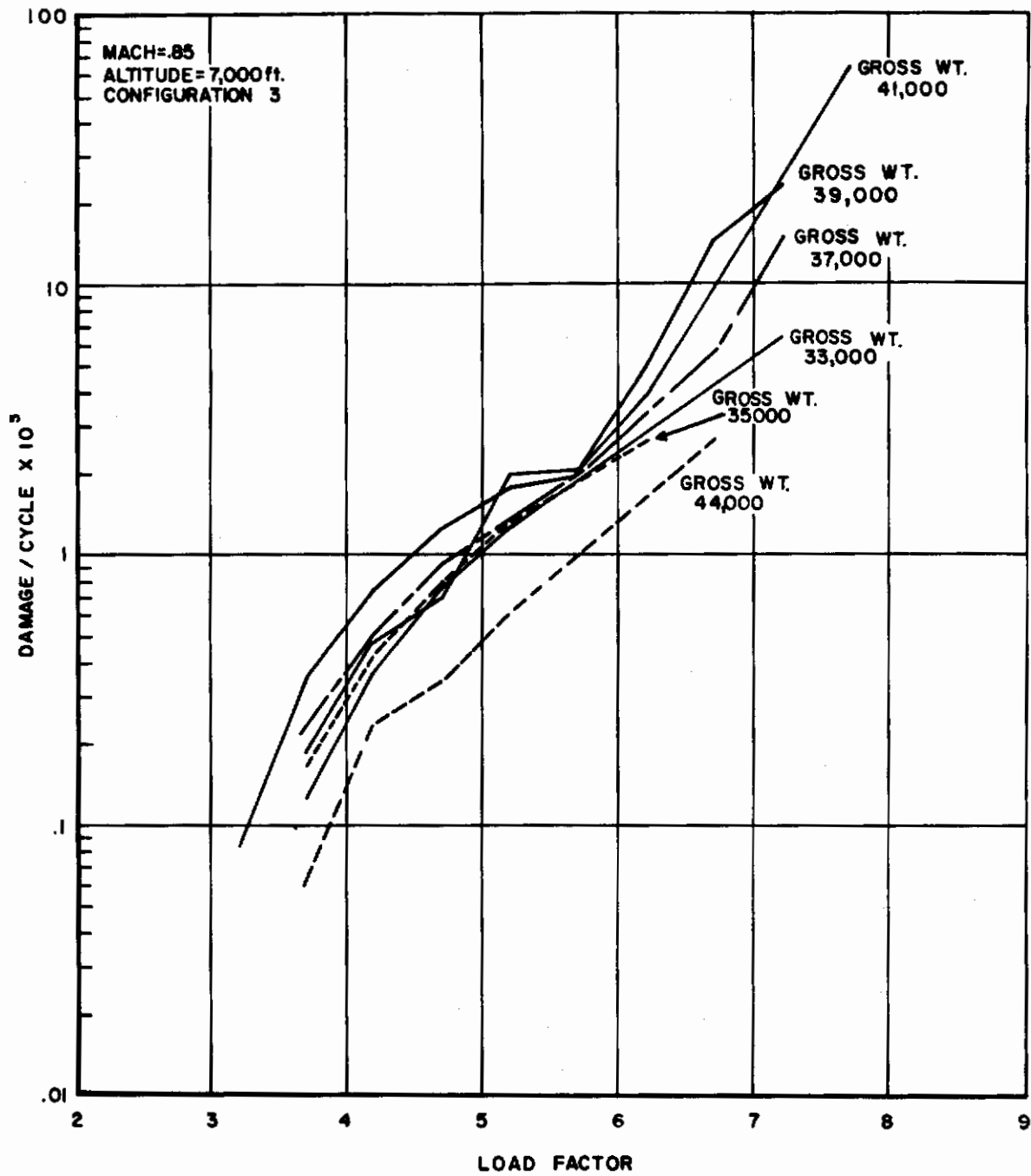


Figure 9 Damage per Cycle vs Load Factor by Gross Weight for the F-105D Top Cover Skin at Fuselage Station 509

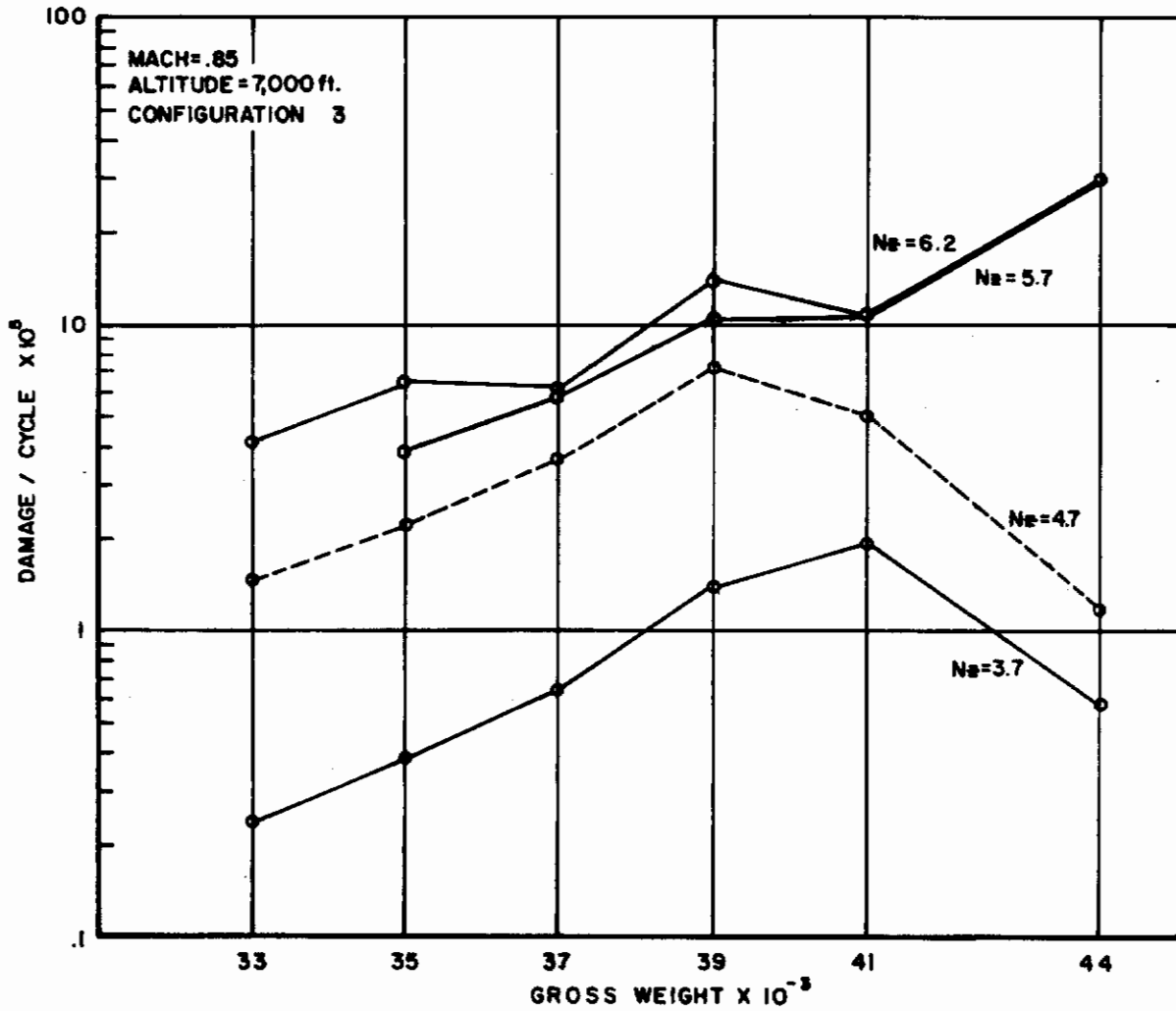


Figure 10 Damage per Cycle vs Gross Weight by Load Factor for the F-105D Transfer Spar at Fuselage Station 442

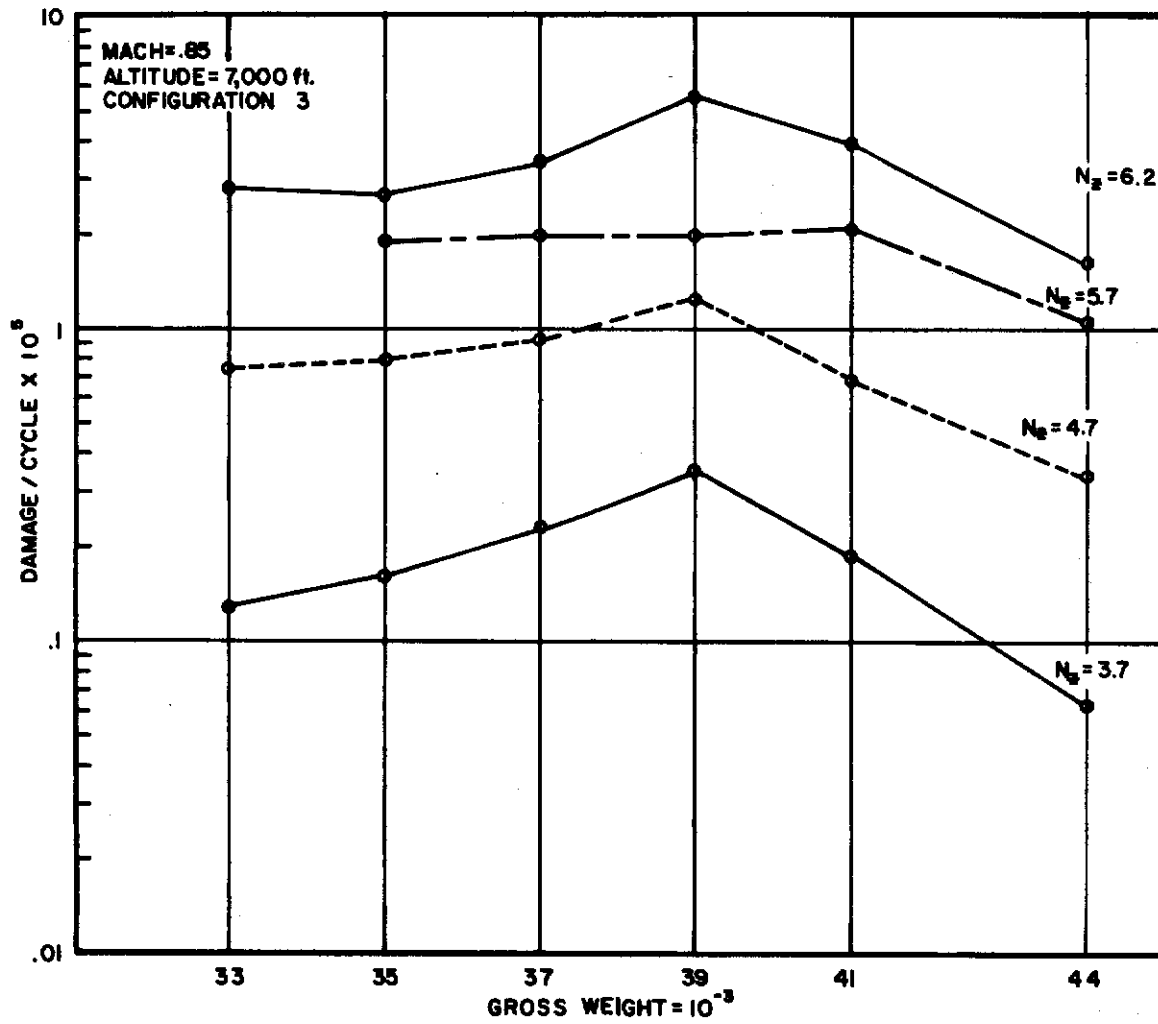


Figure 11 Damage per Cycle vs Gross Weight by Load Factor for the Top Cover Skin at Fuselage Station 509

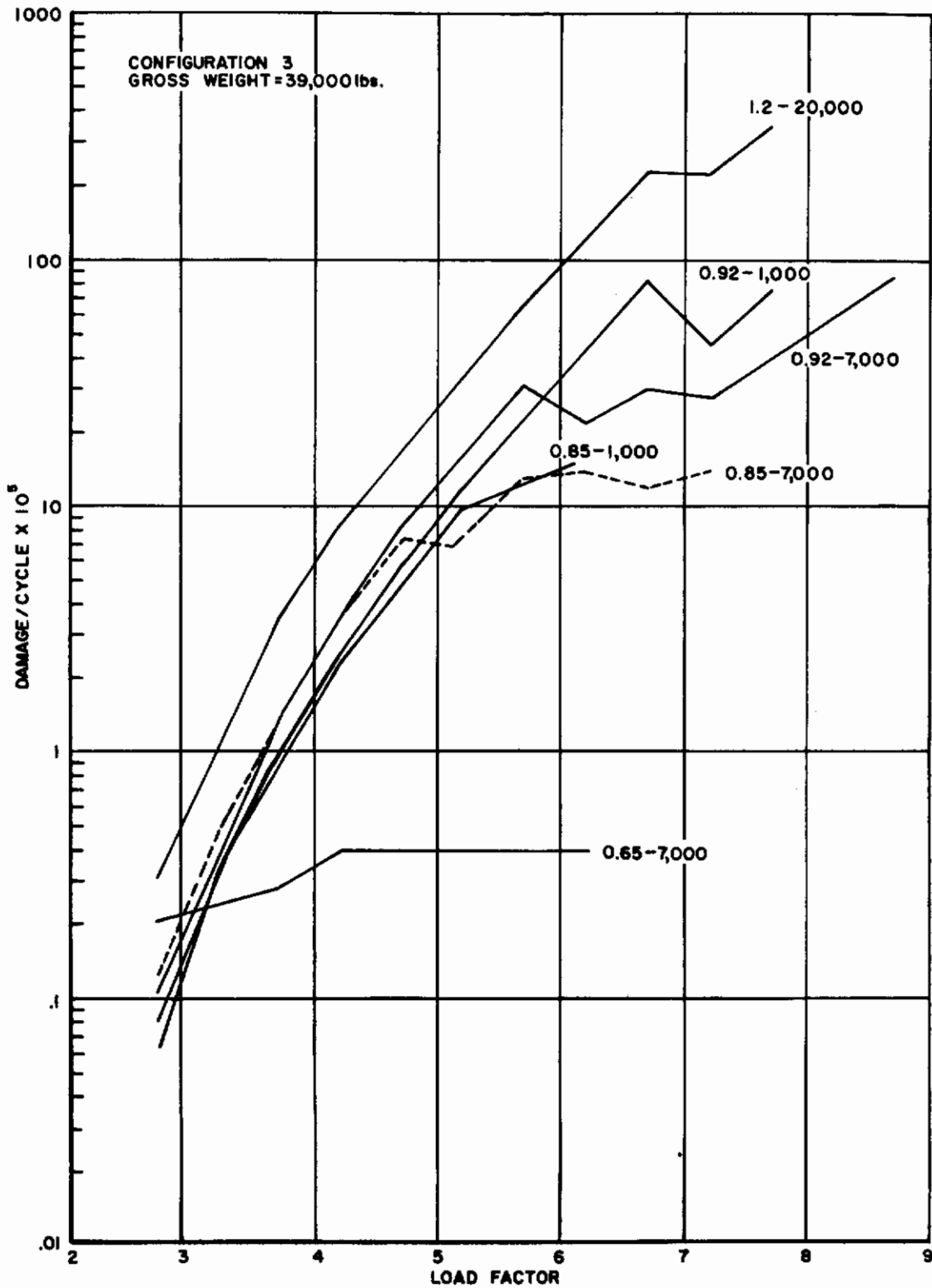


Figure 12 Damage per Cycle vs Load Factor by Mach-Altitude Condition for the F-105D Transfer Spar at Fuselage Station 442

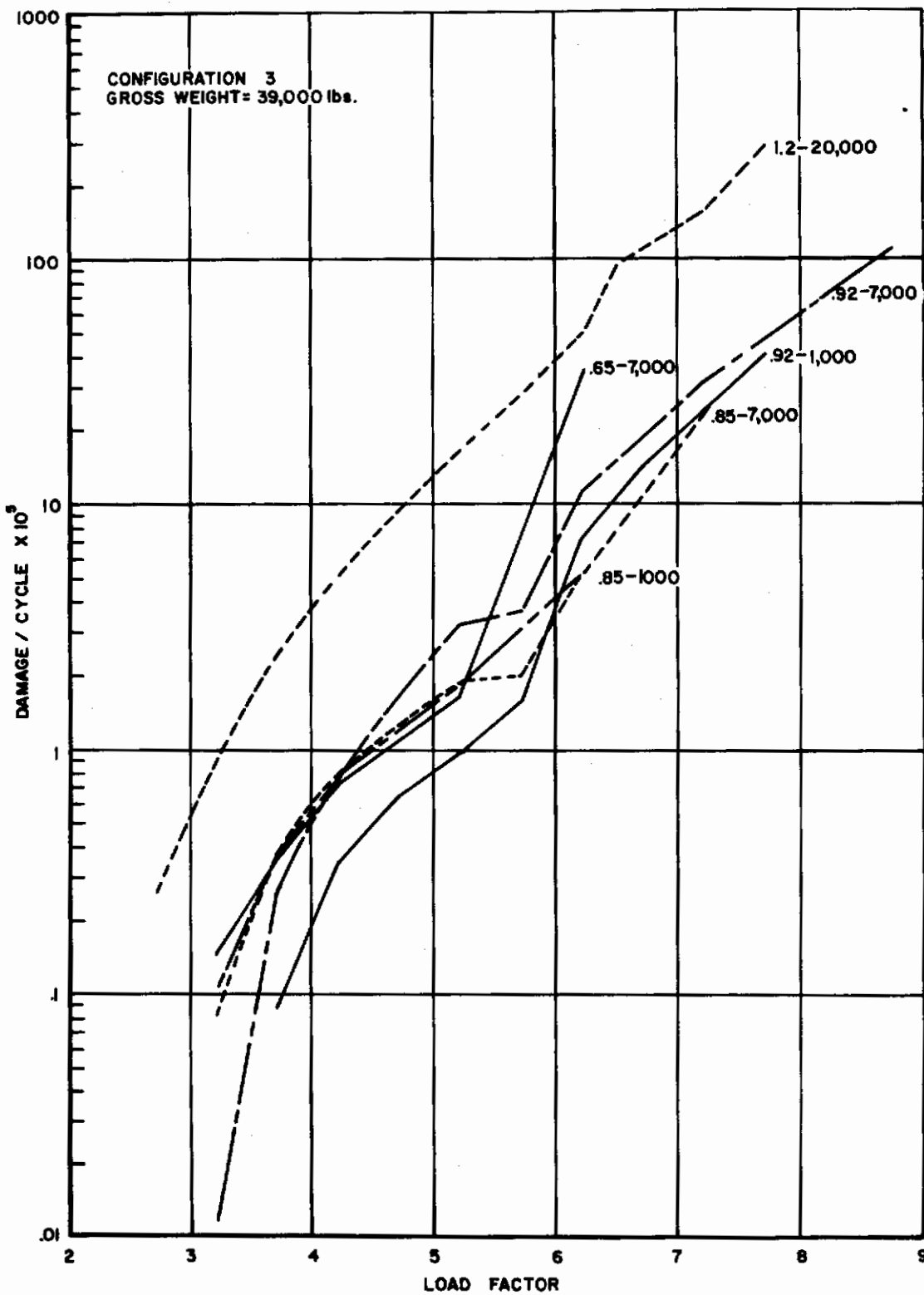


Figure 13 Damage per Cycle vs Load Factor by Mach-Altitude Condition for the F-105D Top Cover Skin at Fuselage Station 509

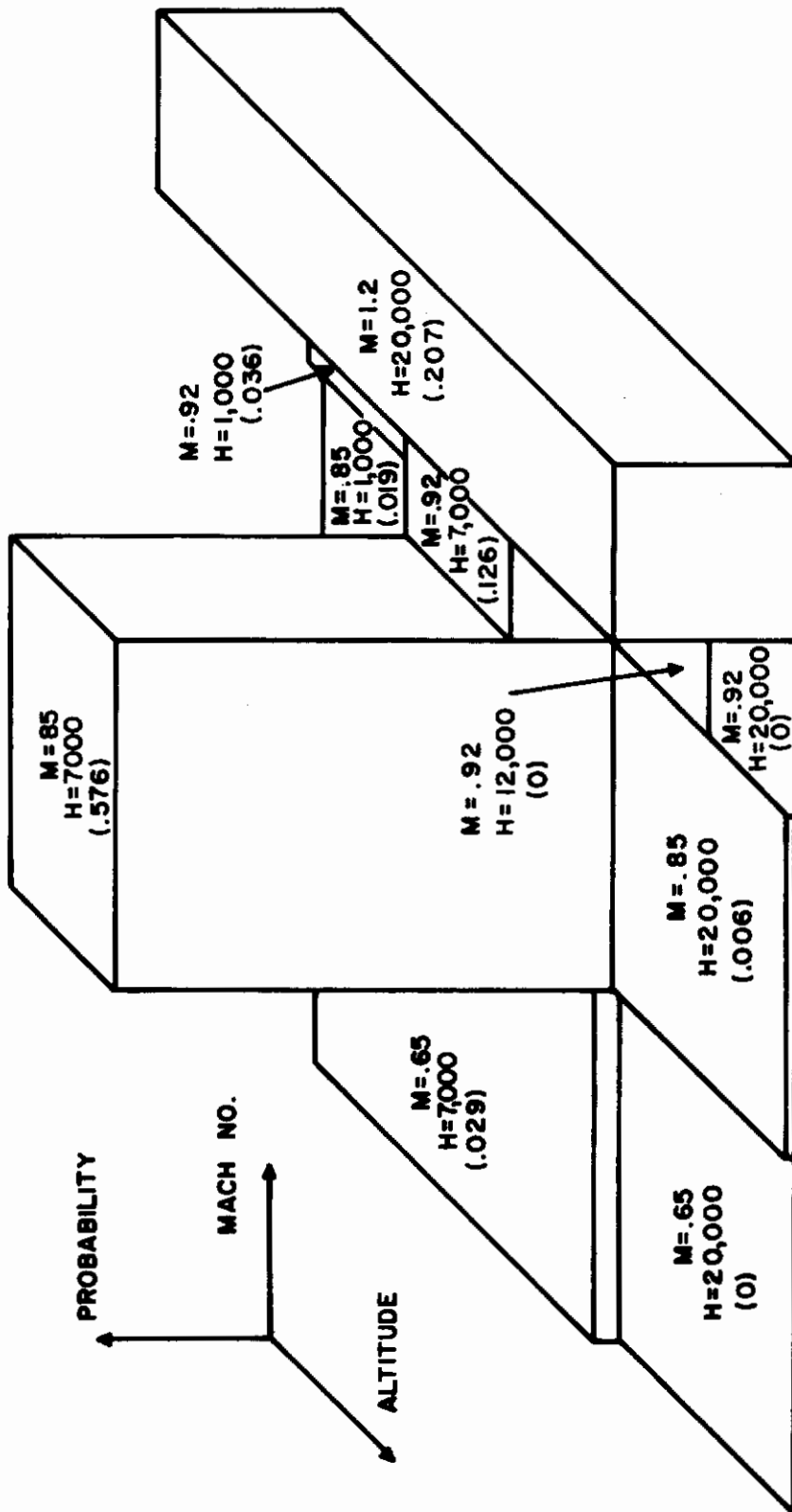


Figure 14 Mach-Altitude Probability Plot for F-105D Pull-up After Weapon Release, Configuration 3, Group 1 Data

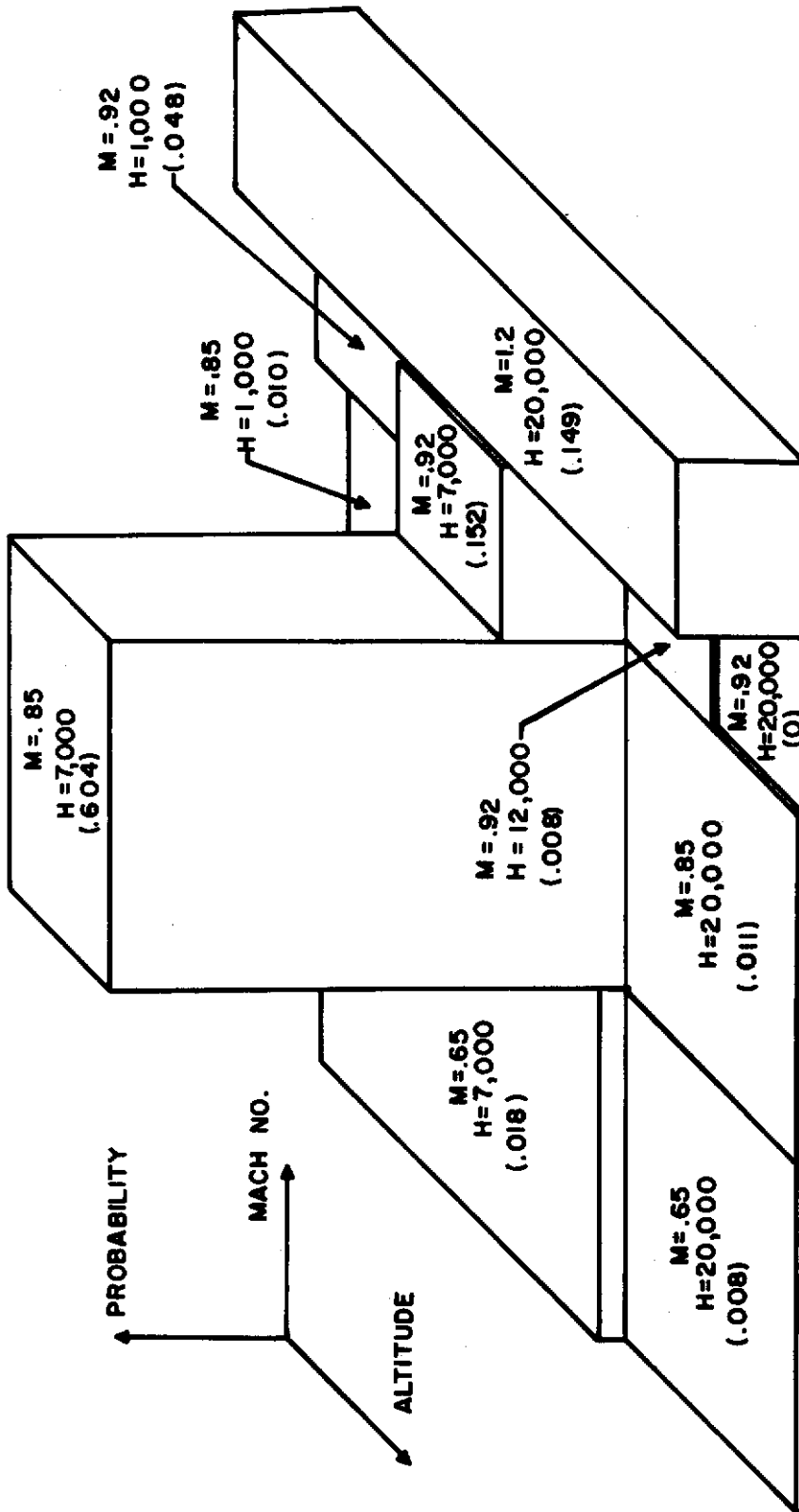


Figure 15 Mach-Altitude Probability Plot for F-105D Pull-up after Weapon Release, Configuration 3 Data

Contrails

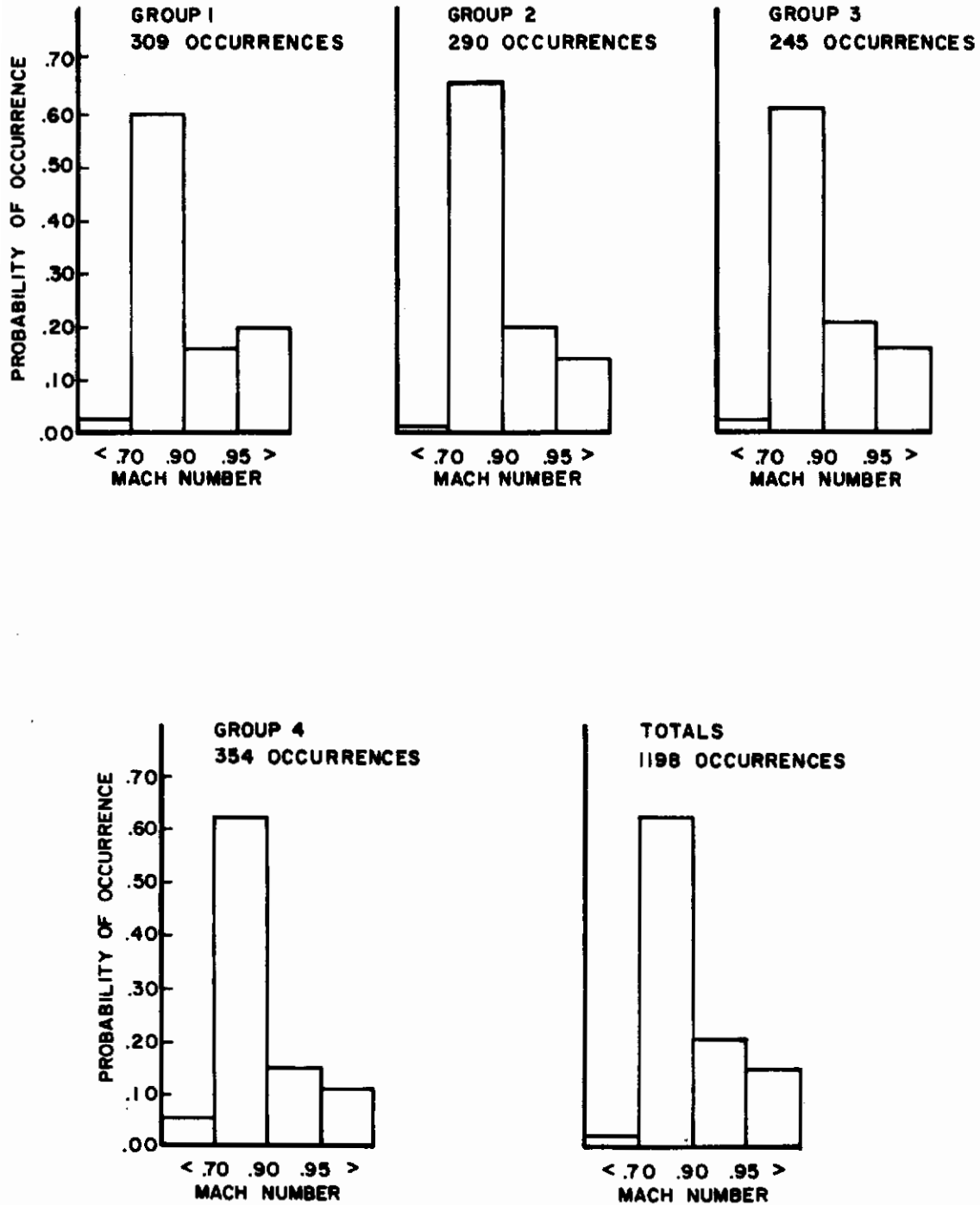


Figure 16 Mach Number Probability by Group for F-105D Pull-up after Weapon Release, Configuration 3 Data

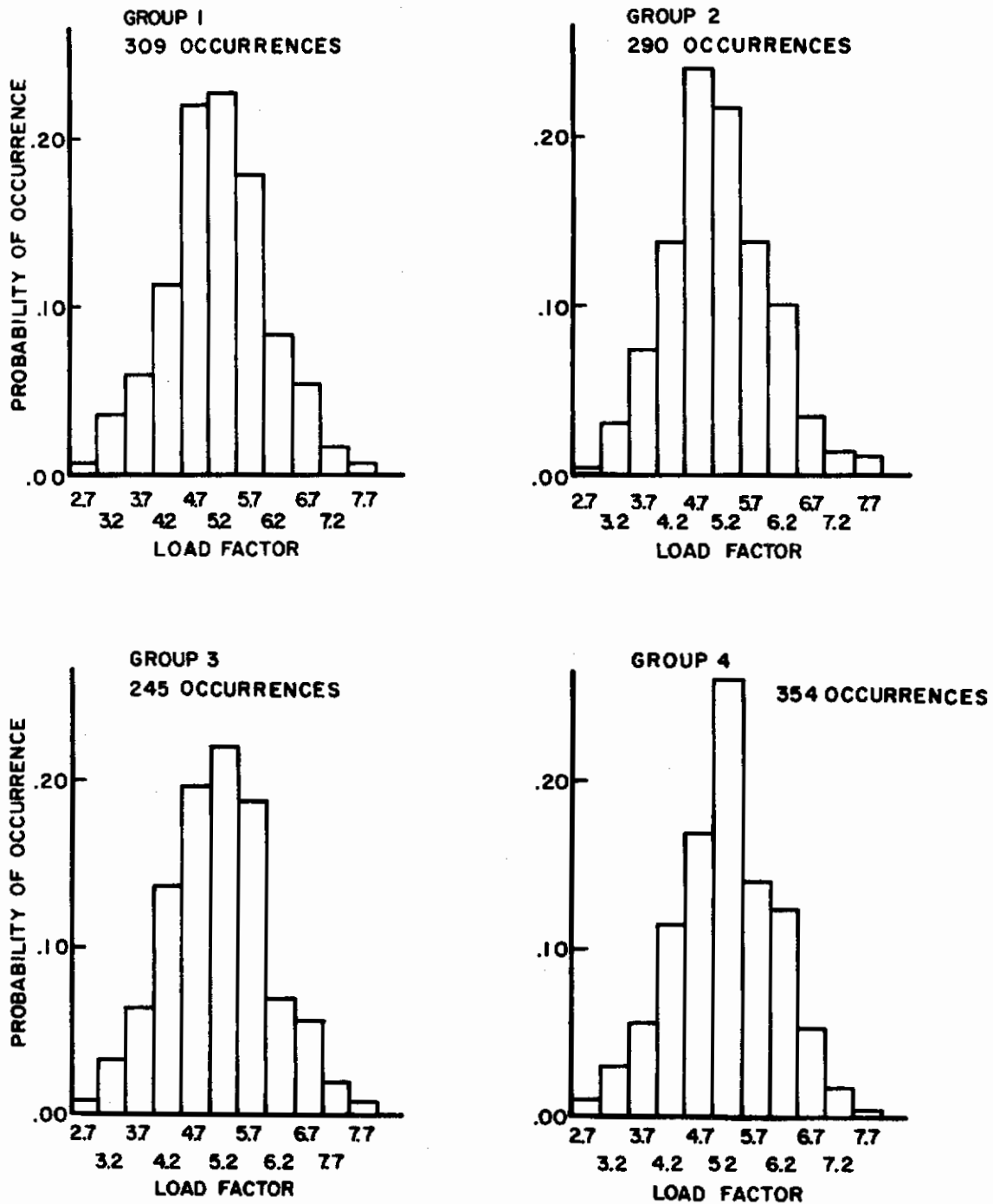


Figure 17 Load Factor Probability by Group for F-105D Pull-up After Weapon Release, Configuration 3 Data

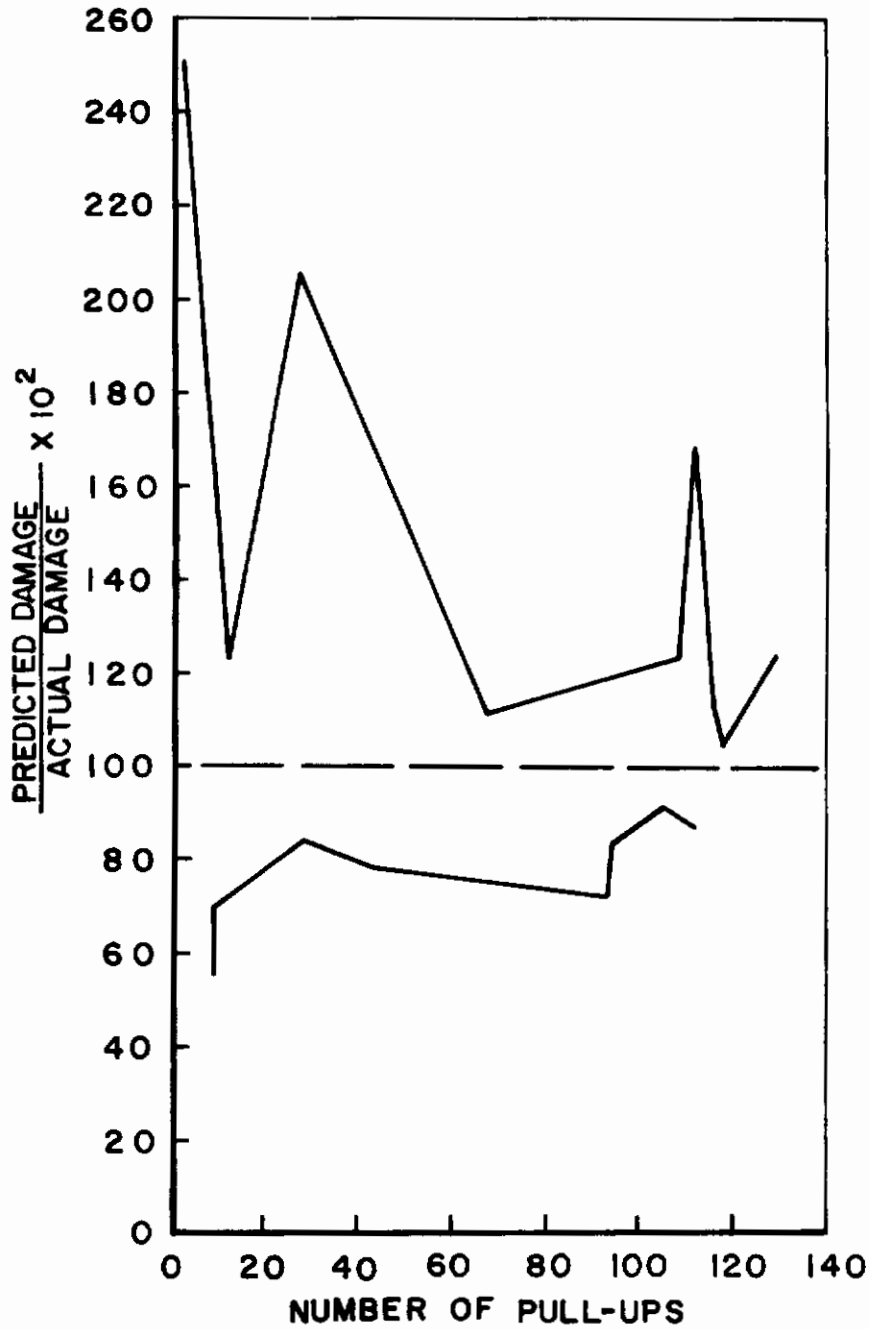


Figure 18 Damage Ratio vs Pull-up Sample Size for Mach-Altitude Probability Damage Prediction Technique Probability Model Based on Total Configuration 3 Pull-ups, Top Skin at Fuselage Station 509 Damage ratios from Table XXI

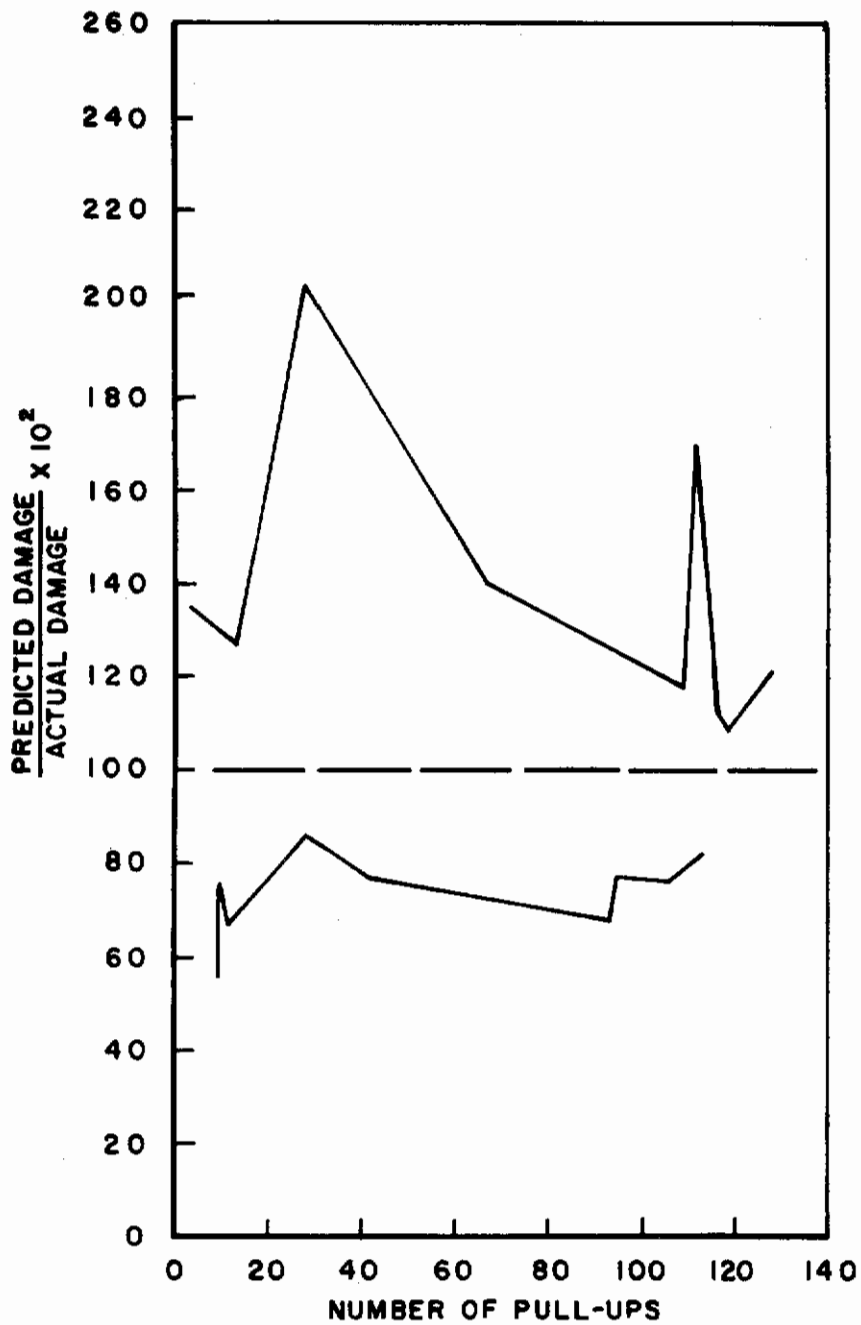


Figure 19 Damage Ratio vs Pull-up Sample Size for Mach-Altitude Probability Damage Prediction Technique
Probability Model based on Total Configuration 3 Pull-ups, Transfer Spar at Fuselage Station 442
Damage ratios from Table XXII

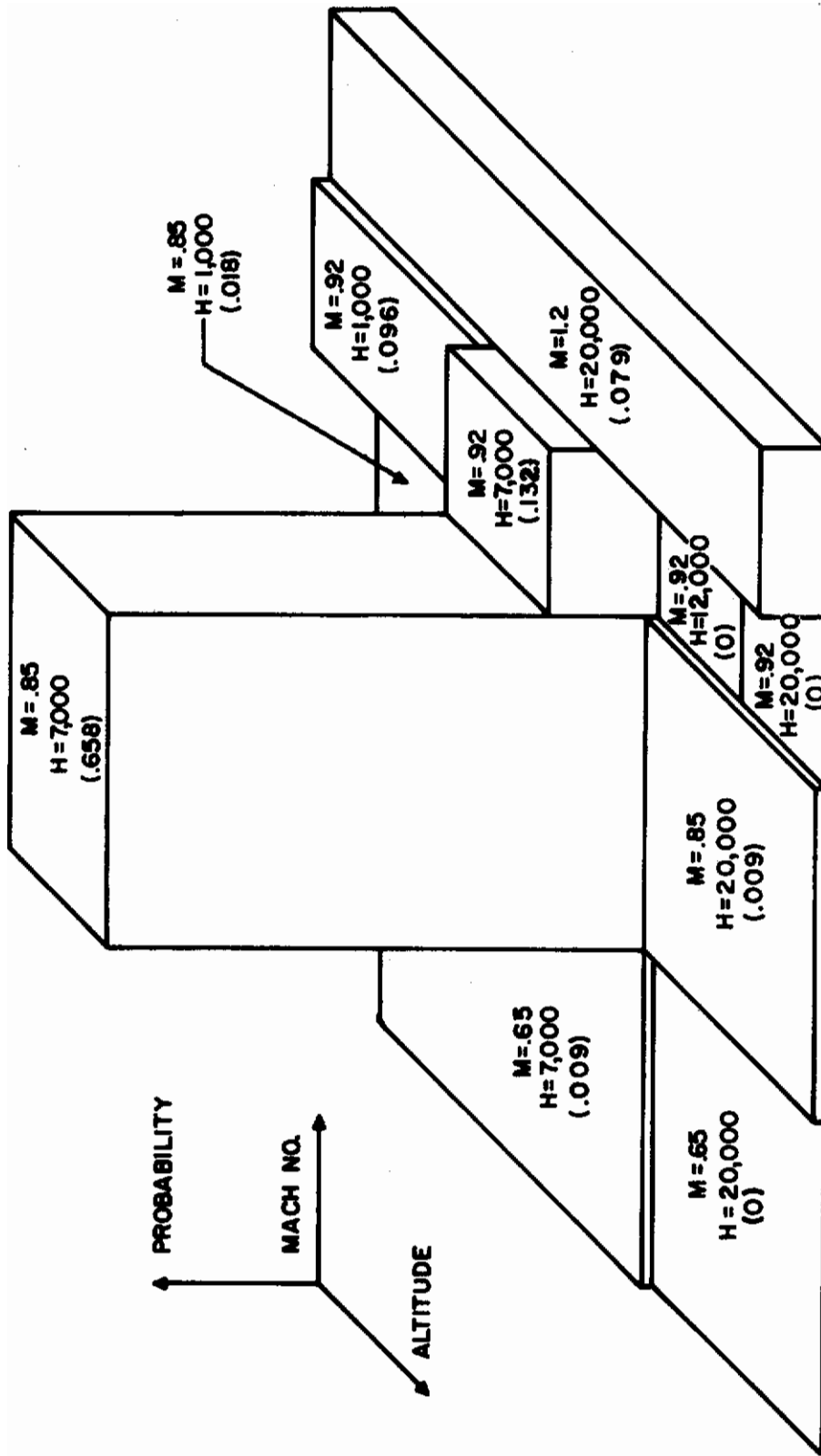


Figure 20 Mach-Altitude Probability Plot for First 114 F-105D Pull-ups after Weapon Release, Configuration 3 Data

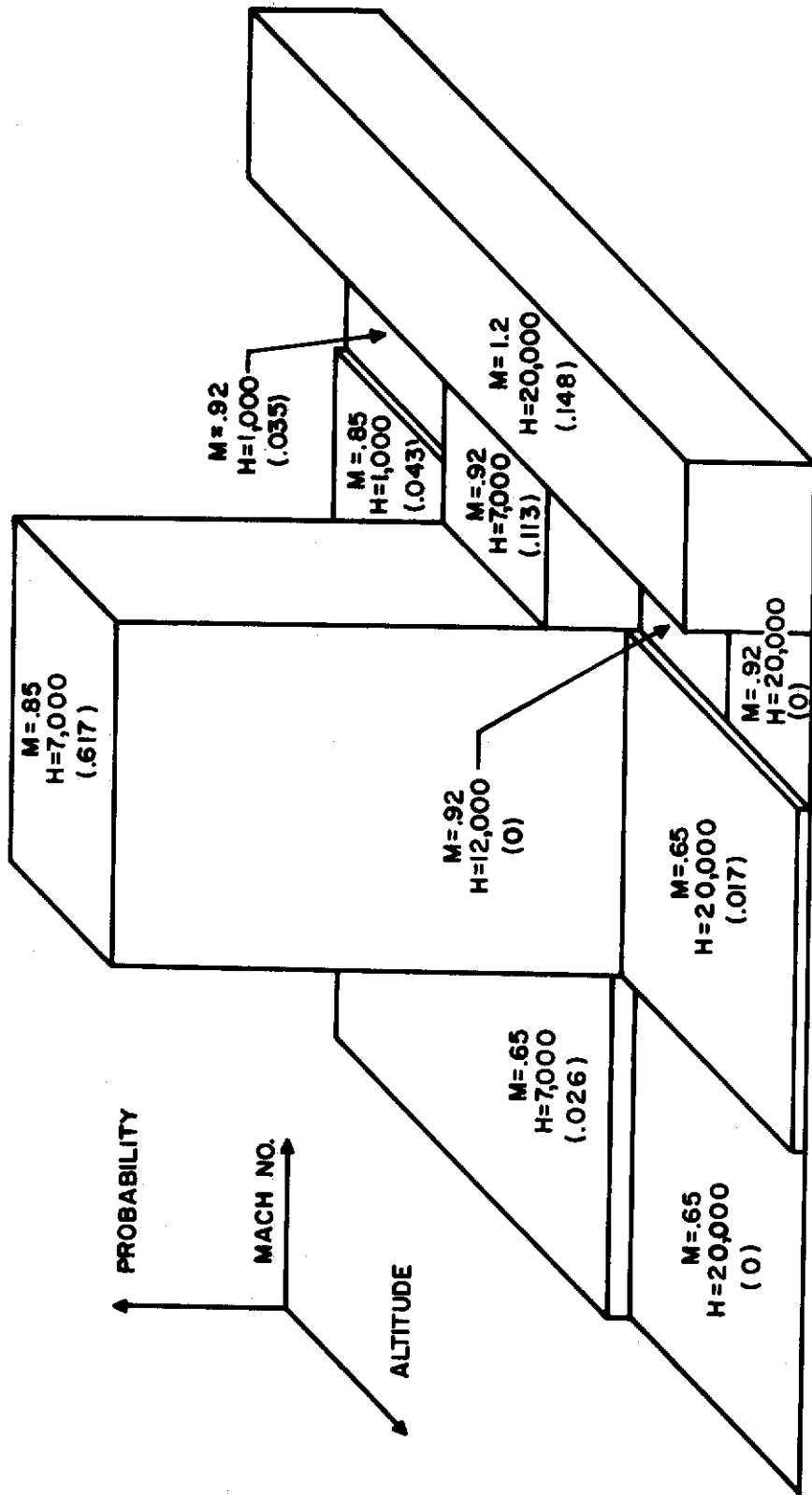


Figure 21 Mach-Altitude Probability Plot for Last 114 F-105D Pull-ups after Weapon Release, Configuration 3 Data

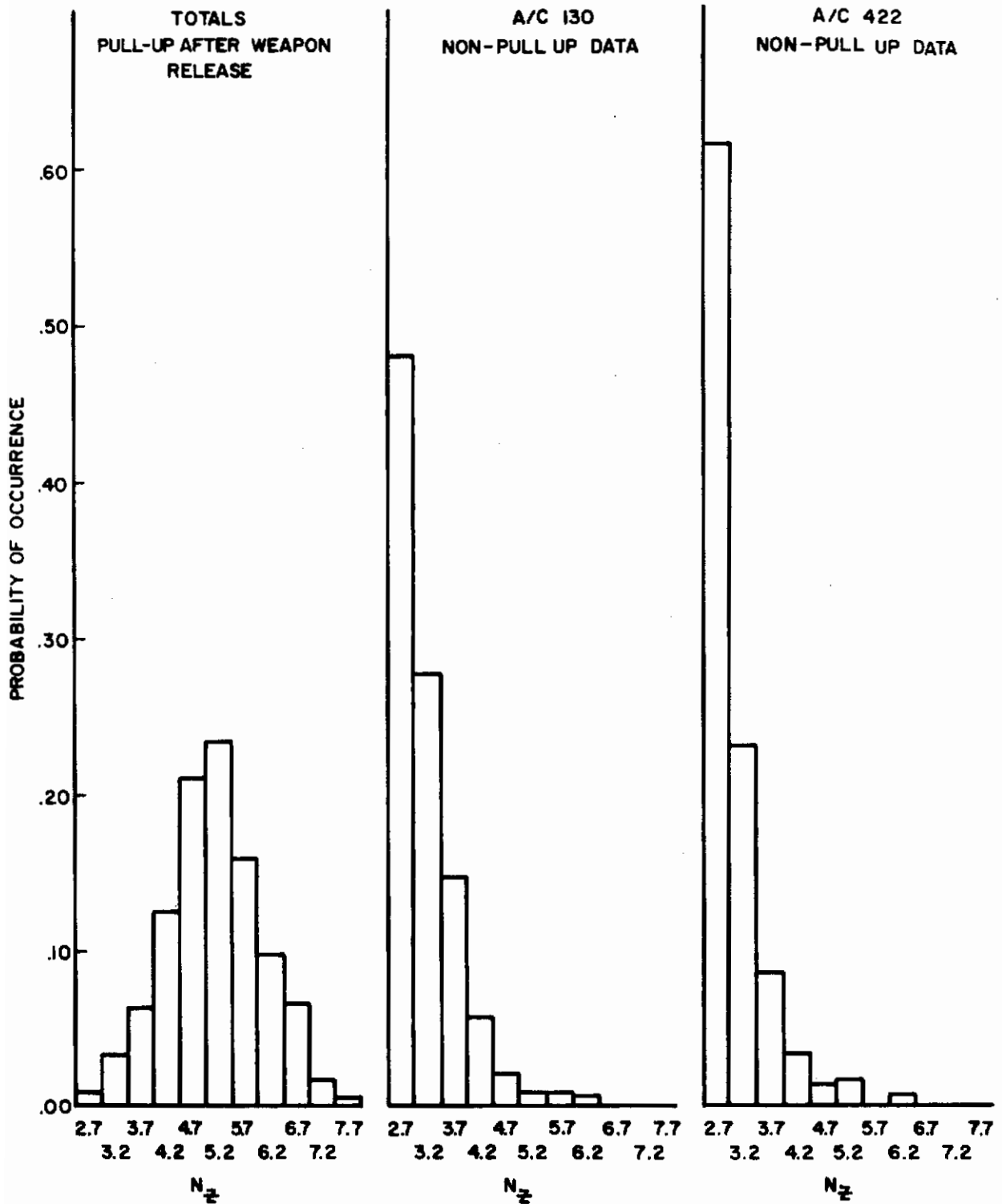
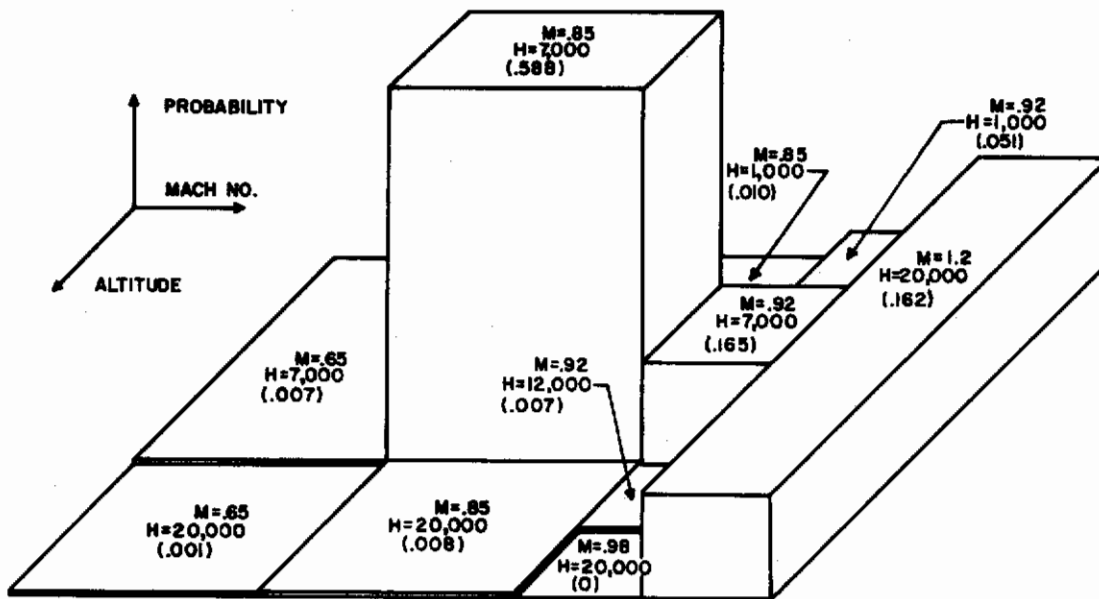


Figure 22 Comparison of Probability of Occurrence by Load Factor for F-105D, Configuration 3 Pull-up and Non Pull-up Data

LOAD FACTOR RANGE
 $4.2 \leq N_z \leq 7.7$
 1074 OCCURRENCE



LOAD FACTOR RANGE
 $2.7 \leq N_z \leq 3.7$
 124 OCCURRENCES

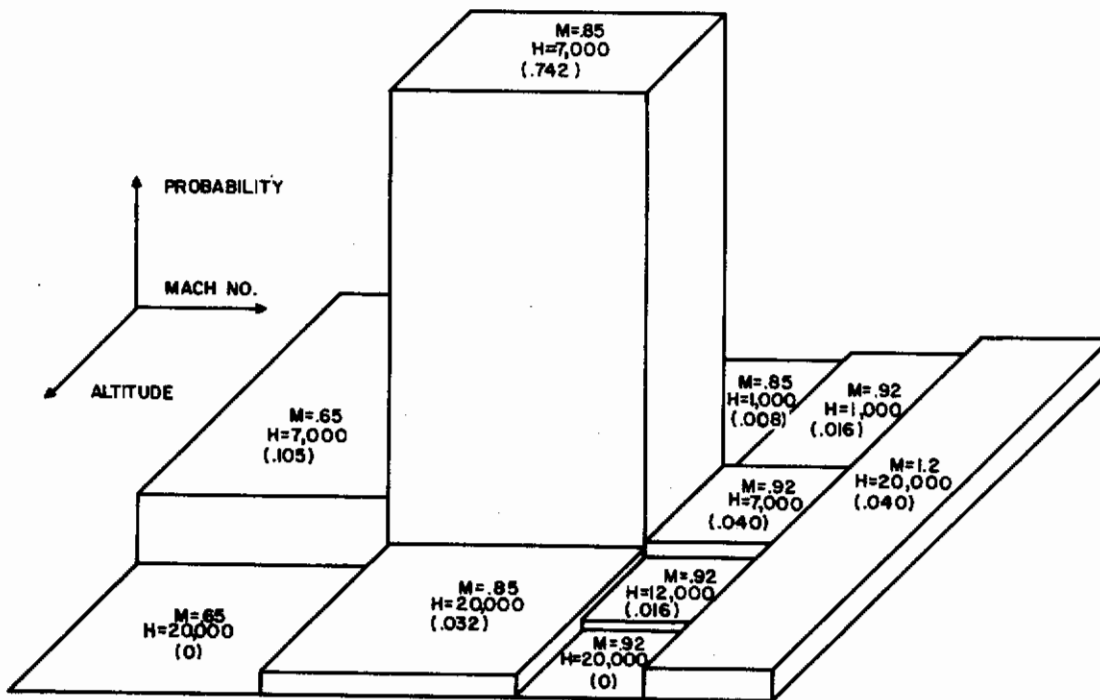
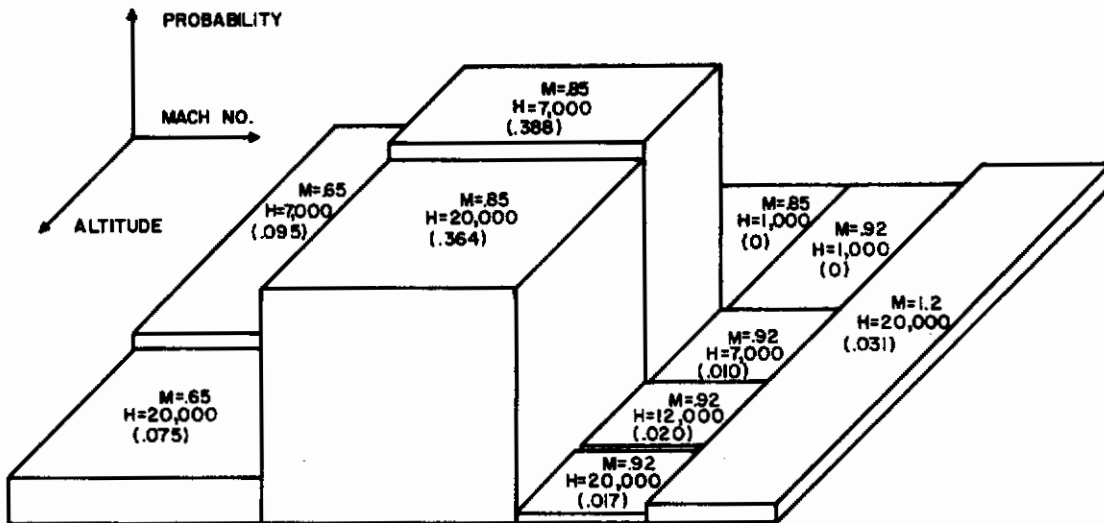


Figure 23 Mach-Altitude Probability Plot by Load Factor Magnitude for F-105D Pull-up after Weapon Release, Configuration 3 Data

A/C 422
294 OCCURRENCES
ALL N₂



A/C 130
357 OCCURRENCES
ALL N₂

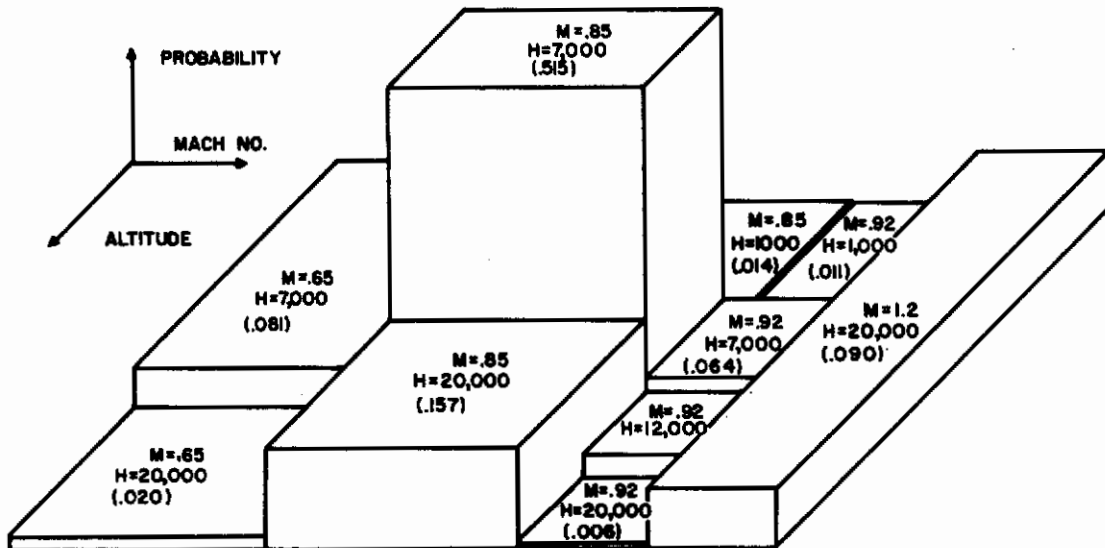


Figure 24 Mach-Altitude Probability Plot for F-105D Non Pull-up, Configuration 3 Data for Two Typical Aircraft

3. F-105F AIRCRAFT

a. Comparison With F-105D Aircraft Analysis

The analysis of the F-105F aircraft was performed using the same basic ground-rules as were employed in the analysis of the F-105D reported in Section II-2 of this report. There are some differences in the basic aircraft as well as differences in the data collection and reduction criteria. These differences, together with assumptions that were made with regard to the following analysis are enumerated below:

(1) The F-105F is a two-place aircraft, whereas the F-105D aircraft is a one-place aircraft. In the absence of stress versus load factor data for the F-105F, the F-105D data was used with the actual F-105F gross weights.

(2) The Mach-altitude subdivisions shown in Table VI of Section II-2 were used for computing fatigue damages to the F-105F.

(3) There was a difference in the criteria used to define the maneuver mission segment for the two flightloads programs, on which the F-105D and F-105F data samples were obtained.

(4) There was a significant variation of the data with respect to mission type for the F-105F data sample. Therefore, it was necessary to consider this additional variable in the F-105F parametric fatigue analysis.

b. Fatigue Damage Analysis

The fatigue damage analysis reported herein is based on a 1,001 hour VGH data sample obtained at two air bases in the Southeast Asia combat zone and reported in Reference 7. This data was recorded on 456 flights. The fatigue damage was calculated for the same fatigue critical locations as were monitored for the F-105D and the remarks with regard to damage calculation, major configuration, Mach-altitude block designation, gross weight and load factor classification contained in Section II-2a of this report are applicable.

(1) Parametric Analysis

The damage sensitivity studies reported in Section II-2a(1) apply to this F-105F analysis. The classification of the data with respect to mission type is defined in Reference 7 and presented in Table XXXIV of this report. The classification of the processed data by mission type and air base is presented in Table XXXV. There is considerable variation in the amount of data recorded by both mission type and air base.

(2) Damage Analysis by Mission Segment

The airborne portion of the flight was classified into the mission segments of ascent, maneuver, cruise, refuel, and descent. Damage was computed for each of the load factor occurrences greater than 2.5 g's by mission

segment. The results are presented in Tables XXXVI and XXXVII for fuselage stations 442 and 509, respectively. More than 99 percent of the total damage, exclusive of the ground-air-ground cycle, occurred during the maneuver mission segment at both aircraft fatigue critical locations.

(3) Analysis of Maneuver Mission Segment Data

On the basis of the data presented in Tables XXXVI and XXXVII, the parametric analysis was confined to the determination of damage in the maneuver mission segment. The damage in the maneuver mission segment was further separated into two categories: pull-up after weapon release or gunfiring, and all other maneuvers. The results of these calculations are presented in Tables XXXVIII and XXXIX for fuselage stations 442 and 509, respectively. Examinations of these figures reveal that approximately 85 percent of the total aircraft damage, exclusive of the ground-air-ground cycle, occurs during pull-up after weapon release or gunfiring for the fatigue critical points under consideration.

c. Damage Prediction Techniques

Based on the relative importance of the load factor occurrences during pull-up after weapon release or gunfiring, the primary effort was directed toward development of a method for predicting this damage.

(1) Mach-Altitude Probability Technique

The F-105F pull-ups after weapon release or gunfiring were classified according to the major exit configuration and mission type. The results are presented in Table XL by air base. These results show that 93 percent of the occurrences at Base 1 are in Major Configuration 1. At Base 2, 98 percent of the occurrences are in Major Configuration 3. This points out a very definite difference in the aircraft configuration at the two bases. However, the use of different Mach-altitude probability models by major configuration would accomplish this separation automatically.

Due to the small sample size available for analysis, and in view of the results obtained for the F-105D, the application of the Mach-altitude probability model damage prediction technique was restricted to the occurrences in exit Configuration Three. The Mach-altitude probabilities for Base 2 are presented by load factor magnitude and independent of gross weight and mission type in Table XLI. These data, with load factor magnitude eliminated as a variable, are presented in the form of a three-dimensional plot in Figure 25. The fatigue damage was predicted as described in Section II-2b(1) of this report, and the results are presented in Table XLII for fuselage stations 442 and 509, respectively.

(2) Calculation of Damages

As shown in Table XL, there is a distinct difference in the exit configuration by base for the F-105F pull-ups after weapon release or gunfiring.

Therefore, the damages based on both the total data sample and by base were computed on a per-hour, per-flight, and per pull-up basis. The resulting damage ratios are presented in Tables XLIII, XLIV, and XLV. The corresponding variances are shown at the bottom of each table. The variances were calculated as described in Section II-2b(2) for a truncated data sample formed by eliminating aircraft serial numbers 8321 and 8278. As shown by the variances, a distinct improvement is realized in the variances by calculating the damages for all three methods on a per-base basis. The improvement at fuselage station 509 is decidedly greater than at fuselage station 442.

The preceding analysis was performed independently of mission type. As was pointed out in Section II-3a(4), there exists a significant variation in the data by mission type. All of the pull-up occurrences in mission types 8 and 9 of Table XL result from night-time missions as shown in Table XXIV. Figure 26 shows the separation of the data by day-time and night-time missions. The probability of occurrences as a function of both load factor level and Mach number is shown. As would be expected, no high magnitude pull-ups were experienced during the night-time missions. Also, the Mach number experience was all in the .70 to .90 range. Therefore, it appears that the damage prediction by any of the techniques being employed would yield better results if this additional parameter were included in the analysis.

d. Discussion

The same general discussion presented for the F-105D in Section II-2c is also pertinent to the F-105F aircraft. Specifically, the F-105F data sample, although somewhat limited in size, pointed out that different utilization can result in the addition or deletion of variables in the fatigue damage analysis of the fighter aircraft. The F-105F fatigue damages were found to be quite sensitive to air base location and time-of-day usage. This serves to point up the fact that not only do the damage rates have to be revised continuously on the basis of aircraft utilization, but also that the number of parameters being considered must also be revised to compensate for different modes of utilization.

TABLE XXXIV

Definition of Mission Type for the F-105F SEA Data Sample

<u>Code</u>	<u>Type Mission</u>
1	Ground Gunnery*
2	Conventional Bombing (Martin)
3	Air Patrol and Air-to-Air Gunnery
4	Special & Search & Rescue [†]
5	Escort
6	Instrumentation, Navigation & Test Hop
7	Conventional Bombing (W. W. Daytime)
8	Conventional Bombing (W. W. Nighttime)
9	Conventional Bombing (Night Raiders)

*Includes Strafing, SAM Strike, and Shrike Launch Missions

[†]Includes Search and Rescue and SAM Search Missions

TABLE XXXV

Recorded Data by Mission Type and Air Base
for F-105F Data Sample

<u>Mission Code</u>	<u>(Base 1) Takhli AB</u>	<u>(Base 2) Korat AB</u>	<u>Total</u>	<u>Percent of Total</u>
1	194.9	135.9	330.8	33.0
2	-	131.7	131.7	13.1
3	-	11.8	11.8	1.2
4	158.9	103.5	262.4	26.2
5	41.6	75.3	116.9	11.7
6	8.8	9.7	18.5	1.9
7	17.4	-	17.4	1.7
8	9.8	31.0	40.8	4.1
9	-	70.9	70.9	7.1
	431.4	569.8	1001.2	100.0

TABLE XXXVI

Tabulation of Damage by Mission Segment for
the F-105F Transfer Spar at Fuselage Station 442
by Aircraft Serial Number

A/C	Damages x 10 ⁵			$\frac{\text{Maneuver}}{\text{Total}} \times 10^2$
	Maneuver Mission Segment	All other Mission Segments	Total	
4436	648.7364	3.5307	652.2671	99.46
8301	1043.2609	3.2982	1046.5591	99.68
8311	1198.3468	4.7994	1203.1462	99.60
8316	842.7527	13.5657	856.3184	98.41
8321	82.0003	1.5050	83.5053	98.19
Base 1	3815.0971	26.6990	3841.7961	99.30
4446	481.6040	6.0914	487.6954	98.75
8302	428.5441	2.0554	430.5995	99.52
8329	1813.7759	4.3401	1818.1160	99.76
8336	631.0819	3.7573	634.8392	99.40
8278	9.0285	4.1070	13.1355	68.73
Base 2	3364.0344	20.3512	3384.3856	99.40
Total	7179.1315	47.0502	7226.1817	99.34

TABLE XXXVII

Tabulation of Damage by Mission Segment for
the F-105F Top Cover Skin at Fuselage Station 509
by Aircraft Serial Number

A/C	Damages x 10 ⁵			<u>Maneuver</u> Total x 10 ²
	Maneuver Mission Segment	All Other Mission Segments	Total	
4436	502.3881	3.9671	506.3552	99.22
8301	1027.7868	2.8694	1030.6562	99.72
8311	1166.6276	4.0279	1170.6555	99.66
8316	918.5769	8.4753	927.0522	99.09
8321	70.8500	0.1325	70.9825	99.81
Base 1	3686.2294	19.4722	3705.7016	99.47
4446	146.3457	2.9242	149.2699	98.04
8302	103.7704	0.7483	104.5187	99.28
8329	421.8694	1.6418	423.5112	99.61
8336	129.9312	0.9207	130.8519	99.30
8278	0.9992	0.7507	1.7499	57.10
Base 2	802.9159	6.9857	809.9016	99.14
Total	4489.1453	26.4579	4515.6032	99.41

TABLE XXXVIII

Tabulation of Damage due to Pull-up after Weapon Release
for Transfer Spar at Fuselage Station 442 on F-105F Aircraft

A/C	<u>Damages x 10⁵</u>		<u>Pull-up</u> Maneuver x 10 ²
	Maneuver Mission Segment	Pull-up after Weapon Release	
4436	648.7364	568.9416	87.70
8301	1043.2609	970.9624	93.07
8311	1198.3468	1041.7746	86.93
8316	842.7527	714.7875	84.82
8321	82.0003	69.4247	84.66
Base 1	3815.0971	3365.8908	88.23
4446	481.6040	329.2365	68.36
8302	428.5441	322.1226	75.17
8329	1813.7759	1665.1987	91.81
8336	631.0819	518.8760	82.22
8278	9.0285	1.0218	11.32
Base 2	3364.0344	2836.4547	84.32
Total	7179.1315	6202.3455	86.39

TABLE XXXIX

Tabulation of Damage due to Pull-up after Weapon Release
for Top Cover Skin at Fuselage Station 509 on F-105F Aircraft

A/C	Damages x 10 ⁵		$\frac{\text{Pull-up}}{\text{Maneuver}} \times 10^2$
	Maneuver Mission Segment	Pull-up after Weapon Release	
4436	502.3881	456.3848	90.84
8301	1027.7868	991.9268	96.51
8311	1166.6276	1063.2190	91.14
8316	918.5769	846.2096	92.12
8321	70.8500	64.6857	91.30
Base 1	3686.2294	3422.4259	92.84
4446	146.3457	99.8291	68.21
8302	103.7704	61.7952	59.55
8329	421.8694	329.7180	78.16
8336	129.9212	89.3597	68.77
8278	0.9992	0.1209	12.10
Base 2	802.9159	580.8229	72.34
Total	4489.1453	4003.2488	89.17

TABLE XL

Pull-up after Weapon Release or Gunfiring Occurrences
by Configuration, Mission Type, and Air Base for F-105F Aircraft

Base 1

Configuration	Mission Type							
	1	2	3	4	5	6	7	8
1	81			31		2	7	
2	2			1				
3	4				2			
4								
5								

Base 2

Configuration	Mission Type								
	1	2	3	4	5	6	7	8	9
1									
2									
3	37	42	4	25	1			7	11
4									
5				2					

TABLE XLI

Mach-Altitude Probability Distribution for F-105F, Base 2,
Configuration 3 Pull-up After Weapon Release

Mach.	.65	.65	.85	.85	.85	.92	.92	.92	.92	1.2
Alt.	7	20	1	7	20	1	7	12	20	20
K Ft.										
2.7				.800	.200					
3.2				.615	.385					
3.7				.778	.112		.112			
4.2		.059		.588	.118		.176			.059
4.7				.500			.273	.091		.136
5.2	.034			.621			.207			.138
5.7				.445	.056		.112	.056		.334
6.2				.250			.250			.500
6.7				.200			.400			.400
7.2										
7.7										

Contrails

TABLE XLII
Damage Predicted for Pull-ups Using Base 2,
Configuration 3 Probability Model for F-105F

A/C	Actual Damage	Predicted Damage	No. Configuration 3 Pull-ups	<u>Predicted Damage</u> Actual Damage
<u>Fuselage Station 509</u>				
4436	1.9316	11.3840	4	5.89
8301	--	--	0	
8311	--	--	0	
8316	0.0	0.0176	1	
8321	0.0	0.0	1	
Subtotal Base 1	1.9316	11.4016	6	5.90
4446	99.7744	136.1765	32	1.36
8302	61.7952	81.9010	21	1.33
8329	329.7180	150.5767	21	0.46
8336	89.3597	205.6577	42	2.30
8278	0.1209	0.0465	11	0.38
Subtotal Base 2	580.7682	574.3584	127	0.99
Totals	582.6998	585.7600	133	1.01
<u>Fuselage Station 442</u>				
4436	13.3438	32.5681	4	2.44
8301	--	--	0	
8311	--	--	0	
8316	0.5862	0.6515	1	1.11
8321	0.0847	0.1576	1	1.86
Subtotal Base 1	14.0147	33.3772	6	2.38
4446	328.4312	452.1126	32	1.38
8302	322.1226	298.3727	21	0.93
8329	1665.1978	768.3214	21	0.46
8336	518.8760	878.6898	42	1.69
8278	1.0218	1.0572	11	1.03
Subtotal Base 2	2835.6494	2398.5537	127	0.85
Totals	2849.6641	2431.9309	133	0.85

TABLE XLIII
 Predicted Damage Ratios per Flight Hour
 for F-105F Data Sample

A/C	Flight Time (hrs)	<u>Predicted Damage</u> <u>Actual Damage</u>			
		Fuselage Station 509		Fuselage Station 442	
		Total	By Base	Total	By Base
4436	77.44	0.69	1.31	0.86	1.06
8301	56.55	0.25	0.47	0.39	0.48
8311	109.17	0.42	0.81	0.65	0.81
8316	164.00	0.80	1.52	1.38	1.71
8321	24.19	1.54	2.93	2.09	2.58
Subtotal					
Base 1	431.35	0.53	1.00	0.81	1.00
4446	135.01	4.08	1.29	2.00	1.64
8302	112.69	4.86	1.53	1.89	1.55
8329	113.86	1.21	0.38	0.45	0.37
8336	131.68	4.54	1.43	1.50	1.23
8278	76.69	197.41	62.21	42.08	34.63
Subtotal					
Base 2	569.83	3.17	1.00	1.22	1.00
Totals		1001.18	1.00	1.00	

$$S^2 = \begin{matrix} & & 4.0295 & .2213 & .4066 & .2694 \end{matrix}$$

$$S^2 = \frac{n \sum (X_i)^2 - (\sum X_i)^2}{n(n-1)}$$

	<u>Damage Rates</u>	
	Station 509	Station 442
Base 1	.0000859	.0000891
Base 2	.0000142	.0000594
Total	.0000451	.0000722

TABLE XLIV
 Predicted Damage Ratios per Flight for F-105F Data Sample

A/C	Number of Flights	<u>Predicted Damage</u> <u>Actual Damage</u>			
		Fuselage Station 509		Fuselage Station 442	
		Total	By Base	Total	By Base
4436	29	0.57	1.22	0.70	0.98
8301	24	0.23	0.50	0.36	0.51
8311	49	0.41	0.89	0.65	0.90
8316	62	0.66	1.42	1.15	1.60
8321	10	1.40	3.00	1.90	2.64
Subtotal					
Base 1	174	0.47	1.00	0.72	1.00
4446	68	4.51	1.31	2.21	1.67
8302	51	4.83	1.40	1.88	1.42
8329	52	1.22	0.35	0.45	0.34
8336	61	4.62	1.34	1.52	1.15
8278	50	282.95	82.06	60.32	45.68
Subtotal					
Base 2	282	3.45	1.00	1.32	1.00
Total	456	1.00		1.00	
	$S^2 =$	4.4494	.1797	.4786	.2362

$$S^2 = \frac{n\sum(X_d)^2 - (\sum X_d)^2}{n(n-1)}$$

	<u>Damage Rates</u>	
	Station 509	Station 442
Base 1	.000213	.000221
Base 2	.000029	.000120
Total	.000099	.000158

TABLE XLV

Predicted Damage Ratio per Pull-up for F-105F Data Sample

A/C	Number of Pull-ups	<u>Predicted Damage</u>			
		<u>Actual Damage</u>			
		<u>Fuselage Station 509</u>		<u>Fuselage Station 442</u>	
		Total	By Base	Total	By Base
4436	20	0.68	1.15	0.84	0.91
8301	18	0.28	0.48	0.44	0.48
8311	36	0.52	0.89	0.83	0.89
8316	50	0.91	1.56	1.68	1.81
8321	6	1.43	2.44	2.07	2.24
Subtotal					
Base 1	130	0.59	1.00	0.92	1.00
4446	34	5.26	1.53	2.47	2.27
8302	21	5.25	1.53	1.56	1.43
8329	21	0.98	0.29	0.30	0.28
8336	42	7.26	2.12	1.94	1.78
8278	11	1406.31	409.65	257.80	236.71
Subtotal					
Base 2	129	3.43	1.00	1.09	1.00
Total					
	259	1.00		1.00	
	$S^2 =$	7.8107	.3769	.5926	.4919

$$S^2 = \frac{n \sum (X_i)^2 - (\sum X_i)^2}{n(n-1)}$$

	<u>Damage Rates</u>	
	Station 509	Station 442
Base 1	.000263	.000259
Base 2	.000045	.000220
Total	.000155	.000239

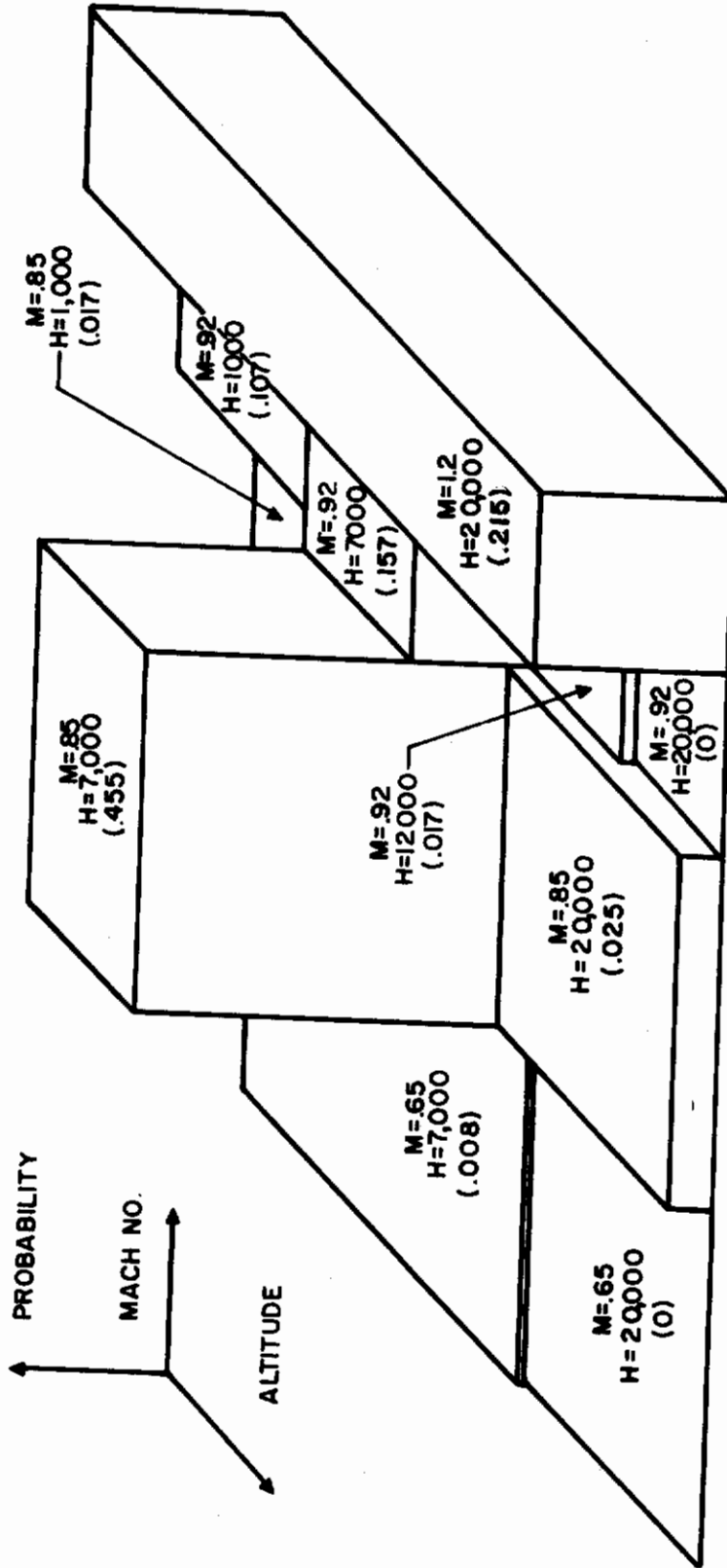


Figure 25 Mach-Altitude Probability Plot for F-105F Configuration 3, Base 2 Pull-ups After Weapon Release or Gunfiring

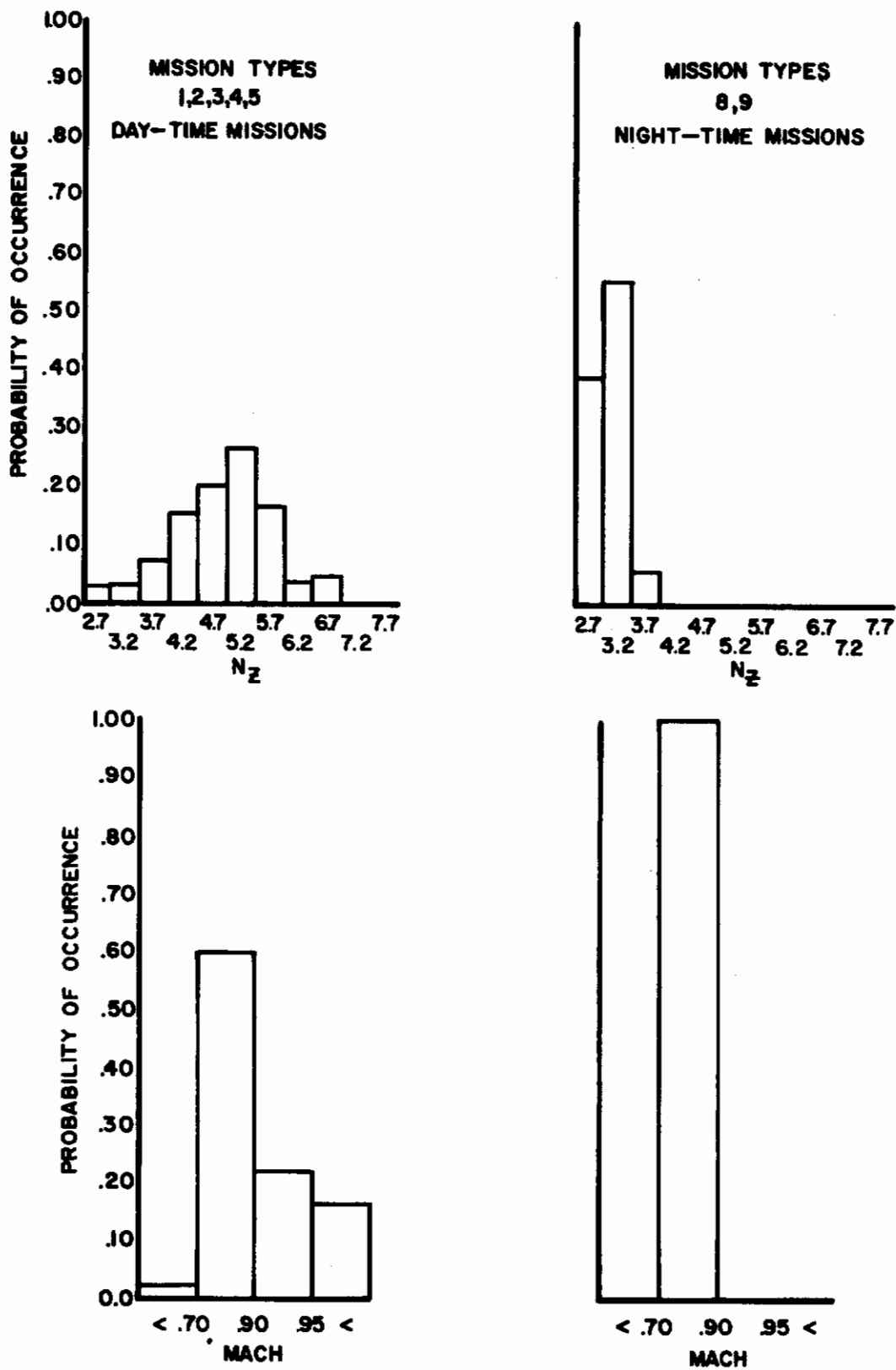


Figure 26 Probability of Occurrence by Load Factor Magnitude and Mach Number for F-105F, Base 2, Configuration 3 Pull-ups

SECTION III

RECORDER DESIGN

1. BACKGROUND

The cumulative fatigue monitoring of fighter-type aircraft presents a very definite challenge to a parametric type of analysis. This analysis is different from that of a bomber or cargo aircraft because the parameters change so rapidly that it is impossible to obtain them from a pilot's log sheet; and equally important is the fact that for fighter aircraft the source of damaging loads is maneuvering rather than gust encounters. Since the damage is a result of pilot-initiated maneuvers, and since the pilot has so much freedom in how he pulls-out after a weapon pass, there is a great amount of variability in the load factor spectrum from aircraft to aircraft. The analysis is further complicated by the large number of combinations of external stores and fuel pods that can be used.

In order to improve on the prediction of the fatigue damage beyond the prediction based on either a per-hour or per-flight average, it will be necessary to use some type of recorded data. The analysis of the F-5A data indicates that a counting accelerometer which segregates the load factor data by stores configuration would provide a more accurate estimate of the damage. The F-105D data indicates that there is little similarity among the various individual aircraft on the basis of Mach number, altitude, or load factor spectra, even for the same weapon configuration. Therefore, to make an accurate calculation of the fatigue damage, a record of the load factor as a function of Mach number, altitude, configuration and gross weight should be made. The measurement of all of the parameters is required so that the stress peaks can be calculated; however, if the stress peaks were to be measured, no other measurements would be required.

Some other observations about the data also warrant the installation of a recording device on each aircraft. For example, on the F-5A: the average damage rates were different for the five recording phases; the data from the first phase (where the gun was being evaluated) should not be included in the overall damage rate; and the period of VGH recording in any one phase was not long enough to establish a good average rate, even though the recordings were made for the duration of the phase. On the F-105F the data from the two bases show a significant difference, primarily due to different external stores, so that the two bases should be handled separately. Also, there was a very significant difference between day and night flights.

The above examples lead to the conclusions that due to the rapid change in mission assignments or usage, it would be necessary to update the usage model very frequently; and also that several models would be in use at any one time.

This would require an elaborate bookkeeping system and a continual analysis of the instrumented fleet to determine when the damage model changed and what the new model should be.

A much simpler system, from an analysis and bookkeeping viewpoint, would be a peak counting strain recorder. Presented below are design concepts of a counting accelerometer and two types of strain recorders.

2. PEAK COUNTING ACCELEROMETER

Peak counting accelerometers have been used by the British Aircraft industry and the United States Navy for some time. The early installations recorded in registers the number of times that a given load factor was equaled or exceeded. These counts were independent of flight condition or aircraft configuration. Recently a new concept in counting accelerometers (References 8 and 9) was introduced for use with the F-111 aircraft. This new counting accelerometer separated the load factors by certain combinations of Mach number and wing sweep angle. This concept allows the calculation of different stresses for the same load factor level, depending on the aircraft's environment and configuration. The following presentation is a discussion of the design of a discriminating counting accelerometer.

A discriminating counting accelerometer can be visualized as an onboard data processing system. Its purpose is to provide a low-cost reliable system for accumulating load factor data and correlating it to other variables. In performing a fatigue analysis of an aircraft fleet, the following calculations are performed: (1) simultaneous time history recordings are obtained of load factor, Mach number, and altitude, (2) these parameters are then blocked into class intervals and a report is prepared that presents the number of times that the load factor peak reached a certain value for each combination of class intervals of Mach number and altitude, along with other parameters such as weight and configuration, and (3) from the calculated curves or tables of stress peak counts and the S-N data for a point on the aircraft, the fatigue damage is calculated.

An onboard counting accelerometer can be designed so that it has a series of accumulating registers which count the number of times that the load factor exceeds a certain value, with all the other parameters constant. This, in effect, is then a stress peak count. The principal disadvantage of this system is the large number of storage registers required to sort the load factor data by combinations of Mach number, altitude, weight, and configuration. In the illustrated system (Figure 27), provision is made for sorting the g-data into three sub-groups according to pre-defined conditions of other variables such as weight or configurations. The components required for this unit are conventional and commercially available; and the circuitry, namely the latching, sorting and dropout circuitry, is well developed and reliable. The cost of the system hinges primarily on the choice of counters, which runs from \$20 per unit to \$70 per unit. Fifteen counters are needed. In high quantity (10,000 counters) the price quoted by one manufacturer drops from \$70 to \$10 per unit.

The counting accelerometer operates as follows: as the acceleration level is increased from the normal 1 - g level, contact is made by the acceleration transducer's wiper to successively increasing level contactors. Such contact, even only momentary, brings the live supply voltage from the wiper to a given contact line and causes the latching relay for that level to momentarily operate. Operation of the latching relay closes a contact on the relay which connects the contact line to the live supply voltage by a route other than the accelerometer wiper. (This other route, for reset purposes, passes through the normally closed contacts of relay R.) Once this alternate route is established the latching relay is "latched on" and the contact line is live even after the accelerometer wiper leaves it. All levels operate in this manner.

To sort g occurrences with respect to weight or configuration, the five lines whether energized or not are routed to three counter banks through three banks of ganged switches (three 5-pole relays). These operate from external commands shown here as configuration command buttons. The buttons would be replaced by two or three logic relays once the desired sorting function is established.

Upon return to the normal g - level or any established threshold, the reset contact is touched by the wiper contact, causing the reset relay R to de-energize all five latching relays, and re-establish the circuits to receive the next g-level signal.

Vibration and/or oscillation of the accelerometer are not counted and neither are cycles in the g value which do not increase from the normal g level position or the established threshold level. This is accomplished by the latching relay mechanism, which holds any given tripped counter in the energized position until the reset contact is touched and relay R de-energizes all five latching relays. When a counter is held energized it is effectively locked, since it is during dropout of the counter solenoid that ratchet action occurs to permit counter advance upon the next energizing pulse. The counters, in effect, store the cumulative frequency of g levels equal to or greater than the level for that register.

3. PEAK COUNTING ELECTRO-MECHANICAL OPTICAL STRAIN TRANSDUCER

The use of a peak counting accelerometer would still require calculations of the response of the aircraft structure to convert load factor magnitudes to stresses at various points on the aircraft. A more direct approach would be to record the number of times that a given strain level was equaled or exceeded at a particular point on the aircraft structure. If the exceedence spectrum of the stresses at a point could be known, it would not be necessary to know anything about the aircraft configuration, weight, or flight environment provided a constant 1 - g trim stress could be assumed.

Contrails

The components of a system to provide such knowledge can be grouped into three areas: (1) the accumulating registers; (2) the mechanical or electronic logic to sort the signal levels into bands; and (3) the strain transducer. The accumulating registers would be the same for all of the systems but the banding mechanisms would be dependent on the type of strain transducer.

One possible type of system would use a conventional dial indicator as the strain transducer with the indicating hand replaced by a drum with a small aperture and a light source inside the drum. Spaced around the outside of the drum would be photocells that would sense the amount of rotation of the drum, which would be proportional to the strain. Each photo cell would be connected to a storage register so that every time a certain magnitude of strain was equaled, the counter would index one count. A schematic drawing of such a system is shown in Figure 28. The wiring diagram of the system is shown in Figure 29. The mechanism of the dial indicator is a rack and pinion with one set of step-up gears, so that for a rack travel of .0001 inches the dial rotates 1.8° . For a two-inch gage length, a stress of 1000 psi would therefore cause a rotation of 3.6° and 36,000 psi would produce 129.6° of rotation.

If five class intervals were used to represent the stress exceedence curve from 12,000 to 36,000 psi, each class interval would be represented by 21.6° of rotation. This sensitivity would give a good resolution for positioning the photocells to distinguish one class interval from another. Assuming that only a peak count of the strains would be necessary, one additional photocell would be located at a threshold level. The strain level would have to decrease below this threshold level before a second peak could be recorded.

One strain channel of such a system is shown on the diagram. As strain increases the aperture slit rotates to illuminate successive photo-resistive cells which then energize their corresponding relay K_1 --- K_5 . Energizing such a relay K_1 --- K_5 closes the contact on that relay which brings current to the corresponding counter. This contact also brings an alternate current to the relay over a path other than through the photocell. This alternate current remains after the photocell is no longer illuminated and serves to latch the relay. This current, however, also passes through the normally closed contact of the reset relay K_0 and de-energizes any and all given relays K_1 --- K_5 , which had been latched. Reset occurs below the level of any desired strain level and hence there is never any conflict of the reset with the energizing and latching of any relay K_1 --- K_5 . Of course, each strain level could be provided with its own reset level with the addition of four more relays. These new reset levels could be placed anywhere other than coincident with the level of the circuit that they are to reset.

There are several advantages of this type of instrument over a load factor recorder. The first and most important is that the accuracy of the fatigue analysis is not dependent on any usage parameters of the aircraft. No pilot log is required.

The storage registers do not have to be read after each flight, but instead perhaps only once a month. The fatigue analysis performed with the strain data is independent of whether the loading was symmetric or asymmetric provided the location of the sensor is such that the transfer factor is a constant for all types of loadings.

At the present time there are a few possible shortcomings of this system, mainly related to the strain transducer. The fatigue life and airworthiness of the dial indicator is unknown; however, any deficiencies should be minor and correctable with a minor effort. There may be some difficulties with transient temperature changes which could cause a differential thermal expansion between the aircraft structure and the dial indicator push rod. Another disadvantage is that one complete system would be required for each fatigue critical location on the structure. This would still require fewer storage registers than an accelerometer system.

The remaining components of the system employ conventional and commercially available counters and relays. Cost of one channel would depend primarily on the price of the counters and the results of the dial indicator tests. The counters could run as high as \$70 each and the latching relays up to \$15 each. However, in large quantity these costs are expected to be more like \$10 and \$3, respectively.

4. RESISTANCE STRAIN GAGE

Another method of monitoring the strain cycles is to use the analog output signal of a conventional resistance strain gage bridge to operate relays at different signal levels. A circuit which would compare the output signal to reference levels is shown in Figure 30, along with a complete circuit diagram of the system.

The counting electrical resistive strain gage is essentially a system which blocks analog strain signals into five preset digital class intervals and then registers the occurrence of each strain level into a counter as it occurs. The proposed system employs a resistive strain gage whose output signal is amplified and thus scaled up by a stable gain but low cost closed loop operational amplifier. The output of this amplifier is compared to a staircase of five voltage levels which are created by an appropriate stack of zener diodes. An alternative voltage staircase could be obtained by use of a resistive divider string. When the output of the amplifier exceeds the voltage level of a given tap on the staircase, the rectifier diode on that branch would become conductive and current would pass through the corresponding relay. A counter could be connected in parallel with this relay, as shown, or energized through a second contact on the relay (not shown) for more reliability if required.

Energizing any given relay also closes the contact on that relay which connects the relay to a current from the staircase string. This latches it and holds it on, even if the amplifier output level changes to a lower level. When the output

level drops to the reset level, the reset relay, which has contacts that are normally open, de-energizes and resets all latched relays. The reset relay is connected to the amplifier output and de-energizes only at near-zero levels of amplifier output and hence at near zero strain levels. This threshold level would be set near the 1 - g trim stress level.

The components suggested in this system require some design considerations and in this regard the system is not as straightforward as an all-relay or electro-mechanical system. However, a logical system is feasible and once designed and tested it should be in every respect as reliable as an all electro-mechanical system.

5. MECHANICAL SCRATCH GAGE

A commercially available scratch strain gage has been evaluated by the USAF for potential use in monitoring fatigue damage for maneuver sensitive aircraft (Reference 10).

The device is a self-contained mechanical extensometer capable of measuring and recording total deformation (and thus average strain) over the effective installed gage length of the member to which it is attached. The gage contains its own brass recording disc and provides a permanent record of each strain excursion above the installation sensitivity threshold limit. During flight tests on a jet trainer (Reference 11) it was determined that the disc capacity would be on the order of 30 hours.

This device is inexpensive (approximately \$100 per installation), requires little maintenance and is self compensated for temperature. The recorded trace is permanent and may be retained for future use once it has been removed from the aircraft.

The discs must be removed and processed to extract the data. Methods of data retract vary from simple, but time consuming manual reading with a calibrated microscope to complex optical scanning equipment. Automated equipment to handle large amounts of discs is considered necessary to successfully warrant the use of the device in service.

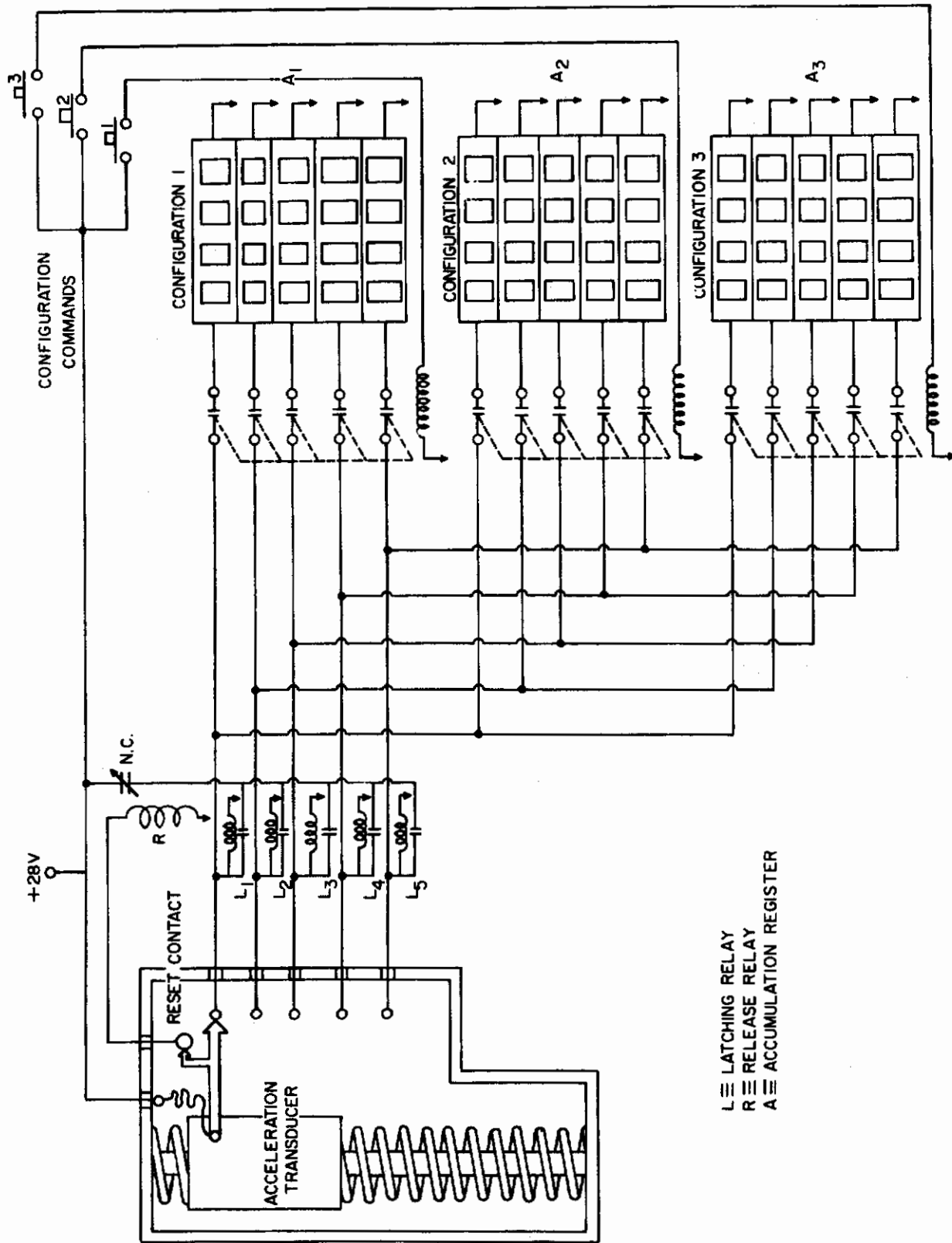


Figure 27 Schematic Diagram of Counting Accelerometer System

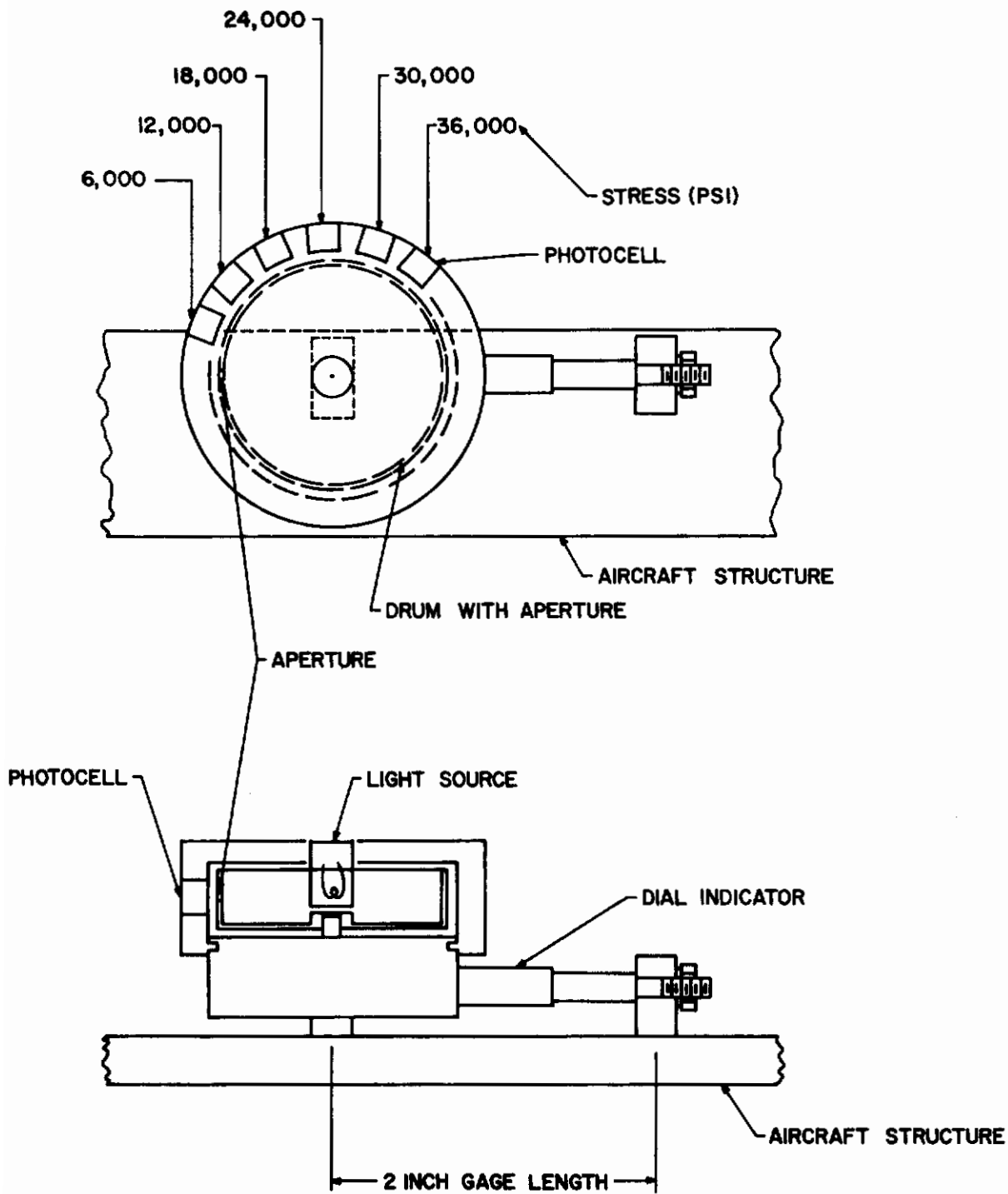


Figure 28 Design Concept of Electro-Mechanical-Optical Peak Strain Transducer

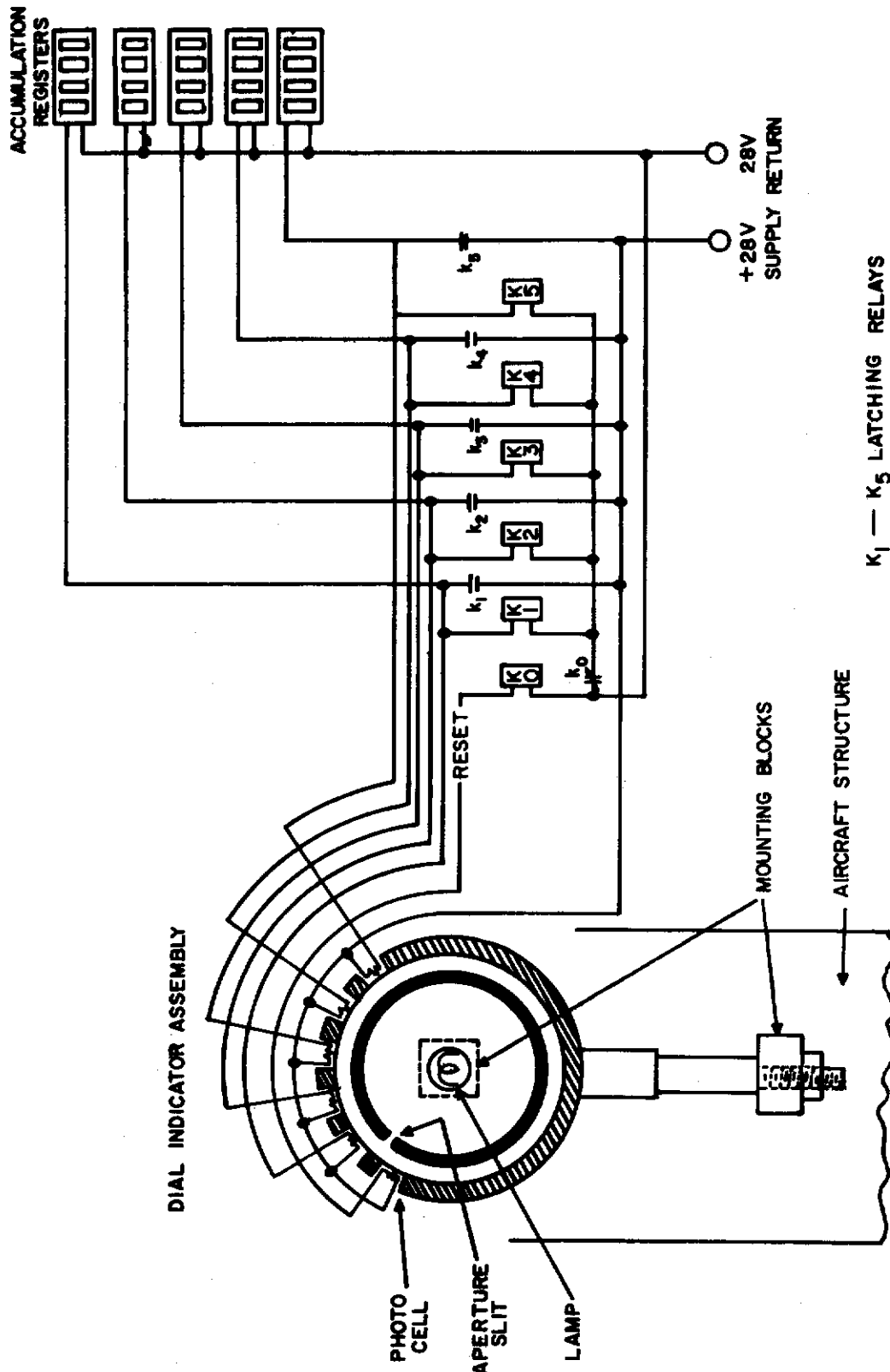


Figure 29 Schematic Diagram of Electro-Mechanical-Optical Peak Strain Counting System

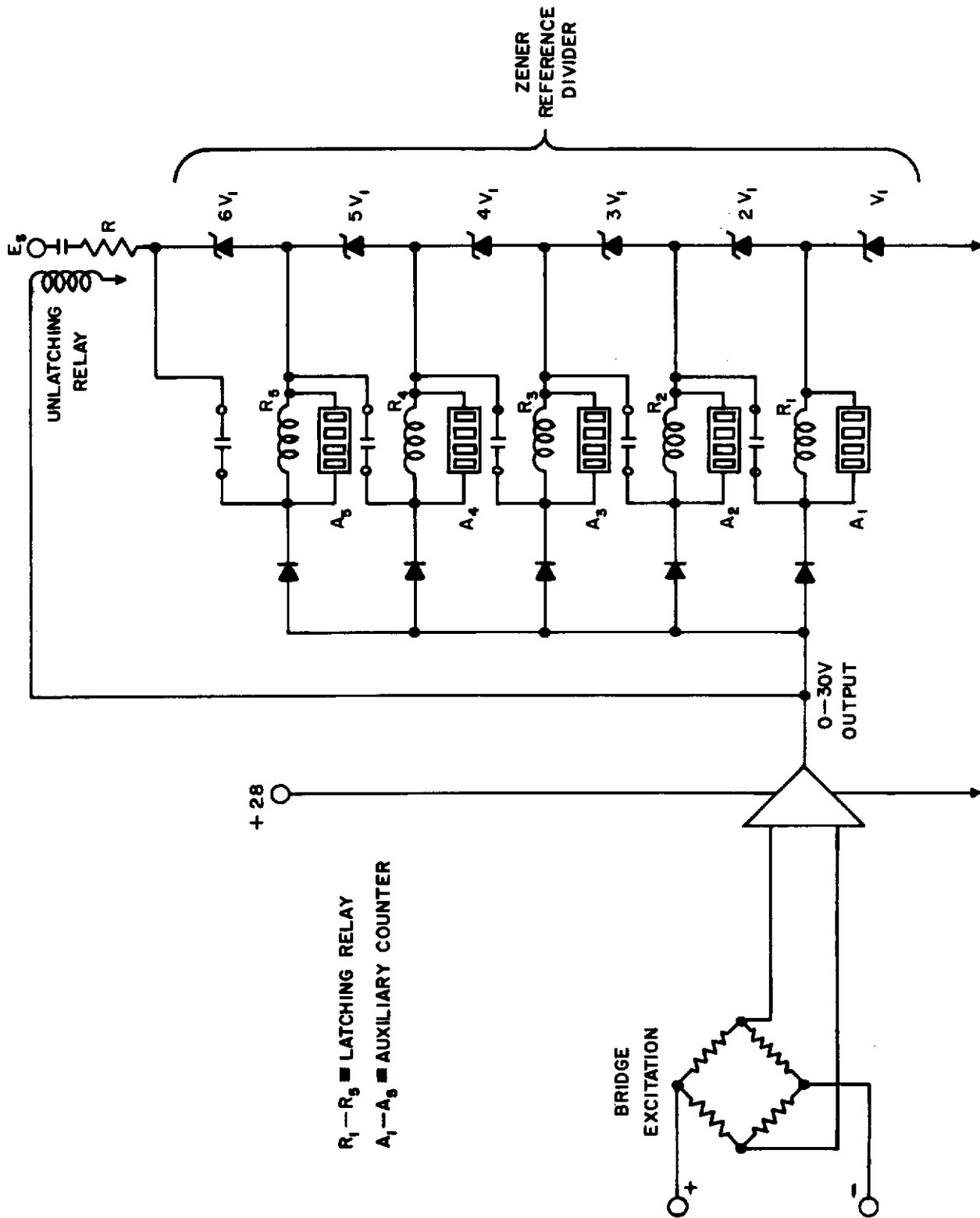


Figure 30 Schematic Diagram of Resistance Strain Gage Peak Strain Counting System

SECTION IV

DISCUSSION

The analysis of the parameters that affect the magnitude of the fatigue damage indicates that for most fighter aircraft, the load factor, gross weight, stores configuration, Mach number and altitude are all important and independent variables. The fact that the magnitude of each variable is independent of each other, and in many cases independent of the type of mission, places a burden on statistics that prevents the construction of any damage model which will accurately predict the damage to individual aircraft. This is true even when the individual aircraft's experience was included in the construction of the model. It is logical to think that for aircraft whose experience is not included in the model, the deviation from the model would be greater than for aircraft which were included in the model.

It has been shown that if the significance of the variables were to be ranked in order of importance, a mean value used for the least important, a probability distribution for the next most important, and the two most important variables were to be measured; then the prediction of the damage naturally was improved. However, the results were still not acceptable.

A comment about the predicted damage based on the Mach-altitude probability model is in order. Referring to Table XLI, it can be seen that at the 6.7 g level for example, there were five occurrences. These five occurrences could have been on five different aircraft. When the model is applied in the prediction of the damage, it would be assumed that 20% of the occurrences were at Mach .85 and 7000 ft. altitude and 40% at Mach .92 and 7000 ft. altitude, etc. The expected average damage rate for a 6.7 g maneuver is then 20% of the damage for an occurrence at Mach .85 altitude 7000, plus 40% of the damage for an occurrence at Mach .92 altitude 7000, plus 40% of the damage for an occurrence at Mach 1.2 altitude 20,000. However, when one applies the model to an individual aircraft there may be only one occurrence of 6.7 g's in the data sample. The true damage is the damage for one of the Mach-altitude combinations listed but the predicted damage is the above described average damage. Therefore, the model cannot be expected to predict the correct damage unless the individual aircraft has enough occurrences of a given load factor level that it has a chance of having a distribution like that used to construct the model.

It appears to the authors that since there are five important variables, it is very unlikely for each aircraft to experience the same number of occurrences of each combination of these variables; and, therefore, some measured data will be required. Now, if it is conceded that a recorded measurement is required, why measure load factor, Mach number, altitude, weight, and

Contrails

configuration, for fleet tracking of fatigue damage by AFLC, since damage is only indirectly related to these? Why not measure the strain at a point, since damage is a function of only the strain? If a reliable peak strain counter is developed, it will provide data for a more accurate fatigue analysis at a lower cost.

SECTION V

CONCLUSIONS

Fighter aircraft deployed in a combat zone experience an almost random stress spectrum. This is due to the large number of parameters (weight, Mach number, altitude, configurations, and load factor) which determine the magnitude of the stress.

Damage rates based on a per-hour or per-flight average may cause errors as large as a factor of 3. Also, the averages depend on the type of mission which changes over a short period of time so that a continual updating of the averages is required.

The Mach-altitude probability model when used with measured load factor data was a better predictor than gross averages but the improvement was not significant.

Due to the variety of missions flown which result in different environmental spectra and weapon configurations, several damage models will be required at any one time.

The use of a peak counting accelerometer that segregates the load factor counts by Mach number, altitude, configuration and gross weight would permit an accurate calculation of fatigue damage but the number of storage registers would be prohibitive.

A peak counting strain indicator would eliminate the requirement for a special pilot's log sheet. This would require the assumption of a constant 1 - g trim stress.

A peak counting strain indicator is the most economical and accurate method of monitoring fatigue damage on fighter aircraft, and to monitor a fleet effectively, each aircraft in the fleet should contain this instrumentation.

REFERENCES

1. G. J. Roth, J. P. Ryan, J. C. Sliemers; Parametric Fatigue Analysis of USAF Aircraft AFFDL TR-67-89, 1967.
2. W. W. Morton, C. G. Peckham; Structural Flight Loads Data From F-5A Aircraft. SEG-TR-66-51, November, 1966.
3. A. P. Berens; Load Factor Data for F-5A and F-105D Aircraft in Weapon Passes AFFDL-TR-68-47, March, 1968.
4. C. M. Kantershi, T. Ishimine; Maneuver Spectra and Fatigue Life from Measured Combat Data. Northrop Corporation, NOR67-28, April, 1967.
5. F-105D Combat Statistical Flight Loads Program. SMNE 68-910, February, 1968.
6. H. Axkrod; F-105 Fatigue Analysis Based on VGH Data. ESAR 105-4 December, 1965.
7. Joseph Militello; F-105F Combat Statistical Flight Loads Program, Technical Report (EFR) 82. 4. 1, May, 1969 (In Publication).
8. J. R. Sturgeon; Fatigue Load Meters. Mechanism Limited, Croydon, England.
9. Maintenance Manual No. 61, Fatigue Recording System Type 25. Mechanism Limited, Croydon, England.
10. T. L. Haglage, H. A. Wood; Scratch Strain Gage Evaluation. AFFDL-TR-69-25, July 1969.
11. T. L. Haglage; Flight Test Evaluation of a Scratch Strain Gage. AFFDL-TR-69-116, November 1969.

Contrails

Unclassified

Security Classification

DOCUMENT CONTROL DATA - R&D		
(Security classification of title, body of abstract and indexing annotation must be entered when the overall report is classified)		
1. ORIGINATING ACTIVITY (Corporate author) University of Dayton Research Institute 300 College Park Dayton, Ohio 45409	2a. REPORT SECURITY CLASSIFICATION Unclassified	
3. REPORT TITLE <p style="text-align: center;">Parametric Fatigue Analysis of USAF Fighter Aircraft</p>		
4. DESCRIPTIVE NOTES (Type of report and inclusive dates) <p style="text-align: center;">Final (13 May 1968 to 1 July 1969)</p>		
5. AUTHOR(S) (Last name, first name, initial) <p style="text-align: center;">Roth, George J. and West, Blaine S.</p>		
6. REPORT DATE <p style="text-align: center;">September 1969</p>	7a. TOTAL NO. OF PAGES <p style="text-align: center;">104</p>	7b. NO. OF REFS <p style="text-align: center;">11</p>
8a. CONTRACT OR GRANT NO. AF 33615-68-C-1494 b. PROJECT NO. <p style="text-align: center;">1467</p> c. Task 146704 d.	9a. ORIGINATOR'S REPORT NUMBER(S) 9b. OTHER REPORT NO(S) (Any other numbers that may be assigned this report) <p style="text-align: center;">AFFDL-TR-69-85</p>	
10. AVAILABILITY/LIMITATION NOTICES This document is subject to special export controls and each transmittal to foreign governments or foreign nationals may be made only with prior approval of the Air Force Flight Dynamics Laboratory (AFSC), Wright-Patterson AFB, Ohio 45433.		
11. SUPPLEMENTARY NOTES	12. SPONSORING MILITARY ACTIVITY Air Flight Dynamics Laboratory Air Force Systems Command Wright-Patterson AFB, Ohio 45433	
13. ABSTRACT <p>This report contains the results of a study of the significant parameters that contribute to the fatigue life of USAF fighter aircraft. The variability of the parameters from one aircraft to another was determined in an attempt to use a mean value or a most probable distribution of some parameters so that they could be eliminated from the log sheet or recorded data. The analysis suggests that there is such a wide variation in the load factors, Mach numbers, altitudes and configurations experienced by the F-105D and F-105F aircraft that an average damage model cannot be used to predict damage to individual aircraft. A peak strain cycle counting recorder is suggested as the most practical method of monitoring fatigue damage to individual fighter aircraft. Design concepts of a counting accelerometer and two types of peak strain counters are presented.</p> <p>This abstract is subject to special export controls and each transmittal to foreign governments or foreign nationals may be made only with prior approval of the AFFDL (FDTR), Wright-Patterson Air Force Base, Ohio 45433.</p>		

DD FORM 1473
1 JAN 64

Unclassified

Security Classification

14.	KEY WORDS	LINK A		LINK B		LINK C	
		ROLE	WT	ROLE	WT	ROLE	WT
	Fatigue Analysis Maneuver Loads Parametric Fatigue Analysis Fatigue Meters						

INSTRUCTIONS

1. **ORIGINATING ACTIVITY:** Enter the name and address of the contractor, subcontractor, grantee, Department of Defense activity or other organization (*corporate author*) issuing the report.
- 2a. **REPORT SECURITY CLASSIFICATION:** Enter the overall security classification of the report. Indicate whether "Restricted Data" is included. Marking is to be in accordance with appropriate security regulations.
- 2b. **GROUP:** Automatic downgrading is specified in DoD Directive 5200.10 and Armed Forces Industrial Manual. Enter the group number. Also, when applicable, show that optional markings have been used for Group 3 and Group 4 as authorized.
3. **REPORT TITLE:** Enter the complete report title in all capital letters. Titles in all cases should be unclassified. If a meaningful title cannot be selected without classification, show title classification in all capitals in parenthesis immediately following the title.
4. **DESCRIPTIVE NOTES:** If appropriate, enter the type of report, e.g., interim, progress, summary, annual, or final. Give the inclusive dates when a specific reporting period is covered.
5. **AUTHOR(S):** Enter the name(s) of author(s) as shown on or in the report. Enter last name, first name, middle initial. If military, show rank and branch of service. The name of the principal author is an absolute minimum requirement.
6. **REPORT DATE:** Enter the date of the report as day, month, year, or month, year. If more than one date appears on the report, use date of publication.
- 7a. **TOTAL NUMBER OF PAGES:** The total page count should follow normal pagination procedures, i.e., enter the number of pages containing information.
- 7b. **NUMBER OF REFERENCES:** Enter the total number of references cited in the report.
- 8a. **CONTRACT OR GRANT NUMBER:** If appropriate, enter the applicable number of the contract or grant under which the report was written.
- 8b, 8c, & 8d. **PROJECT NUMBER:** Enter the appropriate military department identification, such as project number, subproject number, system numbers, task number, etc.
- 9a. **ORIGINATOR'S REPORT NUMBER(S):** Enter the official report number by which the document will be identified and controlled by the originating activity. This number must be unique to this report.
- 9b. **OTHER REPORT NUMBER(S):** If the report has been assigned any other report numbers (*either by the originator or by the sponsor*), also enter this number(s).
10. **AVAILABILITY/LIMITATION NOTICES:** Enter any limitations on further dissemination of the report, other than those

imposed by security classification, using standard statements such as:

- (1) "Qualified requesters may obtain copies of this report from DDC."
- (2) "Foreign announcement and dissemination of this report by DDC is not authorized."
- (3) "U. S. Government agencies may obtain copies of this report directly from DDC. Other qualified DDC users shall request through _____."
- (4) "U. S. military agencies may obtain copies of this report directly from DDC. Other qualified users shall request through _____."
- (5) "All distribution of this report is controlled. Qualified DDC users shall request through _____."

If the report has been furnished to the Office of Technical Services, Department of Commerce, for sale to the public, indicate this fact and enter the price, if known.

11. **SUPPLEMENTARY NOTES:** Use for additional explanatory notes.
12. **SPONSORING MILITARY ACTIVITY:** Enter the name of the departmental project office or laboratory sponsoring (*paying for*) the research and development. Include address.
13. **ABSTRACT:** Enter an abstract giving a brief and factual summary of the document indicative of the report, even though it may also appear elsewhere in the body of the technical report. If additional space is required, a continuation sheet shall be attached.

It is highly desirable that the abstract of classified reports be unclassified. Each paragraph of the abstract shall end with an indication of the military security classification of the information in the paragraph, represented as (TS), (S), (C), or (U).

There is no limitation on the length of the abstract. However, the suggested length is from 150 to 225 words.
14. **KEY WORDS:** Key words are technically meaningful terms or short phrases that characterize a report and may be used as index entries for cataloging the report. Key words must be selected so that no security classification is required. Identifiers, such as equipment model designation, trade name, military project code name, geographic location, may be used as key words but will be followed by an indication of technical context. The assignment of links, rules, and weights is optional.